UNIVERSITY OF PRISTINA-FACULTY OF SCIENCES
KOSOVSKA MITROVICA-REPUBLIC OF SERBIA

THE UNIVERSITY THOUGHT

PUBLICATION IN NATURAL SCIENCES

VOL. 7, N° 1, 2017.

ISSN 1450-7226 (Print)

ISSN 2560-3094 (Online)

UNIVERSITY OF PRISTINA-FACULTY OF SCIENCES
KOSOVSKA MITROVICA-REPUBLIC OF SERBIA
UNIVERSITY THOUGHT-PUBLICATION IN NATURAL SCIENCES

Aims and Scope

The University Thought - Publication in Natural Sciences (Univ. thought, Publ. nat. sci.) is a scientific journal founded in 1994. by the University of Priština, and was published semi annually until 1998.

Today, the University Thought - Publication in Natural Sciences is an international, peer reviewed, Open Access journal, published semi annually in the online and print version by the University of Priština, temporarily settled in Kosovska Mitrovica, Serbia. The Journal publishes articles on all aspects of research in Biology, Chemistry, Geography, Information technologies, Mathematics and Physics in the form of original papers, short communications and reviews (invited) by authors from the country and abroad.

The University Thought - Publication in Natural Sciences serves as an interdisciplinary forum covering a wide range of topics for a truly international audience. Journal is endeavor of the University of Priština to acquaint the scientific world with its achievements and wish to affirm the intellectual potential and natural resources of own region. Our aim is to put forward attitude of principle that science is universal and we invite all scientists to cooperate wherever their scope of research may be. We are convinced that shall contribute to do victory of science over barriers of all kinds erected throughout the Balkans.

Editorial Office

Ive Lola Ribara 29; 38220, Kosovska Mitrovica, Serbia, e-mail: editor.utnsjournal@pr.ac.rs, office.utnsjournal@pr.ac.rs, office.utnsjournal@gmail.com; fax: +381 28 425 397

Available Online

This journal is available online. Please visit http://www.utnsjournal.pr.ac.rs to search and download published articles.

UNIVERSITY THOUGHT-PUBLICATION IN NATURAL SCIENCES

Vol. 7, N^{o} 1, 2017.

CONTENTS

UNIVERSITY THOUGHT
Publication in Natural Sciences, Vol. 7, No. 1, 2017, pp. 1-7.
doi:10.5937/univtho7-13650
Review Paper

THE CIRCADIAN CLOCK AND HUMAN ATHLETIC PERFORMANCE

BILJANA VITOŠEVIĆ[1*]

[1]Faculty of Sport and Physical Education, Leposavić, University of Priština, Kosovska Mitrovica, Serbia

ABSTRACT

The importance of circadian clock in managing of key muscle physiological processes, and therefore the impact on athletic performance is well studied. Specifically chronobiology examines the mechanisms of the biological clock and the consequences of disrupting its rhythm. Although a body of literature indicates that the peak performance of notable indicators of athletic performance exerts mainly in the afternoon and evening hours which is attributed to increased temperature of the body, certain variables such as vigilance, alertness and cognitive domains can influence the shift of the peak performance during the day. In addition, athletes face issues of desynchronization of their circadian rhythm during frequent transcontinental travels, since their performance is reduced and the adjustment of the biological clock requires some recommendations in the training process and behavioral approach. This review focuses on some current studies on endogenous and exogenous factors which affect the circadian rhythm in order to achieve better sport results, evaluation of the impact chronotype through chronometric tests and revising more valuable determinants of sport performance, as well as the application of new mathematical models in individual treatment of recovery of athletes in the phase of resynchronization.

Keywords: circadian clock, chronobiology, athletic performance, circadian disruption.

INTRODUCTION

That the man is indeed a part of nature and in a harmonious relationship with it, indicating the fact that although the biological rhythms are endogenous, they are adjusted to external stimuli. It has long been recognized that the circadian rhythm regulates many physiological processes, like secretion of hormones, sleep-wake cycle, body temperature and activity patterns. The term circadian rhythm is of Latin origin and means fluctuations set for a period of about 24 hours, or more precisely 24.5, which are synchronized with the cycle of light in the environment (Brown et al., 2005). That internal generator of rhythms, called "biological clock" is located in the suprachiasmatic nucleus (SCN) of the hypothalamus, which directly receives the information about light and the darkness through retinal-hypothalamic fibers. Information obtained from the outside are processed and through a central circadian clock sent to the other peripheral clocks of various tissues and cells whose work can be aligned or may be autonomous. The circadian synthesis and secretion of melatonin by the pineal gland is generated in the SCN and entrained primarily by the light-dark cycle (Cajochen et al., 2003). The molecular mechanism behind this cell-autonomous rhythm involve a complex network of negative transcription–translation-based feedback loop (Okamura et al., 2002). Many opposite research results are explained just with that powerful autonomy of peripheral clocks. These external signals or natural time synchronisers are in literature referred to as the German term "zeitgeber" and have the ability to "rewind" the biological clock and thus can regulate circadian rhythms. Light as the leading zeitgeber, in addition to transmission along retinal-hypothalamic tract, also affects a number of other physiological rhythms, including plasma cortisol and plasma melatonin, which like its precursor serotonin plays an important role in the regulation of sleep (Carrier & Monk, 2001). In addition to brightness, the timing of nutrition, physical activity and some social and psychological factors are also considered as zeitgebers and through the main biological clock, affect the peripheral oscillators that regulate many important physiological functions of metabolism. As the "gold standard" or key biological marker of human circadian rhythm is considered the temperature of the body which raises a number of physiological rhythms that manage an important metabolic variables (Wever, 1979).

The science that studies the mechanisms of biological clocks as well as the potential consequences of disrupting this system is referred to as chronobiology. A key component of this transdisciplinary science is the biological rhythm which is characterized by its frequency, period length, amplitude (acrophase-peak, mesor-mean and nadir-trough), as well as the phase (phase advance- shift to an earlier time or phase delay-shift to a later time in the 24 hour cycle) of the particular parameter (Lee-Chiong, 2008). Another sphere of interest of chronobiologists is the clock mechanism and factors affecting the rhythm of the endogenous processes (Drust et al., 2005). Chronobiological systems are not isolated, but rather are associated with other irreversible homeostatic processes that define the metabolism (Reilly & Waterhouse, 2009). Since the circadian changes are interrelated and synchronized with many external factors, there are a variety of scientific disciplines that study the coherence. Thus there is chrono-pharmacology that

* Corresponding author: home.vitosevic@gmail.com

studies the optimal timing of medication, improving metabolic activity in respect of time of administration; chrono-nutrition that studies the relationship between the food and the the system of circadian rhythm; chrono-therapy in terms of medication in the coordination with the circadian rhythm in order to increase the effectiveness and reducing side effects (eg. corticosteroids in dosages that simulate adrenocortical cycle), and more recently sports-chronobiology, which examine the physical skills and their respective biochemical, physiological and psychological functions in a time frame. The main goal of these subdisciplines of chronobiology is to monitor the periodisation of sport trainings, particularly focusing on the adaptive mechanisms and timing in sports performance in terms of its optimization or elimination of desynchronisation factors (Jančokova et al., 2013).

CIRCADIAN RHZTHM AND ATHLETIC PERFORMANCE

In early publications, (Winget et al., 1985) pointed out the connection between circadian rhythm with many physiological functions associated with sports performance, such as motor and psychomotor skills, perceptual and cognitive functions. Biological rhythms are coordinated in accordance with the environment by adjusting the circadian clock primarily in relation to light, but also to physical activity. As mentioned, the main biological marker of human circadian rhythm is considered the temperature of the body. Increase in body temperature can increase the utilization of carbohydrates compared to fat as an energy source and eventually facilitate the actin and myosin mechanics in the musculoskeletal structures, which may result in improved physical performance through better skeletal muscle contractile properties (Starkie et al., 1999). A body of literature indicates that body core temperature is lowest in the morning around 04:30h and increases gradually during the day with acrophase around 18.00h in the afternoon. Increased temperature in the afternoon is in line with the increased coordination, the highest reaction time, increasing muscle strength and cardiovascular efficiency (Atkinson & Reilly, 1996; Shibata & Tahara, 2014; Smolensky & Lamberg, 2000). In addition, anaerobic power output and flexibility of joints are also the highest in the late afternoon (Racinais et al., 2005). But, when it comes to performance speeds, the best results were obtained between 08:30 h and 10:30h in the morning (Huguet et al., 1995). Reasons for the worse performance among athletes in the morning are associated with lower glycogen as a result of a night fasting, stiffness of joints after periods of rest and sleep, the less warming up the muscles in the morning compared to subsequent active period of the day and the fact that they are not yet sufficiently awake to keep their activity at a high level (Kline et al., 2007).

The heterogeneity in some studies and daily variations in the strength, power and force of skeletal muscle attributes to the peripheral clocks that possess temperature-dependent and temperature-independent mechanisms (Robinson et al., 2013). Many authors emphasize that although the temperature is the chief marker of sports performance, some variables such as the state of vigilance and alertness, and mood levels (which are the highest in the morning) can affect athletic performance (Atkinson & Speirs, 1998; Reilly et al., 2003). Interestingly, simple mental actions such as reaction time are mainly associated with the core body temperature (neural activity and conduction, for example, increase with temperature) and they show a peak in the afternoon, while more complex mental actions that require cognitive and neuromuscular coordination, like, decision making, concentration and calculations show peak earlier, around noon. This data could be the reason for shifts peak sports performance in some studies (Valdez et al., 2008). Conducting of circadian rhythm in short-term (1 min or less) performance is controversial and can rely on the type of exercise and the muscle group tested (Bernard et al., 1998).

That the temperature associated with the functionality of skeletal muscles, (Taylor et al., 2011) are demonstrated by extending the active warm-up training session in the morning for 20 min, and in the results achieved a reduction of the force and strength loss in the vertical jumps, which are obtained identical conditions of temperature in the afternoon training session. This result suggests that the protocol of warming-up in order to increase the temperature of the body could be helpful in reducing the diurnal difference in performance and improving performance especially in colder climates. Possible intercellular mechanisms include intercellular calcium and inorganic phosphate concentrations. For example, certain deviations from the traditional point of view of the relationship of the temperature of the body and sports performance is explained in the study of (Martin et al., 1999), by analyzing the role of circadian rhythm on the neural activation and the contractile ability of human adductor pollicis muscle. They found that the force during maximal voluntary contraction was higher in the evening than in the morning, with the increase in twitch and tetanus force, so they assume that peripheral mechanisms rather than central activation, have a predominant role in the diurnal fluctuation. The obtained results are attributable to the increase of calcium release from the sarcoplasmic reticulum, an increased sensitivity of calcium ion of contractile proteins actin and myosin and the changed-myosin ATPase activity. Subsequently, (Stephenson & Williams, 1985) suggested that calcium concentration and temperature have a valuable effect on force at temperatures below 25°C, with a decrease of interacting sites of the thin actin-myosin filament system, but little effect at temperatures above 25°C. Indeed, this is confirmed in human studies, and it has been proven that there are fundamental thermodynamic differences in amplitude and sensitivity of the Ca2+, which further induces changes in protein binding, contraction and significant decline in force (Fitts, 2008).

Another effect that can affect the diurnal variation, are the hormones testosterone and cortisol. Under normal conditions, the circadian profiles of testosterone and cortisol are very similar, with their peak early in the morning and a progressive decline during the day, and hence morning hours are less suitable for high catabolic activity of training (endurance and long running or resistance training with high repetition), therefore they are recommended in the late afternoon when the ratio T / C is highest. In fact it is known that cortisol primarily affects the degradation of proteins, so its decline increased skeletal muscle hypertrophy through a reduction in the degradation of proteins (Hayes et al., 2012; Hayes et al., 2010). Much more work remains to be done in this area considering that both steroid hormones are very important for adaptation in the bouts of exercise. However, different types of exercise, their duration, intensity and recovery periods are parameters which often give different general results, so that consideration of some major conclusions are difficult to achieve. What is certain is that it is obvious that their influence is very important in neuromuscular function, in metabolic pathways, as well as to fluctuations in certain neurotransmitters (GABA, dopamine and serotonin) (Monti & Jantos, 2008). So additional research with uniform conditions is required, with similar loadings in the sports performances and to be replicated in larger studies, by including more respondents.

Table 1. Summary of some findings in impact of circadian rhythm on performance

Study	Mode	Subjects, Gender	Skills	Results
Rahnama et al. (2009)	Soccer	12, M	Flexibility, socer skills	The values were better in the evening than morning
Reilly et al. (2007)	Soccer	8+8, M	Flexibility, reaction time, grip strenght, football specific skills	Peaks occurred between 16:00 and 20:00 h, daytime changes paralleled the temperature rhythm
Gharbi et al. (2013)	Soccer	15, M	Agility, dribbling, Coordination	Higher at 17,00h; No time-of-day effect was observed for the coordination and skill index
Chtourou et al. (2013)	Soccer	20, M	Vertical jump height (SJ, CMJ)	Lower morning values in vertical jump height
Atkinson et al. (2005)	Cycling	8, M	Power output	16.1-km cycling performance is worse in the morning than in the afternoon, even they perform a vigorous 25-min warm-up
Souissi et al. (2012)	Cycling	22, M	Wingate tests (muscle power), mean-power-frequency (MPF), Neuromuscular efficiency (NME)	MPF and NME are higher in the evening during the Wingate cycling test and the evening improvement in muscle power and fatigue is due to an enhancement of muscle contract. Propertis
Rai & Tiwari, (2015)	Volleyball	30, M	Agility, explosive strenght, speed ability	Diurnal variation does not affect the performance of volleyball players on selected motor fitness components
Souissi et al. (2013)	Judo	12, M	Wingate tests	Muscle power and strength were significantly higher at 16:00 than 09:00 hours ($p<0.05$)
Jarraya et al. (2014)	Handball's goalkeeper	12, M	Reaction time Cognitive tasks	Significantly higher at evening; Cognitive performances of GK are time-of-day-dependent with the highest values observed in the morning

In addition, different results in peak athletic performance may be the result of inter-individual variation in circadian rhythmicity. Morning- and evening-type (an early "lark" or a late "owl") endogenously individuals differ in the circadian phase of their biological clocks. Sometimes these chronotypes cope better with the training sessions at different times of the day (Kerkhof

et al., 1996). In recent times, new research focuses on the chronometric tests as novel approach, which is based on the fact that the main predictor of peak performance is actually time since entrained awakening, and not time of day. A recent study of (Facer-Childs & Brandstaetter, 2015) with the participation of 121 athletes competitors, showed that the time of the entrained awakening reflects the internal biological clock, and varies by about 26% compared to the real time of day. Consequently, these differences entail the different physiology, such as different levels of cortisol and melatonin. These studies have provided important insights into peak performance between circadian phenotypes in real time and in a time of awakening, which can be used to better optimize performance. They concluded that it does not matter in which time of the day is the best performance of a person, but how many hours after waking up is a performance or competition carried out.

Some studies of sports performance and their different skills in relation to the time of day, are summarized in Table 1. Most of results have shown a better value in the afternoon and evening which is coherent with some general viewpoint in line with circadian rhythm. By contrast, (Rai & Tiwari, 2015) did not observe that diurnal variations have an impact on performance of volleyball players in selected motor fitness. Similarly, cognitive performance of handball goalkeepers showed the highest values in the morning, which is desynchronized from rhythm of core temperature, but are in accordance with some opinion that fatigue occurs later in the day (Jarraya et al., 2014).

MECHANISMS OF MOLECULAR BACKGROUND

As it is known, SCN achieves it regulatory role directly, by nervous and humoral paths, and indirectly, through the body temperature, physical activity or feeding rhythms. However, regulation of the individual cell type or organ is usually complex and involves multiple pathways. The largest number of efferent pathways from the SCN includes neurotransmitters that enable endocrine responses. Through various endocrine hormone target tissues are then prepared for certain changes. Glucocorticoids, whose rhythm is regulated by these pathways, are extremely important to reset or synchronize many peripheral clocks in the body (Dickmeis, 2009; Chung et al., 2011). It is known that GABAergic neurons are responsible for the inhibitory effect of SCN on the secretion of melatonin during the day, while glutamatergic neurons stimulate the release of melatonin at night. Melatonin, as well as glucocorticoids, however, has a regulatory role in the circadian activity of many tissues (Kalsbeek et al., 2006; Hirota & Fukada, 2004). Each of these hormones acting on receptors in various tissues, and therefore transmitted a message to the target tissue.

Molecular clock of mammals consisting of a primary loop comprising the basic clock genes (core clock genes) and additional, regulatory loop, which altogether gives a complex network of negative feedback loops. The availability and activity of the protein clocks regulates at post-transcriptional and post-translational level. The main positive regulators or activators of these loops are CLOCK (Circadian Locomotor Output Cycles Kaput) and BMAL1 (Brain and Muscle Arnt-like 1) and the other two are repressors (PER-Period 1, 2 and 3), and CRY-Cryptochrome 1 and 2), with a set of kinases and phosphatases as adjusters and stabilizers (Partch et al, 2014). But what initiates and drives all the action between SCN, neuronal networks, neurotransmitter release to cellular functions and coordinate their work at the intracellular level, are calcium ions (Ca2+), because once they enter the cytosol, they exert different effects on proteins and coordinates numerous cell functions (Enoki et al., 2017). The research done by shutting down the input pathway by tetrodotoxin (TTX) reduces the amplitude of Ca2+ rhythms by approximately 30%, assuming that intracellular Ca2+ levels are managed by both input pathways to the core loop and output pathways from the loop to diverse cellular functions (Enoki et al., 2012). All this indicates not only the importance of the role of calcium ions, but also the synchronization and correlation of all these components because disruption of one factor destabilizes the entire system. Although most of the data comes from experimental work with animal, humans appear to have a similar set and mechanisms of clock genes (Cermakian & Boivin, 2003). Accordingly, some studies have shown that different types, intensity and duration of exercise may affect different transcriptional output of the biological clock. A study by (Zambon et al., 2003) found that resistance exercise may alter the expression of circadian clock regulatory genes in human skeletal muscle. These findings are important because they support the view that sometimes peripheral clocks are independent in their regulation of SCN. But the specific mechanisms of regulation of individual genes of oscillators and their expression in the different loads in exercise, and their behavior in different time spans, remains unclear. Also, the independence of the peripheral clock with respect to SCN is not always determined, which remains an unexplored area and requires further investigation.

DESYNCHRONIZATION OF CIRCADIAN RHYTHM

The change of external factors, such as changes in the cycle of light and darkness at the trans-continental flights or work shift, can result in desynchronization of circadian rhythm. Adaptation to change, as well as resynchronization are individual, requiring several days and takes place in stages. Jet leg is transient disturbance occurring by desynchronization of steady physiological and biological rhythms. It manifests itself on travelling where the flight passes through the three or more time zones to the final destination. The first phase of desynchronization can be accompanied by symptoms such as fatigue, headache, nausea, decrease of concentration, insomnia, but as the organism adjusts the biological clock to a new time zone, these symptoms slowly disappear (phase of

resynchronization). Adaptation to changes in circadian rhythms are individual, so that younger adapt faster than elderly. It was established that for every time zone crossed, one day is required to restore normal rhythm. Crossing over six time zones requires about two days up to two weeks. Faster adaptation is present in flying to the west because it extends the day and gets more time compared to those flying to the east. During the adjustment period of the biological clock to a new time zone, physical performance may be impaired because it maintains the parallelism with the temperature of the body and the biological clock and is not adequately prepared for the new destination. In addition, the mental performance may be reduced and further exacerbated by insomnia (Waterhouse et al., 2001). (Lemmer et al., 2001) suggests that elite athletes travelling to the west or east destinations over six to eight time zones demonstrated modified grip strenght and weak performance in training sessions or several days after the flight.

While the biological clock is adjusted and completely remodeled, it is recommended to establish the normal daily behavior, exposure to sunlight, rhythm activities, rest, taking a meal, waking and sleep in relation to the local time in order to normalize biological rhythms as soon as possible. The type of food and timing of meals are also important aspects in the adaptation to a shifted zone. It is known that high-protein food stimulates an adrenaline path that increases alertness and readiness, so it is recommended for breakfast, but foods rich in carbohydrates increases the secretion of insulin, which facilitates the uptake of tryptophan, an essential amino acid which is then converted into serotonin, and promotes drowsiness, so this kind of food is recommended in the evening. Adequate hydration is implied because it eliminates fatigue that often accompanies jet leg (Reilly et al., 2007c; Reilly et al., 2007).

With regard to the important sports events, quality assurance of sports performance requires serious planning of travelling. Thus it is recommended previous training in the time that is in line with the future time zone, as well as planning the arrival earlier and thus adequate adaptation. Behavioral approach involves timing and intensity of training, and gradual build-up of the level of training (without strenuous and risky exercise in the initial sessions in order to avoid possible injuries). Food timing is certainly a better approach than pharmacological, but not should be avoided supplementation and maintaining sleep through low dose of melatonin, bearing in mind the direction and purpose of adjusting the biological clock, as some side effects of melatonin (headache, dizziness, morning drowsiness). Alternative therapies recommended as antidotes for jet-lag comprise homeopathic remedies, massage and relaxation are without any evidence of their effectiveness (Reilly et al., 2007). There is little evidence based on for re-timer eyeglasses that emit green light, which is supposed to mimic natural sunlight and is believed to help reset the biological clock.

The idea of mathematical models of performance is not new, but has previously relied on the different models, the first one implying that the homeostatic and circadian processes are independent and additive and others who implies their interaction (Carrier & Monk, 2000). Other types of models have studied the dynamics of the SCN, both the main pacemaker and peripheral oscillators and trying to numerically determine the behavior. The latest model conceived by (Lu et al., 2016) unified the dynamics of many individual oscillators and held them up to the macroscopic level. The advantage of this model, according to the authors, is its simplicity compared to previous models, ease of interpretation and applicability. As base they used sinusoidally forced Kuramoto model from animal experiments (direct measurements of SCN oscillators are not available for humans but is used as an indirect deduction), and added external parameters such as the sensitivity of an individual's response to sunlight, cloud distribution, geographical latitude, and seasonality. This is the most actual model and its value consists of the facts that may help explain how eastward and westward travel can have different effects on the individual recovery of circadian rhythms. They suggest further research in the field of resynchronization including a more realistic approach of the oscillators and better analysis of SCN complex network.

CONCLUSION

Interpretation of sports chronobiology is based on the premise that the fusion of endogenous and exogenous mechanisms has a strong influence on the circadian rhythm in sports performance. In addition to light, physical activity is important zeitgeber that through the main biological clock operates on the peripheral oscillators, and then they initiate a myriad of physiological functions that raise hormones, enzymes and neurotransmitters, and through a complex network of negative feedback loops can define the response and adaptation of the organism. That response, although tightly bound to the internal biological clock, may shift its limits in relation to environmental conditions. This space represents a major enigma for scientists, although it is being explored for a long time now. Most of the borders of peak performance in physical skills are generally known. Physical skills such as strength, agility and flexibility has its peak in the afternoon and evening, which is associated with an increase in temperature as the main marker of biological rhythms. However, many other variables such as vigilance, alertness and cognitive abilities may affect the outcome of the performance and display fine alterations. This shift is explained by the influence of the peripheral clocks, but also by numerous other factors, endogenous (different chronotype) or exogenous (different environmental conditions, methodology of research). Some new approaches to the evaluation of circadian rhythms deserve great attention and suggest correction of analysis regarding the peak performance of the day and propose that circadian phenotypes are also taken into

considerations and performance inquiry as a function of time since awakening.

On the other hand, often cited that the biggest enemy of athletes is the syndrome of jet lag, considering the frequent transcontinental travells. Although the response and adaptation in athletes are individual, sometimes these circadian disruptions may affect the reduction in athletes performance. This requires serious prior preparation for travel, training and time of food intake in order to minimize these issues. Recently, a lot of attention is devoted to the application of mathematical models that can individually calculate the required recovery in distant eastward and westward journeys, which translated into practice can be of great help to athletes in the phase of resynchronization.

REFERENCES

Atkinson, G., & Reilly, T. 1996. Circadian variation in sports performance. Sports Med, 21(4), pp. 292-312. pmid:8726347. doi:10.2165/00007256-199621040-00005

Atkinson, G., & Speirs, L. 1998. Diurnal variation in tennis service. Percept Mot Skills, 86(3 Pt 2), pp. 1335-8. pmid:9700810

Atkinson, G., Todd, C., Reilly, T., & Waterhouse, J. 2005. Diurnal variation in cycling performance: Influence of warm-up. J Sports Sci, 23(3), pp. 321-9. pmid:15966350. doi:10.1080/02640410410001729919

Bernard, T., Giacomoni, M., Gavarry, O., Seymat, M., & Falgairette, G. 1998. Time-of-day effects in maximal anaerobic leg excercise. Eur. J. Appl. Physiol, 77(3), pp. 133-138. pmid:9459533

Brown, S.A., Fleury-Olela, F., Nagoshi, E., Hauser, C., Juge, C., Meier, C.A., . . . Schibler, U. 2005. The period length of fibroblast circadian gene expression varies widely among human individuals. PLoS Biol., 3(10), p. 338. pmid:16167846. doi:10.1371/journal.pbio.0030338

Cajochen, C., Kräuchi, K., & Wirz-Justice, A. 2003. Role of melatonin in the regulation of human circadian rhythms and sleep. J. Neuroendocrinol., 15(4), pp. 432-7. pmid:12622846

Carrier, J., & Monk, T.H. 2000. Circadian rhythms of performance: New trends. Chronobiol. Int., 17(6), pp. 719-32. pmid:11128289

Cermakian, N., & Boivin, D.B. 2003. A molecular perspective of human circadian rhythm disorders. Brain Research Reviews, 42, pp. 204-220. pmid:12791440

Chtourou, H., Aloui, A., Hammouda, O., Chaouachi, A., Chamari, K., & Souissi, N. 2013. Effect of static and dynamic stretching on the diurnal variations of jump performance in soccer players. PLoS ONE, 8(8), p. 70534. pmid:23940589. doi:10.1371/journal.pone.0070534

Chung, S., Son, G.H., & Kim, K. 2011. Circadian rhythm of adrenal glucocorticoid: Its regulation and clinical implications. Biochim. Biophys. Acta, 1812(5), pp. 581-91. pmid:21320597. doi:10.1016/j.bbadis.2011.02.003

Dickmeis, T. 2009. Glucocorticoids and the circadian clock. J. Endocrinol, 200(1), p. 322. doi:10.1677/JOE-08-0415

Drust, B., Waterhouse, J., Atkinson, G., Edwards, B., & Reilly, T. 2005. Circadian rhythms in sports performance: An update. Chronobiol. Int., 22(1), pp. 21-44. pmid:15865319. doi:10.1081/CBI-200041039

Enoki, R., Kuroda, S., Ono, D., Hasan, M.T., Ueda, T., Honma, S., & Honma, K. 2012. Topological specificity and hierarchical network of the circadian calcium rhythm in the suprachiasmatic nucleus. Proc. Natl. Acad. Sci. USA, 109(52), pp. 21498-21503. doi:10.1073/pnas.1214415110

Enoki, R., Ono, D., Kuroda, S., Honma, S., & Honma, K. 2017. Dual origins of the intracellular circadian calcium rhythm in the suprachiasmatic nucleus. Sci. Rep., 7, p. 41733. doi:10.1038/srep41733

Facer-Childs, E., & Brandstaetter, R. 2015. The impact of circadian phenotype and time since awakening on diurnal performance in athletes. Current biology , 25(4), pp. 518-22. pmid:25639241. doi:10.1016/j.cub.2014.12.036

Fitts, R.H. 2008. The cross-bridge cycle and skeletal muscle fatigue. J. Appl. Physiol., 104(2), pp. 551-8. pmid:18162480. doi:10.1152/japplphysiol.01200.2007

Gharbi, A., Masmoudi, L., Ghorbel, S., Noureddine, B., Maalej, R., Tabka, Z., & Zaouali, M. 2013. Time of Day Effect on Soccer-Specific Field Tests in Tunisian Boy Players. Advances in Physical Education, 3(2), pp. 71-75. doi:10.4236/ape.2013.32011

Hayes, L.D., Bickerstaff, G.F., & Baker, J.S. 2010. Interactions of cortisol, testosterone, and resistance training: Influence of circadian rhythms. Chronobiol. Int., 27(4), pp. 675-705. pmid:20560706. doi:10.3109/07420521003778773

Hayes, L.D., Grace, F.M., Kilgore, J.L., Young, J.D., & Baker, J.S. 2012. Diurnal variation of cortisol, testosterone and their ratio in apparently healthy males. Sport SPA, 9(1), pp. 5-13.

Huguet, G., Touitou, Y., & Reinberg, A. 1995. Diurnal changes in sport performance of 9- to 11year-old school children. Chronobiol Intl., 12, pp. 351-362.

Jančokova, L. 2013. Chronobiology from theory to sports practice.Krakow: Towarzystwo Slowakow w Posce., p. 30. Monograph ed..

Jarraya, S., Jarraya, M., Chtourou, H., & Souissi, N. 2014. Diurnal variations on cognitive performance in handball goalkeepers. Biological Rhythm Research, 45(1), pp. 93-101. doi:10.1080/09291016.2013.811032

Kalsbeek, A., Palm, I.F., La, F.S.E., Scheer, F.A.J.L., Perreau-Lenz, S., Ruiter, M., . . . Buijs, R.M. 2006. SCN outputs and the hypothalamic balance of life. J. Biol. Rhythms, 21(6), pp. 458-69. pmid:17107936. doi:10.1177/0748730406293854

Kerkhof, G.A., & van Dongen, H.P.A. 1996. Morning-type and evening-type individuals differ in the phase position of their endogenous circadian oscillator. Neurosci Lett, 218, pp. 153-156.

Kline, C.E., Durstine, L.J., Davis, M.J., Moore, T.A., Devlin, T.M., Zielinski, M.R., & Youngstedt, S.D. 2007. Circadian variation in swim performance. J. Appl. Physiol., 102(2), pp. 641-9. pmid:17095634. doi:10.1152/japplphysiol.00910.2006

Lee-Chiong, T.L. 2008. Sleep medicine: Essentials and review. In .Oxford - New York: Oxford University Press. ISBN-13: 978-0195306590.

Lemmer, B., Kern, R., Nold, G., & Lohrer, H. 2002. Jet lag in athletes after eastward and westward time-zone transition. Chronobiol. Int., 19(4), pp. 743-64. pmid:12182501

Lu, Z., Klein-Cardeña, K., Lee, S., Antonsen, T.M., Girvan, M., & Ott, E. 2016. Resynchronization of circadian oscillators and the east-west asymmetry of jet-lag. Chaos, 26(9), p. 94811. pmid:27781473. doi:10.1063/1.4954275

Martin, A., Carpentier, A., Guissard, N., van Hoecke, J., & Duchateau, J. 1999. Effect of time of day on force variation in a human muscle. Muscle Nerve, 22(10), pp. 1380-7. pmid:10487904. doi:10.1002/(SICI)1097-4598(199910)22:10<1380::AID-MUS7>3.0.CO;2-U

Okamura, H., Yamaguchi, S., & Yagita, K. 2002. Molecular machinery of the circadian clock in mammals. Cell Tissue Res., 309, pp. 47-56. doi:10.1007/s00441-002-0572-5

Partch, C.L., Green, C.B., & Takahashi, J.S. 2014. Molecular architecture of the mammalian circadian clock. Trends Cell Biol., 24(2), pp. 90-9. pmid:23916625. doi:10.1016/j.tcb.2013.07.002

Racinais, S., Blonc, S., Jonville, S., & Hue, O. 2005. Time of day influences the environmental effects on muscle force and contractility. Med Sci Sports Exerc, 37(2), pp. 256-61. pmid:15692321. doi:10.1249/01.MSS.0000149885.82163.9F

Rahnama, N., Sajjadi, N., Bambaeichi, E., Sadeghipour, H.R., Daneshjoo, H., & Nazar, B. 2009. Diurnal Variation on the Performance of Soccer-Specific Skills. World Journal of Sport Sciences, 2(1), pp. 27-30.

Rai, V., & Tiwari, L.M. 2015. Diurnal variation on the performance of selected motor fitness components of volleyball Players. International Journal of Physical Education, Sports and Health, 2(2), pp. 86-88.

Reilly, T., Atkinson, G., Edwards, B., & et al., 2007. Coping with jet-lag: A position statement for the European College of Sport Science. Eur J Sport Sci., 7, pp. 1-7. doi:10.1080/17461390701216823

Reilly, T., Waterhouse, J., Burke, L.M., & Alonso, J.M. 2007. Nutrition for travel. Journal of Sports Sciences, 25(1), pp. 125-134. doi:10.1080/02640410701607445

Reilly, T., & Waterhouse, J. 2009. Chronobiology and Exercise. Medicina Sportiva, 13(1), pp. 54-60.

Reilly, T., Atkinson, G., Edwards, B., Waterhouse, J., Farrelly, K., & Fairhurst, E. 2007. Diurnal variation in temperature, mental and physical performance, and tasks specifically related to football (soccer). Chronobiol. Int., 24(3), pp. 507-19. pmid:17612948. doi:10.1080/07420520701420709

Reilly, T., Farrelly, K., Edwards, B., & Watehouse, J. 2003. Time of day and performance test in male Football players. Book of abstracts. . In: The 5th Word Congress of Science and Football Portugal. , pp. 268-270

Robinson, W.R., Pullinger, S.A., Kerry, J.W., Giacomoni, M., Robertson, C.M., Burniston, J.G., . . . Edwards, B.J. 2013. Does lowering evening rectal temperature to morning levels offset the diurnal variation in muscle force production?. Chronobiol. Int., 30(8), pp. 998-1010. pmid:23863092. doi:10.3109/07420528.2012.741174

Shibata, S., & Tahara, Y. 2014. Circadian rhythm and exercise. The Journal of Physical Fitness and Sports Medicine, 3(1), pp. 65-72. doi:10.7600/jpfsm.3.65

Smolensky, M., & Lamberg, L. 2000. The Body Clock Guide to Better Health: How to Use your Body's Natural Clock to Fight Illness and Achieve Maximum Health, 1st ed.New York: Henry Holt and Co..

Souissi, H., Chtourou, H., Chaouachi, A., Chamari, K., Souissi, N., & Amri, M. 2012. Time-of-day effects on EMG parameters during the Wingate test in boys. J Sports Sci Med., 11, pp. 380-386. PMC3737921. pmid:24149343

Souissi, N., Chtourou, H., Aloui, A., Hammouda, O., Dogui, M., Chaouachi, A., & Chamari, K. 2013. Effects of Time-of-Day and Partial Sleep Deprivation on Short-Term Maximal Performances of Judo Competitors. Journal of Strength & Conditioning Research, 27(9), pp. 2473-2480. doi:10.1519/JSC.0b013e31827f4792

Starkie, R.L., Hargreaves, M., Lambert, D.L., Proietto, J., & Febbraio, M.A. 1999. Effect of temperature on muscle metabolism during submaximal exercise in humans. Exp. Physiol., 84(4), pp. 775-84. pmid:10481233

Stephenson, D.G., & Williams.D.A., 1985. Temperature-dependent calcium sensitivity changes in skinned muscle fibres of the rat and toad. Journal of Physiology, 360, pp. 1-12.

Taylor, K., Cronin, J.B., Gill, N., Chapman, D.W., & Sheppard, J.M. 2011. Warm-up affects diurnal variation in power output. Int J Sports Med, 32(3), pp. 185-9. pmid:21305444. doi:10.1055/s-0030-1268437

Valdez, P., Reilly, T., & Waterhouse, J. 2008. Rhythms of Mental Performance. Mind, Brain, and Education, 2(1), pp. 7-16. doi:10.1111/j.1751-228X.2008.00023.x

Zambon, A.C., McDearmon, E.L., Salomonis, N., Vranizan, K.M., Johansen, K.L., Adey, D., . . . Conklin, B.R. 2003. Time- and exercise-dependent gene regulation in human skeletal muscle. Genome Biol., 4(10), p. 61. pmid:14519196. doi:10.1186/gb-2003-4-10-r61

Waterhouse, J., Minors, D., Akerstedt, T., & et. al., 2001. Rhythms of human performance. In J. Takahashi, F. Turek, & R. Moore Eds., Handbook of behavioral neurobiology: Circadian clocks.New York: Kluver Academic/Plenum Publishers., pp. 571-601.

Wever, R.A. 1979. The circadian system of man: Results of experiments under temporal isolation.New York: Springer-Verlag.

Winget, C.M., DeRoshia, C.W., & Holley, D.C. 1985. Circadian rhythms and athletic performance. Med Sci Sports Exerc, 17(5), pp. 498-516. pmid:3906341

UNIVERSITY THOUGHT
Publication in Natural Sciences, Vol. 7, No. 1, 2017, pp. 8-12.
doi:10.5937/univtho7-14038
Review Paper

CAVE MOTH AND BUTTERFLY FAUNA (Insecta: Lepidoptera) OF SERBIA: CURRENT STATE AND FUTURE PROSPECTS

PREDRAG JAKŠIĆ[1*]

[1]Faculty of Sciences and Mathematics, University of Niš, Niš, Serbia

ABSTRACT

A history of the study of Lepidoptera in caves in Serbia is given. On this basis, a comparative analysis with Lepidoptera species in neighboring countries – Croatia, Romania and Bulgaria, was carried out. The presence of cavernicolous habitats and ecological niches suitable for Lepidoptera was investigated. There is a need to investigate these groups of organisms in Serbia and it is suggested that caves in Serbia be a priority in this research.

Keywords: Lepidoptera, caves, habitats, Serbia.

INTRODUCTION

Carbonate sedimentary rocks (limestone and dolomites) are widespread on the Balkan Peninsula and possess a variety of speleological features, including caves, which are very important to wildlife. It is thought that there are several thousand caves, each providing a suitable habitat for a variety of living organisms. The Balkan Peninsula is considered to be an important center of cave fauna diversity in the world.

In Serbia, parts of the Dinarides and Carpatho-Balkan Mountains are found, with numerous caves, giving it an advantage over other Balkan countries. However, this advantage has not been adequately exploited in the case of cave fauna. There are very few studies on the cave fauna of Serbia. Pretner (1963) registers around 30 endemic species, predominantly Coleoptera, in the caves of Serbia. Ćurčićet et al. (1997), lists 29 species representing different groups in the Zlotska Cave, among which 13 are endemic in caves of the Carpatho-Balkan loop. Every year, intensive research describes numerous species new to science, but a summary of the results depicting the wealth of cave fauna in Serbia is still to come.

Results so far offer little specific data regarding representatives of the Lepidoptera order in caves in Serbia. The goal of this work was to present the current situation and future prospects in the study of Lepidoptera in Serbian caves, and to compare the faunistic abundance in Serbia with that of this group of insects in neighboring countries. One of the tasks was to analyze the cave habitats suitable for the survival of Lepidoptera according to contemporary habitat classification systems, and to show the specific elements of Lepidoptera ecology conditioned by living in caves. It is also important to underline the importance of the protection and monitoring of cave-dwelling Lepidoptera, and to encourage the study of this group of organisms in Serbia.

MATERIALS AND METHODS

By analyzing the literature for Serbia and the countries chosen for comparison – Croatia, Romania and Bulgaria, a list of Lepidoptera species found caves was made. The taxonomic order and nomenclature assigned to the species are according to Karsholt & Razowski (1996). The ecological status of these species (troglophile, trogloxene, subtroglophile) is based on the reports of the authors of the works given in Table 1. An overview of the cavernicolous habitats suitable for Lepidoptera is presented according to the EUNIS habitat classification (Anonymous, 2007-2012). The overview of ecological niches suitable for Lepidoptera is according to Jakšić (2005).

RESULTS

Jovanović (1891), was the first to report the finding of moths in one of the caves in the Sićevo Gorge. The systematic study of Lepidoptera fauna in Serbian caves dates from the period between the two World Wars. In 1923, the Institute of Speleology "Emil Racoviță", Cluj, Romania, organized a study of the cave fauna of Serbia. This research was led by Dr. René Jeannel (1879-1965) and Dr. Siniša Stanković (1892-1974) with a team of four biospeleologists. During June and July, the team visited over 20 caves in eastern and western Serbia. Lepidoptera material was also collected in Hadži Prodan's Cave, but the names of the species were not given Jeannel & Stanković (1924). More detailed results were reported later Jeannel & Racovitza (1929), when the presence of Lepidoptera in four caves was cited, without specifying the species. In 1933, biospeleological research was conducted in the caves of eastern and western Serbia, as well as eastern Montenegro (around Pljevlja), led by Dr. Paul Remy (1894-1962). In the published report, four species of Lepidoptera found in caves around Prijepolje are presented. In his analysis of habitats in Lazar's (Zlotska) Cave, Jakšić (2005) noted the presence of two species of Lepidoptera.

* Corresponding author: jaksicpredrag@gmail.com

These results show that five species of Lepidoptera have been found in the caves of Serbia. Table 1 presents the overall data regarding the presence of Lepidoptera in Serbia and the neighboring countries of Croatia, Romania and Bulgaria.

Table 1. Comparative overview of cave fauna. The species identification number (ID) is according to Karsholt & Razowski (1996). Croatia: (Kučinić, 1990; 2002; Matočec & Ozimec, 2001). Romania: (Rakosy, 2003-2004. Serbia: (Remy, 1953; Jakšić, 2005). Bulgaria: (Beron, 1994, 2016; Beshkov & Langourov, 2004, 2011; Beshkov & Petrov, 1996; Kostova et al., 2016; Zagulajev, 2000). Ecological status (ES): Tp – troglophile, Tx – trogloxene, Stp – subtroglophile.

Nbr.	ID	Family and species	Croatia	Romania	Serbia	Bulgaria	ES
		Fam. **TINEIDAE**					
1	475	*Haplotinea ditella* (Pierce & Diakonoff, 1938)		●			
2	623	*Nemapogon granella* (Linnaeus, 1758)		●			Tx, Tp
3	624	*Nemapogon cloacella* (Haworth, 1828)		●			Tp
4	481	*Cephimallota angusticostella* (Zeller, 1839)		●			Tp
5	568	*Infurcitinea olympica* (G. Petersen, 1958)		●			Tp
6	576	*Lichenotinea pustulatella* (Zeller, 1852)		●			Tp
7	579	*Ischnoscia borreonella* (Millière, 1874)		●			Tp
8	657	*Fermocelina liguriella* (Millière, 1879)		●			Tp
9	661	*Trichophaga tapetzella* (Linnaeus, 1758)		●			Tp
10	682	*Tinea nonimella* (Zagulajev, 1955)		●			Tp
11	700	*Monopis laevigella* (D. & S., 1775)		●		●	Tp
12	704	*Monopis obviella* (D. & S., 1775)	●	●		●	Tp
13	705	*Monopis crocicapitella* (Clemens, 1859)		●			Tp
14	707	*Monopis imella* (Hübner, 1813)		●			Tp
15	709	*Monopis christophi* (G. Petersen, 1957)		●			Tp
16	710	*Monopis pallidella* (Zagulajev, 1955)		●			Tp
17	711	*Monopis fenestratella* (Heyden, 1863)		●			Tp
		Fam. **ACROLEPIIDAE**					
18	1534	*Rhigognostis wolfschlaegeri* (Rebel, 1940)				●	Tx
19	1556	*Digitivalva pulicariae* (Klimesch, 1956)		●		●	Stp, Tx
20	1562	*Digitivalva granitella* (Treitschke, 1833)		●		●	Tp
		Fam. **DEPRESSARIIDAE**					
21	1714	*Agonopterzx atomella* (D. & S., 1775)	●				
22	1719	*Agonopterix arenella* (D. & S., 1775)		●			Tx
23	1738	*Agonopterix banatica* (Georgesco, 1965)		●			Tx
		Fam. **ALUCITIDAE**					
24	5322	*Alucita cymatodactyla* (Zeller, 1852)				●	Stp
25	5323	*Alucita hexadactyla* (Linnaeus, 1758)		●		●	Tx
26	5325	*Alucita huebneri* (Wallengren, 1859)		●		●	Tx
27	5327	*Alucita grammodactyla* (Zeller, 1841)		●			Tx
28	5329	*Alucita desmodactyla* (Zeller, 1847)		●			Tx
29	–	*Alucita bulgaria* (Zagulajev, 2000)				●	Tx
		Fam. **PYRALIDAE**					
30	5627	*Pyralis farinalis* (Linnaeus, 1758)		●			Tx
31	5632	*Aglossa caprealis* (Hübner, 1809)		●			Tx
32	5633	*Aglossa pinguinalis* (Linnaeus, 1758)		●			Tx
		Fam. **CRAMBIDAE**					
33	6607	*Pyrausta falcatalis* (Guenée, 1854)		●			Tx
		Fam. **SATURNIIDAE**					
34	6795	*Saturnia spini* (D. & S., 1775)				●	Tx
		Fam. **SPHINGIDAE**					
35	6843	*Macroglossum stellatarum* (Linnaeus, 1758)		●		●	Tx

		Fam. **GEOMETRIDAE**					
36	7847	*Gnophos furvata* (D. & S., 1775)		●			Tx
37	7852	*Odontognophos dumetata* (Treitschke, 1827)		●			Tx
38	8028	*Timandra comae* (A. Schmidt, 1931)				●	Tx
39	8256	*Xanthorhoe fluctuata* (Linnaeus, 1758)				●	Tx
40	8258	*Xanthorhoe axybiata* (Millière, 1872)				●	Tx
41	8289	*Camptogramma bilineata* (Linnaeus, 1758)		●			Tx
42	8319	*Cosmorhoe ocellata* (Linnaeus, 1758)				●	Tx
43	8325	*Nebula nebulata* (Treitschke, 1825)				●	Tx
44	8391	*Hydriomena furcata* (Thunberg, 1784)		●			Tx
45	8411	*Melanthia procellata* (D. & S., 1775)		●			Tx
46	8421	*Rheumaptera cervinalis* (Scopoli, 1763)		●			Tx
47	8427	*Triphosa sabaudiata* (Duponchel, 1830)	●	●	●	●	Tx
48	8428	*Triphosa dubitata* (Linnaeus, 1758)	●	●	●	●	Tx
49	8457	*Perizoma hydrata* (Treitschke, 1829)		●			Tx
50	8458	*Perizoma lugdunaria* (Herrich-Schäffer, 1855)		●			Tx
51	8496	*Eupithecia undata* (Freyer, 1840)				●	Tx
52	8681	*Acasis viretata* (Hübner, 1799)		●			Tx
		Fam. **NOCTUIDAE**					
53	8877	*Catocala elocata* (Esper, 1787)				●	Tx
54	8940	*Apopestes spectrum* (Esper, 1787)	●	●		●	Tx
55	8944	*Autophila dilucida* (Hübner, 1808)		●		●	Tx
56	8945	*Autophila limbata* (Staudinger, 1871)				●	Tx
57	8948	*Autophila ligaminosa* (Eversmann, 1851)				●	Tx
58	8984	*Scoliopteryx libatrix* (Linnaeus, 1758)	●	●	●	●	Tx
59	8995	*Hypena rostralis* (Linnaeus, 1758)		●		●	Tx
60	8996	*Hypena obesalis* Treitschke, 1829	●	●		●	Tx
61	8997	*Hypena obsitalis* (Hübner, 1813)	●				
62	8998	*Hypena palpalis* (Hübner, 1796)	●			●	Tx, Stp
63	9305	*Pyrois effusa* (Boisduval, 1828)	●			●	Tx
64	9490	*Mormo maura* (Linnaeus, 1758)	●	●		●	Tx
65	9638	*Dasypolia templi* (Thunberg, 1792)				●	Tx
66	10096	*Noctua pronuba* (Linnaeus, 1758)		●			Tx
67	10139	*Rhyacia simulans* (Hufnagel, 1766)				●	Tx
68	10163	*Spaelotis ravida* (D. & S., 1775)		●			Tx
69	10218	*Eugraphe sigma* (D. & S., 1775)		●			Tx
		Fam. **NYMPHALIDAE**					
70	7247	*Inachis io* (Linnaeus, 1758)		●	●	●	Tx
71	7250	*Aglais urticae* (Linnaeus, 1758)		●		●	Tx
72	7258	*Nymphalis polychloros* (Linnaeus, 1758)		●		●	Tx
73	7312	*Lasiommata maera* (Linnaeus, 1758)		●	●		Tx

CONCLUSION

Based on the literature, the cavernicolous habitats and ecological niches in which the studied species are found were determined.

Results show that 73 species of Lepidoptera, representing 10 families, were found in speleological habitats in the countries analyzed. The 73 identified species make up 80% of the 90 known species found in caves worldwide Turquin (1994), reflecting the richness of the fauna. Fifty-four species of Lepidoptera were identified in Romania, 35 in Bulgaria, 12 in Croatia and 5 in Serbia. The caves in eastern Serbia are found in the central part of the Carpatho-Balkan system. It is therefore realistic to deduce their faunistic potential to be around 50 species. The given quantitative data points out the inadequate level of research into Lepidoptera in the caves of Serbia.

The most abundant species are from the families of Tineidae and Noctuidae, with 17 species each. Analysis showed that the number of identified species depends on the targeted research of specialized lepidopterists. Beron (1994), who is not a lepidopterist, recorded only 16 species in the caves of Bulgaria. It was only the targeted research of experienced lepidopterists (Beshkov & Petrov, 1996) that doubled this number. In Romania, there is a rich biospeleological tradition from the period of Emil Racoviță (E. Rakovitza, 1868-1947) and there are several lepidopterists, so that the number of identified species is greater. The number of species in Serbia and Croatia is small because no

one has taken an interest in cavernicolous Lepidoptera. Just how neglected the faunistic study of this group is in Serbia is clear when compared to the cavernicolous systems in Luxembourg where 18 species of Lepidoptera have been identified (Werno et al., 2013).

The ecological presence of Lepidoptera in caves is determined by habitat and ecological niche. According to the degree of dependence of the identified Lepidoptera species on cavernicolous habitats, three groups of Lepidoptera are singled out: troglophiles (Tp), trogloxenes (Tx) and subtroglophiles (Stp) (Table 1). Interesting to this analysis are the troglophiles, organisms that are adapted to conditions of cave life but which are not exclusive to caves. The results show that there are 17 of this type of species. With the exception of the species *Digitivalva granitella* (Treitschke, 1833), the others belong to the Tineidae family. Robinson (1980), conducted a more detailed study of them as cave-dwelling Lepidoptera. Three of the mentioned species are also found in caves in Romania and Bulgaria, and they are most probably present in caves in Serbia. The number of these species is probably higher because in Serbia and Bulgaria there are no lepidopterists specializing in representatives of the Tineidae family. In Romania, this group of moth fauna is well-researched and there is a book of national fauna dedicated to it (Cãpuşe, 1968). Six of the 17 mentioned species, *N. granella, N. cloacella, C. angusticostella, M. laevigella, M. obviella* and *M. imella*, are present in Serbian fauna, but are only found outside caves (Jakšić, 2016).

The ecological niches of all 73 identified Lepidoptera species can be divided into two groups: species that occupy the niche at the entrance of caves ("the Twilight Zone"), where temperature and humidity are variable and conditioned by the outside environment, and these are mostly trogloxene species. They are found here during winter hibernation, summer estivation, or by chance, in the search for temporary shelter. Here can also be found species that feed on fungi and lichens (fungivore or mycophagous), as well as those that feed on hair and feathers (keratinophilic), such as *Monopis obviella* (Denis & Schiffermüller, 1775) and *Monopis crocicapitella* (Clemens, 1859).

Many bird species in Serbia, such as *Neophron percnopterus, Gypaetus barbatus, Columba livia, Bubo bubo, Hirundo daurica, Pyrrhocorax graculus*, etc. (Rašajski, 2000) build their nests at the entrances of caves. It is worth mentioning the moth species *Galleria mellonella* (Linnaeus, 1758), whose caterpillars live in the nests of wasps, bees and bumblebees (often built at cave entrances) and feed on wax. Unlike them, the second group - troglophile species occupy the interior of caves, without light and with a relatively constant temperature and humidity. They are mostly found on the guano of cave-dwelling bats or carcasses of animals that enter the caves before dying.

The data indicate that the greatest faunistic potential in Serbian caves is that of troglophile species of Lepidoptera, primarily representatives of the Tineidae family. The larvae of Tineidae species feed on fungi, lichens (fungivores), hair, bird feathers, nails, claws, etc. (keratophiles) and the body parts of dead animals and feces (detritivores or saprovores). The fossils of many groups of vertebrates found in Balkan caves confirm the long existence of these systems, i.e. the long-term adaptation of species from the Tineidae family to the specific habitat conditions. Many species brought their prey into the caves; others died in them. Such organic mass is an ideal ecological niche for the larvae of Tineidae.

Table 2. Sites of bats in Serbian caves: +++ − large colonies with over 1000 individuals; ++ − middle sized colonies with several hundred individuals; + − small colonies with 50-100 individuals. Type of habitat according to the IUCN classification scheme: 1.4.2 – deciduous broadleaved forests; 3.5.3 – warm and temperate grasses and shrubs; 5.1 – perennial rivers, brooks, streams (including waterfalls) (according to (Paunović, 2016) and simplified)

Sites	Bor, Zlot village **Lazar's Cave**	Bor, Zlot village **Vernjikica Cave**	Ražanj, Skorica village, **Pečurski kamen Cave**	Radavac village, **Radavac Cave**	Valjevo, Degurić village, **DegurićCave**	Valjevo, Brežđe village, **Šalitrena Cave**	Valjevo, Petnica village, **Petnica Cave**	Valjevo, Jovanja village, **Čebić Cave**	Ćuprija, Senje village**Ravanička Cave**
m a.s.l.	308	450	430	631	240	285	209	330	235
UTM	EP77	EP77	EP54	DN43	DP19	DP29	DP19	DQ00	EP36
Type of habitat around the cave	3.5.3	3.5.3	1.4.2	1.4.2	5.1	5.1	1.4.2	3.5.3	3.5.3
Colony size	+++	+++	+++	+++	+++	+++	++	++	++
Number of bat Species	13	10	7	5	5	4	14	11	8

Representatives of the Tineidae family that are detritivores prefer the guano of bats (Mammalia: Chiroptera). Ulrich et al. (2007), analyzed the correlation of the faunistic abundance of bats in 58 European countries with the size of territory, altitude, temperature conditions (the number of days in a year with temperatures < 0^0 C), richness of vascular flora and distance from Turkey. Optimal conditions are in the geographical latitude of 46^o N, where Croatia has 34 bat species, and Serbia 30 (Paunović, 2016). Luxembourg has 18 species of bat and the same number of cave-dwelling Lepidoptera species, indicating the possibility that Serbia could have 50 species of cave-dwelling Lepidoptera. Altitude is also an important factor for the distribution of bats; the majority prefers altitudes up to 600 m, as has been established for bats in Serbia (Paunović, 2016). The richness of vascular flora has no effect on the number of bat species. The presented data suggest that the presence of bats is the key factor as to which speleological structures in Serbia should be researched in the search for troglophilic species of Lepidoptera. It is fortunate that Paunović (2016) provided data that are important to this study. The author points out that the most important habitats for bats in Serbia are caves, and he provides information about the character of these habitats (Table 2). To summarize, we can conclude that despite the diversity of cavernicolous habitats on the Balkan Peninsula and in Serbia, there has not been enough research into Lepidoptera fauna. The reason for this is the appeal of other groups, particularly with respect to faunistic richness and endemism, which have attracted the attention of researchers away from Lepidoptera. Additionally, there is the traditional belief that there are no Lepidoptera in caves, that their presence is occasional and fortuitous, that they are not really cave organisms. This belief was dismissed by Robinson (1980) who, in the case of species from the Tineidae family, pointed out that 11 of the 20 identified species permanently exist in cave populations and have not been found outside, and that their larvae feed on guano (guanophiles). The presented data show that the study of the cavernicolous fauna of Lepidoptera in Serbia is both justified and necessary.

REFERENCES

Anonymous, 2007. EUNIS habitat classification. 2007 (Revised descriptions 2012). Retrieved from http://www.eea.europa.eu/themes/biodiversity/eunis/eunis-habitat-classification/habitats/eunis-habitats-complete-with-descriptions.xls

Beron, P. 1994. Résultats des recherches biospéléologiques en Bulgarie de 1971 à 1994 et liste des animaux cavernicoles Bulgares.Sofia: Editions de la Féderation bulgare de Spéléologie., pp. 1-137.

Beron, P. 2016. Terrestrial cave invertebrates of the Vrachanska Planina Mountains. – In: Bechev, D. & Georgiev, D. (Eds.): Faunistic diversity of Vrachansky Balkan Nature Park. ZooNotes, 3, pp. 185-230. Suppl. Plovdiv..

Beshkov, S., & Petrov, B. 1996. A catalogue of the Bulgarian Lepidoptera species reported and collected from the caves and galleries in Bulgaria (Insecta Lepidoptera). Atalanta Würzburg, 27(1/2), pp. 433-448.

Jeannel, R., & Stanković, S. 1924. Prilog poznavanju pećinske faune i pećina u Srbiji. Glas Srpske kraljevske akademije, Beograd, 113(50), pp. 97-105.

Jakšić, P. 2005. Staništa i ekološke niše u speleološkim objektima istočne Srbije prema savremenim klasifikacionim sistemima (CORINE, EUNIS). . In: Drugi naučni skup o geonasleđu Srbije, 2004-06-22, Beograd. , pp. 189-196

Jakšić, P. 2016. Tentative Check List of Serbian Microlepidoptera. Ecologica Montenegrina Podgorica, 7, pp. 33-258.

Jeannel, R., & Racovitza, E.G. 1929. Énumération des grottes visitées 1918-1927 (septieme serie). Archives de zoologie expérimentale et génèrale Paris, 68, pp. 293-608. II.

Jovanović, Đ. 1891. Sićevačka klisura, pećine, dupke i potkapine. Otadžbina, Beograd, 29, pp. 401-419.

Karsholt, O., & Razowski, J. 1996. The Lepidoptera of Europe. A Distributional Checklist.Stenstrup: Apollo Books., pp. 1-380.

Kučinić, M. 2002. Lepidoptera and Trichoptera. In: Gottstein-Matočec, S. (ed.) An overview of the cave and interstitial biota of Croatia. Natura croatica, Zagreb, 11(1), pp. 1-112. (Suppl.).

Paunović, M. 2016. Rasprostranjenje, ekologija i centri diverziteta slepih miševa (Mammalia: Chiroptera) u Srbiji.Univerzitet u Beogradu - Biološki fakultet., pp. 1-474. Doktorska disertacija I-IX +.

Pretner, E. 1963. Biospeleološka istraživanja u Srbiji. Poročila Acta Carsologica, Ljubljana, 3, pp. 139-147.

Rašajski, J. 2000. Ptice Srbije (Birds of Serbia).Novi Sad: Prometej.

Remy, P. 1953. Description des grottes Yougoslaves. Bulletin du museum d'histoire naturelle du Pays Serbe, Beograd, 5-6, pp. 175-233.

Robinson, G. 1980. Cave dwelling tineid moths: A taxonomic review of the World species (Lepidoptera: Tineidae). Trans. British Cave Research Assoc, 7(2), pp. 83-120.

Turquin, M.J. 1994. Lepidoptera. Encyclopedia Biospeleologica. In: C. Juberthie& V. Decu Eds., . Moulis - Bucarest: Société Biospéologie., pp. 333-339 I.

Cãpuşe, I. 1968. Fauna Republicii Socialiste Romãnia. Insecta Volumul XI, Fascicula 9. Fam. Tineidae.Bucuresti: Editura Academiei RS Romãnia.

Ćurčić, B.P.M., Dimitrijević, R.N., Makarov, S.E., Lučić, L.R., Karamata, O.S., & Tomić, V.T. 1997. The Zlot Cave: A unique faunal refuge (Serbia, Yugoslavia). Arch. Biol. Sci. Belgrade, 49(3-4), pp. 29-30.

Ulrich, W., Sachanowicz, K., & Michalak, M. 2007. Environmental correlations of species richness of European bats (Mammalia: Chiroptera). Acta chiropterologica, 9(2), pp. 347-360.

Werno, A., Weber, D., & Meyer, M. 2013. Schmetterlinge (Insecta, Lepidoptera) aus Höhlen des Großherzogtums Luxemburg. In: Weber, D. (ed.): Die Höhlenfauna Luxemburgs. Ferrantia, 69, pp. 388-394.

UNIVERSITY THOUGHT
Publication in Natural Sciences, Vol. 7, No. 1, 2017, pp. 13-16.
doi:10.5937/univtho7-13688
Original Scientific Paper

SYNTHESIS AND SPECTROSCOPIC CHARACTERIZATION OF LITHIUM SALTS OF COPPER(II) AND NICKEL(II) COMPLEXES WITH 1,3-PROPANEDIAMINE-*N,N,N',N'*-TETRAACETATE

NENAD S. DRAŠKOVIĆ[1*], DEJAN M. GUREŠIĆ[2]

[1]Faculty of Agriculture, University of Priština, Lešak, Serbia
[2]Faculty of Tehnological Sciences, University of Priština, Kosovska Mitrovica, Serbia.

ABSTRACT

The complexes $Li_2[Ni(1,3\text{-pdta})]\cdot 5H_2O$ and $Li_2[Cu(1,3\text{-pdta})]\cdot 5H_2O$ (where 1,3-pdta represents the 1,3-propanediaminetetraacetate anion) have been synthesized and characterized by applying IR and UV-vis spectroscopy. The obtained spectroscopic results of these complexes are discussed in relation to those for $Mg[M(1,3\text{-pdta})].8H_2O$ complexes (M = Ni(II) and Cu(II)) of known crystal structure.

Keywords. Nickel(II) complexes, Copper(II) complexes, 1,3-pdta, IR spectroscopy, UV-vis spectrophotometry.

INTRODUCTION

The hexadentate 1,3-pdta ligand (1,3-pdta = 1,3-propanediamine-N,N,N',N'-tetraacetate anion) has been used for preparation of complexes with many transition metal ions (Herak et al., 1984; Rychlewska et al., 2000; Radanović et al., 2001; Radanović et al., 2003; Radanović et al., 2004; Rychlewska et al., 2005; Rychlewska et al., 2007; Rychlewska et al., 2011). In relation to edta (edta = ethylenediamine-N,N,N',N'-tetraacetate), the 1,3-pdta ligand has longer diamine chain and is expected to coordinate hexadentatedly to metal ions of various size.

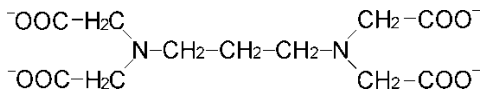

1,3-pdta

The structural 1,3-pdta characteristics of the numerous hexadentate complexes of the type $M[M'(1,3\text{-pdta})]\cdot 8H_2O$ (M = Mg(II), Co(II), Zn(II), Sr(II); M' = Cu(II), Ni(II), Co(II), Mg(II), Zn(II) and Sr(II)) have been determined by single-crystal X-ray diffraction analysis (Rychlewska et al., 2000; Radanović et al., 2001; Radanović et al., 2003; Radanović et al., 2004; Rychlewska et al., 2005; Rychlewska et al., 2011). Previous attempts to isolate 1,3-pdta-M(II) complexes with monovalent cations as counter ion did not give the expected results. Recently, in our laboratory by ion exchange column chromatography, $Li_2[Co(1,3\text{-pdta})]\cdot 5H_2O$ complex was isolated (Rychlewska et al., 2008). This complex constitutes the first example of $[M(1,3\text{-pdta})]^{2-}$ complex with a monovalent cation as counter ion (Rychlewska et al., 2008). The structure of this complex consists of two tetrahedrally coordinated Li^+ cations, an octahedral $[Co(1,3\text{-pdta})]^{2-}$ anion and five water molecules, two of which are crystalline water molecules. As a continuation of our research, in the present paper, we report synthesis and spectroscopic characterization of two new Cu(II) and Ni(II) complexes with general formula $Li_2[M(1,3\text{-pdta})]\cdot 5H_2O$.

EXPERIMENTAL

Materials and methods

All commercially obtained reagent-grade chemicals were used without further purification. The preparation of $Ba_2(1,3\text{-pdta})\cdot 2H_2O$ has been reported elsewhere (Radanovic et al., 2000). The IR spectra were recorded on a Perkin-Elmer Spectrum One FT-IR spectrometer using the KBr pellet technique. The UV-vis spectra of Ni(II) and Cu(II) complexes were recorded on a Perkin-Elmer spectrophotometer. The following concentrations of aqua solutions have been used for these measurements: 10^{-2} M for Ni(II) and 10^{-3} M for Cu(II) complexes. Elemental microanalysis for carbon, hydrogen and nitrogen were performed by the Microanalytical Laboratory, Department of Chemistry, Faculty of Science, University of Belgrade.

*Synthesis of $Li_2[Ni(1,3\text{-pdta})]\cdot 5H_2O$ (**1**) and $Li_2[Cu(1,3\text{-pdta})]\cdot 5H_2O$ (**2**) complexes*

0.01 mol of $CuSO_4\cdot 5H_2O$ (2.50 g) or $NiSO_4\cdot 7H_2O$ (2.83 g) in 60 ml of H_2O was stirred at 80 °C for 10 min. To this solution, solid $Ba_2(1,3\text{-pdta})\cdot 2H_2O$ (6.13 g, 0.01 mol) was added and the obtained solution (pH = 7) was stirred at 80 °C for 3 h. The precipitated $BaSO_4$ was filtered off and to the obtained filtrate, the solid $MgSO_4\cdot 6H_2O$ (2.28 g; 0.01 mol) was added and stirring with heating at 60 °C was continued for the next 20 min. The precipitated $BaSO_4$ was again filtered off. To the obtained filtrate, 5–6 ml of ethanol was added and the solution was left to stand in a refrigerator for several days. The crystals of $Mg[Cu(1,3\text{-pdta})]\cdot 8H_2O$ (3.34 g, 66%) and $Mg[Ni(1,3\text{-pdta})]\cdot 8H_2O$ (3.38 g, 63%) were collected, washed with ethanol, then ether and air-dried.

* Corresponding author: nenad.draskovic@pr.ac.rs

Anal. Calc. for Mg[Cu(1,3-pdta)]·8H_2O, $MgCuC_{11}H_{30}N_2O_{16}$ (FW = 534.21): C, 24.73; H, 5.66; N, 5.24%. Found: C, 24.84; H, 4.84; N, 5.04%.

Anal.Calc. for Mg[Ni(1,3pdta)]·8H_2O, $MgNiC_{11}H_{30}N_2O_{16}$ (FW = 529.36): C, 24.96; H, 5.71; N, 5.29%. Found: C, 24.90; H, 5.82; N, 5.32%.

The aqueous solutions of Mg[Ni(1,3pdta)]·8H_2O (Radanović et al., 2001) and Mg[Cu(1,3-pdta)]·8H_2O (Radanović et al., 2000) were passed through a column packed with Merck I cation exchanger in the Li^+ form. The eluates were evaporated at room temperature to a volume of 2 ml and Li_2[Ni(1,3-pdta)]·5H_2O **(1)** and Li_2[Cu(1,3-pdta)]·5H_2O **(2)** complexes were crystallized after addition of ethanol and cooling in a refrigerator for 2 days. The crystals were removed by filtration and air-dried.

Anal. Calc. for Li_2[Ni(1,3-pdta)]·5H_2O **(1)**, $Li_2NiC_{11}H_{24}N_2O_{13}$**(**FW = 464.89): C, 28.42; H, 5.20; N, 6.03. Found: C, 28.27; H, 5.22; N 6.05%.

Anal. Calc. for Li_2[Cu(1,3-pdta)]·5H_2O **(2)**, $Li_2CuC_{11}H_{24}N_2O_{13}$ (FW = 469.74): C, 28.13; H, 5.15; N, 5.96. Found: C, 27.93; H, 5.16; N, 5.96%.

RESULTS AND DISCUSSION

In this work two Li_2[M(1,3-pdta)]·5H_2O complexes (M = Ni(II), **1** and Cu(II), **2**) were synthesized and characterized by IR and UV-vis spectroscopy. The schematic presentation of the procedure for synthesis of **1** and **2** is presented in Figure 1. The spectroscopic results of these complexes are discussed in relation to those for Mg[Ni(1,3pdta)]·8H_2O and Mg[Cu(1,3-pdta)]·8H_2O complexes of known crystal structure (Radanović et al., 2001; Rychlewska et al., 2000).

*Comparative analysis of the spectroscopic data for **1** and **2** with those for Mg[Ni(1,3-pdta)]•8H_2O and Mg[Cu(1,3-pdta)]•8H_2O complexes of known crystal structure IR spectra*

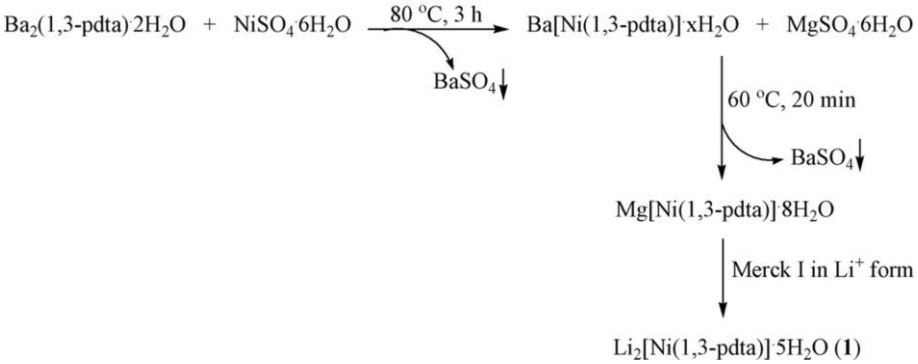

Figure 1. Schematic presentation of the procedure for the preparation of Li_2[Ni(1,3-pdta)]·5H_2O (**1**). The same method is used for the synthesis of Li_2[Cu(1,3-pdta)]·5H_2O (**2**).

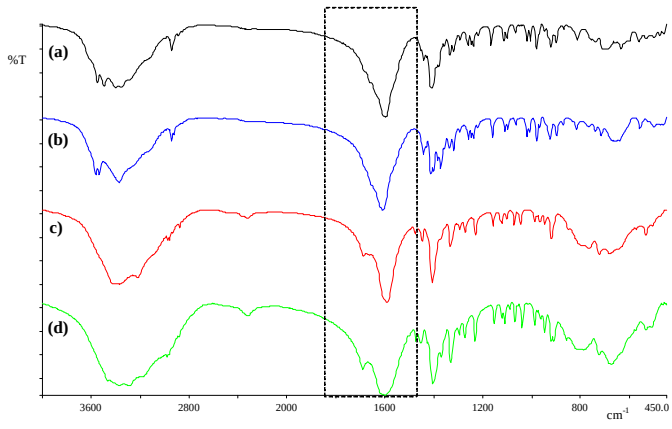

Figure 2. IR spectra of Ni(II) and Cu(II) complexes with hexadentate coordinated 1,3-pdta ligand: (a) Li_2[Ni(1,3-pdta)]·5H_2O **(1)**, (b) Li_2[Cu(1,3-pdta)]·5H_2O **(2)**, (c) Mg[Ni(1,3-pdta)]·8H_2O and (d) Mg[Cu(1,3-pdta)]·8H_2O.

The IR spectra of **1** and **2** are given in Figure 2. These spectra have been compared with the corresponding for Mg[Ni(1,3-pdta)]·8H_2O and Mg[Cu(1,3-pdta)]·8H_2O complexes having the same hexadentate coordinated 1,3-pdta ligand and Mg^{2+} ion as counter cation. The crystal structures of the latter two complexes have been previously determined by single crystal X-ray diffraction analysis (Radanović et al., 2001; Rychlewska et al., 2000). The IR data of these complexes, in the region for the asymmetric carboxylate stretching frequencies, are presented in Table 1. The interpretation of these spectra was done in accordance to the previously established rule that the protonated and uncoordinated asymmetric carboxylate stretching frequencies occur at 1750 – 1700 cm^{-1}, whereas these frequencies for the ionized and coordinated carboxylate groups are at 1650 – 1590 cm^{-1} (Nakamoto, 1963). As it was shown in Figure 2 and Table 1, complexes **1** and **2** in the region for the asymmetric carboxylate stretching frequencies have only one very strong and symmetric band at 1598 and 1610 cm^{-1}, respectively. This is in accordance to the fact that carboxylate groups of 1,3-pdta ligand in these two complexes are coordinated to the corresponding metal ion. Moreover, symmetric shape of these bands indicates that all glycinate rings in these complexes are equivalent. The IR spectra of **1** and **2** are very similar to those for Mg[Ni(1,3-pdta)]·8H_2O and Mg[Cu(1,3-pdta)]·8H_2O complexes. The latter two complexes in the carboxylate region

for coordinated glycinates showed very strong and broad band at 1590 and at 1599 cm^{-1} for Ni(II) and Cu(II) complexes, respectively (Table 1). Additionally, from Table 1 it can be seen that these two bands are slightly shifted to the higher energy in respect to those for complexes **1** and **2**. Moreover, the carboxylate stretching band for Mg[Ni(1,3-pdta)]·$8H_2O$ and Mg[Cu(1,3-pdta)]·$8H_2O$ complexes showed evidence for splitting on the higher energy side resulting in appearance of small band at 1688 for Ni(II) and 1692 cm^{-1} for Cu(II) complex.

Table 1. IR asymmetric carboxylate stretching frequencies of Ni(II) and Cu(II) complexes with 1,3-pdta ligand

Complex	**ν_{asym} (cm^{-1})**
Li_2[Ni(1,3-pdta)]·$5H_2O$ **(1)**	1598
Li_2[Cu(1,3-pdta)]·$5H_2O$ **(2)**	1610
Mg[Ni(1,3-pdta)]·$8H_2O$	1590; 1688(sh)
Mg[Cu(1,3-pdta)]·$8H_2O$	1599; 1691(sh)

UV-vis spectra

Difference in the position and shape of the asymmetric carboxylate stretching frequencies for **1** and **2** in respect to those for Mg[Ni(1,3-pdta)]·$8H_2O$ and Mg[Cu(1,3-pdta)]·$8H_2O$ can be attributed to the presence of different counter cation in these two pairs of 1,3-pdta complexes. The presence of different cation in these complexes can result in their different packing in the crystal lattice as well as in different interactions between coordinated water molecules of Li^+ and Mg^{2+} counter cation and carboxylate group of $[M(1,3\text{-pdta})]^{2-}$ complex anion (M = Ni(II) and Cu(II)).

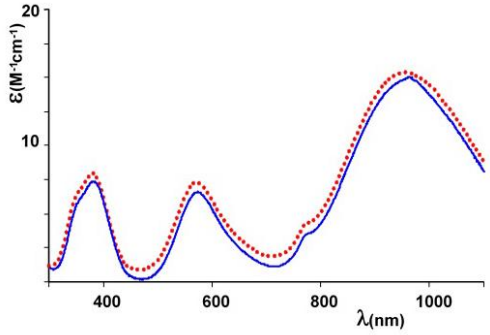

Figure 3. UV-vis spectra of **1** (···) and Mg[Ni(1,3-pdta)]·$8H_2O$ (Radanović et al., 2001).

The UV-vis spectra of **1** and Mg[Ni(1,3pdta)]·$8H_2O$ complexes and their numerical data are presented in Figure 3. and Table 2. The UV-vis spectrum of Mg[Ni(1,3-pdta)]·$8H_2O$ has been previously discussed in detail (Radanović et al., 2001), and here it has only been repeated for the sake of comparison with the spectrum of **1**. In general, it has been shown that the spectra of Ni(II)-1,3-pdta-type complexes containing the six-membered diamine ring (**T** ring), with respect to Ni(II)-edta-type complexes with five-membered diamine ring (**E** ring), exhibit broadening of the first absorption band(D_{4h} model) (Radanović et al., 2001).

In accordance to previously established results for the Ni(II)-edta-type and most other Ni(II) complexes, the interpretation of the UV-vis spectra of **1** and Mg[Ni(1,3-pdta)]·$8H_2O$ (Radanović et al., 2001) has been done by using an octahedral model (O_h): $^3A_{2g}\rightarrow{}^3T_{2g}$ (*F*) (band I); $^3A_{2g}\rightarrow{}^3T_{1g}$ (*F*) (band III) and $^3A_{2g}\rightarrow{}^3T_{1g}$ (*P*) (band IV) (Table 2). From Figure 3 it can be seen that UV-vis spectra of **1** and Mg[Ni(1,3-pdta)]·$8H_2O$ (Radanović et al., 2001) are almost identical in the shape and intensities of absorption maxima. This undoubtedly leads to the conclusion that anionic part of these two molecules are the same and represents octahedral complex containing hexadentate coordinated 1,3-pdta ligand. As it was abovementioned, the influence of counter cation on the shape and position of the carboxylate stretching frequencies was observed after measuring IR spectra of these complexes in the solid state. However, no influence of Li^+ and Mg^{2+} counter cation was observed on the shape and position of absorption maxima in the UV-vis spectra of these complexes measured in water solvent.

UV-vis spectra of **2** and Mg[Cu(1,3-pdta)]·$8H_2O$ (Rychlewska et al., 2000) and corresponding numerical data are given in Figure 4 and Table 2. The UV-vis spectrum of Mg[Cu(1,3-pdta)]·$8H_2O$ complex has been previously reported (Rychlewska et al., 2000) and, in the present work, it has been repeated for comparison with the spectrum of **2**. As it can be seen from Figure 4, complexes **2** and Mg[Cu(1,3-pdta)]·$8H_2O$ have one unsymmetrical absorption band in the expected region, what is in accordance to the fact that these complexes have the same N_2O_4 donor system and C_2 molecular symmetry.

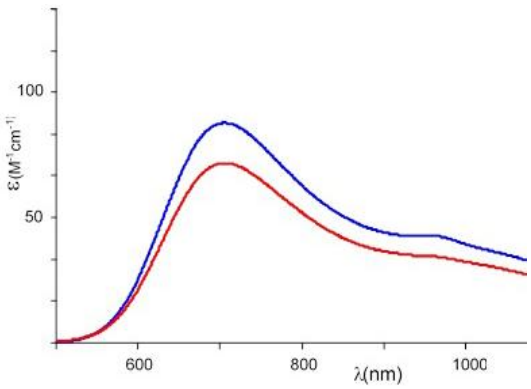

Figure 4. UV-vis spectra of **2** and Mg[Cu(1,3-pdta)]·$8H_2O$ (Rychlewska et al., 2000).

This band can be assigned to the d_z^2, d_{xy}, d_{xz}, $d_{yx}\rightarrow d_{x^2-y^2}$ transitions with a $d_{x^2-y^2}$ ground state. The UV-vis spectra of **2** and Mg[Cu(1,3-pdta)]·$8H_2O$ complexes are identical in the position of the absorption maxima. However, there is small difference in the intensity of these absorption bands resulted in

the presence of different counter cation and number of water molecules in these two complexes.

Table 2. UV-vis numerical data of **1** and **2** in comparison to those for $Mg[Ni(1,3\text{-pdta})]\cdot 8H_2O$ (Radanović et al., 2001) and $Mg[Cu(1,3\text{-pdta})]\cdot 8H_2O$ (Rychlewska et al., 2000) complexes with hexadentate 1,3-pdta ligand

Complex	Absorption			Assignments
		λ (nm)	ε ($M^{-1}cm^{-1}$)	O_h
$Mg[Ni(1,3\text{-pdta})]\cdot 8H_2O$	I	959.9	15.4	$^3A_{2g}\rightarrow{}^3T_{2g}(F)$
	II	770.3	3.9	$\rightarrow{}^1E_g(D)$
	III	571.5	7.3	$\rightarrow{}^3T_{1g}(F)$
	IV	379.7 (sh)	7.9	$\rightarrow{}^3T_{1g}(P)$
$Li_2[Ni(1,3\text{-pdta})]\cdot 5H_2O$ (**1**)	I	962.1	15.8	
	II	775.6	4.1	
	III	573.2	7.3	
	IV	380.9	8.2	
$Mg[Cu(1,3\text{-pdta})]\cdot 8H_2O$		706.0	85.0	
$Li_2[Cu(1,3\text{-pdta})]\cdot 5H_2O$ **(2)**		705.1	86.0	

CONCLUSION

In this paper, the new method for preparation of $[Ni(1,3\text{-pdta})]^{2-}$ (**1**) and $[Cu(1,3\text{-pdta})]^{2-}$ (**2**) complexes with Li^+ counter cation has been presented. The hexadentate coordination of 1,3-pdta ligand in these complexes was confirmed by comparison of their IR and UV-vis spectra with those for $Mg[Ni(1,3\text{-pdta})]\bullet 8H_2O$ and $Mg[Cu(1,3\text{-pdta})]\bullet 8H_2O$ complexes of known crystal structure (Radanović et al., 2001; Rychlewska et al., 2000). The IR spectra of **1** and **2** are slightly different from those for $Mg[Ni(1,3\text{-pdta})]\bullet 8H_2O$ and $Mg[Cu(1,3\text{-pdta})]\bullet 8H_2O$ complexes, what can be attributed to the presence of different counter cation in these two pairs of 1,3-pdta complexes. On the other hand, no difference in the UV-vis spectra of these complexes was observed.

ACKNOWLEGMENTS

This work was funded in part by the Ministry of Education, Science and Technological Development of the Republic of Serbia (Project No. 172036).

REFERENCES

Nakamoto, K. 1963. Infrared Spectra of Inorganic and Coordination Compounds. New York, N. Y.: John Wiley & Sons, Inc..

Herak, R., Srdanov, G., Djuran, M.I., Radanović, D.J., & Bruvo, M. 1984. Crystal structures of $Na[M(1,3\text{-pdta})]\cdot 3H_2O$ (M = Cr, Rh;1,3-pdta = 1,3-propanediaminetetraacetate), and the absolute configuration of the (-)D-Isomer of the Rh complex. Inorg. Chim. Acta, 83, pp. 55-64.

Radanović, D.J., Ama, T., Kawaguchi, H., Drašković, N.S., Ristanović, D., & Janićijević, S. 2001. Synthesis and X-Ray Structural Study of Magnesium (1,3-propanediaminetetraacetato)nickelate(II) Octahydrate, $Mg[Ni(1,3\text{-pdta})]\cdot 8H_2O$. Structural Parameters and Strain Analysis of $[M(1,3\text{-pdta})]_n$: Complexes in Relation to Their Octahedral Distortion. Bull. Chem. Soc. Jpn., 74, pp. 701-706.

Radanović, D.D., Rychlewska, U., Djuran, M.I., Drašković, N.S., Vasojević, M., Hodžić, I., & Radanović, D.J. 2003. Simple synthetic method and structural characteristics of (1,3-propanediaminetetraacetato)cobalt(II) complexes: Uniform crystal packing in a series of metal(II) complexes with 1,3-propanediaminetetraacetate ligand. Polyhedron, 22, pp. 2745-2753.

Radanović, D.D., Rychlewska, U., Djuran, M.I., Warżajtis, B., Drašković, N.S., & Gurešić, D.M. 2004. Alkaline earth metal complexes of the edta-type with a six-membered diamine chelate ring: Crystal structures of $[Mg(H_2O)_6][Mg(1,3\text{-pdta})]\cdot 2H_2O$ and $[Ca(H_2O)_3Ca(1,3\text{-pdta})(H_2O)]\cdot 2H_2O$: Comparative stereochemistry of edta-type complexes. Polyhedron, 23, pp. 2183-2192.

Rychlewska, U., Radanović, D.D., Jevtović, V.S., & Radanović, D.J. 2000. Synthesis and X-ray structural study of magnesium (1,3-propanediaminetetraacetato)-cuprate(II) octahydrate, $Mg[Cu(1,3\text{-pdta})]\cdot 8H_2O$.: Stereochemistry of hexadentate copper(II)–edta-type complexes in relation to the structure of the ligand. Polyhedron, 19, pp. 1-5.

Rychlewska, U., Gurešić, D.M., Warżajtis, B., Radanović, D.D., & Djuran, M.I. 2005. Highly selective crystallization of metal(II) ions with 1,3-pdta ligand: Syntheses and crystal structures of the $[Mg(H_2O)_6][Cd(1,3\text{-pdta})(H_2O)]\cdot 2H_2O$ and two isomorphic $[Zn(1,3\text{-pdta})]^{2-}$ complexes. Polyhedron, 24, pp. 2009-2016.

Rychlewska, U., Warżajtis, B., Cvetić, D., Radanović, D.D., Gurešić, D.M., & Djuran, M.I. 2007. Two distinct manganese(II) complexes with hexadentate 1,3-propanediaminetetraacetate ligand: The ability of metal(II) complexes with 1,3-pdta ligand to form solid solutions. Polyhedron, 26, pp. 1717-1724.

Rychlewska, U., Wazajtis, B., Radanovic, D.D., Draškovic, N.S., Stanojevic, I.M., & Djuran, M.I. 2011. Structural diversification of the coordination mode of divalent metals with 1,3-propanediaminetetraacetate (1,3-pdta): The missing crystal structure of the s-block metal complex $[Sr_2(1,3\text{-pdta})(H_2O)_6]\cdot H_2O$. Polyhedron, 30(6), pp. 983-989.

Rychlewska, U., Warżajtis, B., Djuran, M.I., Radanović, D.D., Dimitrijević, M., & Rajković, S. 2008. Coordination behaviour and two-dimensional-network formation in poly[[μ-aqua-di-aqua(μ5-propane-1,3-diyldinitrilotetraacetato)dilithium(I)-cobalt(II)] dihydrate]: The first example of an M^{II}-1,3-pdta complex with a monovalent metal counter-ion. Acta Cryst C.,64, pp. 217-220.

UNIVERSITY THOUGHT
Publication in Natural Sciences, Vol. 7, No. 1, 2017, pp. 17-23.
doi:10.5937/univtho7-13649
Original Scientific Paper

DEVELOPMENT AND APPLICATION OF POTENTIOMETRIC STRIPPING ANALYSIS

LJILJANA M. BABINCEV[1*], DEJAN M. GUREŠIĆ[1], RANKO M. SIMONOVIĆ[2]

[1]Faculty of Technical Sciences, University of Priština, Kosovska Mitrovica, Serbia
[2]Faculty of Natural Sciences and Mathematical, University of Priština, Kosovska Mitrovica, Serbia

ABSTRACT

This paper focuses on the voltammetric determination of lead, cadmium and zinc in water. Two ways of determining were investigated: individually and all three metals simultaneously. The experiments were performed using the Potentiometric Stripping Analysis (PSA). Determination of metals in real samples was preceded by preliminary tests. Preliminary investigations were performed in order to determine the optimal conditions of measurement. It was concluded that the process of determining was for most part influenced by: pH, time of metals extraction, stirring rate of the solution and the thickness of the mercury layer on the working electrode. The smallest concentrations of metals which can be determined using this method are: for lead 22.48 μg dm^{-3}, for cadmium 16.23 μg dm^{-3} and for zinc 18.75 μg dm^{-3}. The obtained results deviated from the actual 1.12% for lead, 1.91% for cadmium and 1.81% for zinc. All tests (individually and simultaneously) were conducted from model solution with concentration as follows: 44.96 μg dm^{-3} for lead, 32.47 μg dm^{-3} for cadmium and 37.50 μg dm^{-3} for zinc. The results of individual measurements deviated by 1.02% lead, 1.90% for cadmium and 1.89% for zinc. Simultaneously the contents were lower than real for: −4.58% for lead, cadmium for −1.91% and −1.89% for zinc. For the conditions determined, except for lead, deviations did not exceed ±2%. This indicates that Potentiometric Stripping Analysis is a good way of individual and simultaneous determination of lead, cadmium and zinc and for determination of their concentrations in water (river and groundwater).

Keywords: Lead, Cadmium, Zinc, Potentiometric Stripping Analysis, Waters.

INTRODUCTION

Heavy metals are natural constituents of soil whence are due into waterways and via of plants and in the food chain (Kastori, 1997; Sekulić et al., 2003; Kastori et al., 2006). They are characterized by toxic effects which are manifested in traces. Testing area is the northern part of Kosovo and Metohija. This part is directly affected by 100 million tons of existing flotation landfills of Trepča, which occupy an area of about 350 ha. A voltammetric technique used to determine traces of heavy metals in the surrounding surface water (river) and groundwater (natural spring and borehole) was Potentiometric Stripping Analysis (Wang, 1985; Jin et al., 1997). Determination of metals, by a three-electrode electrolytic system, was preceded by reduction and oxidation processes After reduction of metal ions on the working electrode, at a give potential, extracted metal ions are oxidized with oxygen from the solution and in terms of diffusion mass transfer they return to solution while monitoring the dependence of the potentials from oxidation time (Jagner, 1979; Marjanović et al., 1987; Riso et al, 1999;). This dependence is proportional to material concentrations. The potential of the working electrode does not change until the entire concentrations of the separate elements are oxidized. After complete oxidation of one, the working electrode potential increases to the characteristic potentials at which oxidation of the following element takes place (Suturović, 1985; Suturović, 1992; Stanković et al., 2007; Suturović, 2003).

The aim of this study was: I) To establish conditions for the simultaneous determination of lead, cadmium and zinc using Potentiometric Stripping Analysis; II) Sampling and sample preparation as well as the reduction to a single sample is suitable for Potentiometric Stripping Analysis; III) Application of simultaneous Potentiometric Stripping Analysis for the determination of lead, cadmium and zinc in water samples.

EXPERIMENTAL

Apparatus

The tests in this paper were performed on the device for Potentiometric Stripping Analysis, Striping analyzer M1 (Faculty of Technology in Novi Sad, Symmetry in Leskovac, Serbia). Basis of this system's functioning is a three-electrode electrolytic cell consisting of: disk working electrode of glassy carbon, the total area of 7.07 mm^2, which is used as an inert carrier for the mercury layer; a reference silver−silver chloride electrode (Ag/AgCl/KCl/3.5 mol dm^{-3}) and a platinum auxiliary electrode. Metal content using Potentiometric Stripping Analysis were determined by standard addition method (Babincev, 2004).

* Corresponding author: ljiljana.babincev@pr.ac.rs

Reagents

All the solutions for the execution of this experiment were prepared from high purity chemicals (supprapur, Merck). The basic solutions were prepared by standard lead, cadmium, zinc and mercury (1.000 g dm^{-3}) while working solutions were prepared from the basic standards in the concentrations as follows: for the lead 90 mg dm^{-3}3, zinc 75 mg dm^{-3}, for cadmium 65 mg dm^{-3}. In addition to standard solutions, the following ones were also used: hydrochloric acid (HCl, 30%), nitric-acid (HNO3, 65%), di-methyl ketone (CH3COCH3, 99.5%), copper-sulfate (CuSO4) and gallium-chloride ($GaCl_3$). The solutions were stored in polyethylene bottles (Babincev, 2004).

Sample preparation

Sample preparation for Potentiometric Stripping Analysis was done so that the certain amount of filtered water was evaporated after adding 5 ml of concentrated nitrate. The process was repeated three times in order to transform metals into the shape of ions. Following separation and evaporation, the dry residue was dissolved with 5 ml chlorine acid, and adding the ionized water, it has been transferred into the measuring pot of 100 ml. Aliquot of 20 ml has been transferred into the glass for electrolytic determination by Potentiometric Stripping Analysis (Babincev et al., 2011; Babincev, 2012a; Babincev, 2012b).

Procedure

Metal determination was preceded by the formation of the working electrode on the surface of glassy carbon from acidic solution of mercury(II)-ion concentration 10 mg dm^{-3}. Mercury film formation at glassy carbon electrode was performed at a constant current of −48.90 μA for the time of 240 s. In order to define optimal experimental conditions for determination of metals, the series of solutions (model solutions) of 20.0 ml of deionized water and 0.5−200 μl working standard solutions of lead, cadmium and zinc were prepared (Babincev, 2012c). Working standards were added to a micropipettes with variable volume of 0.10 (±0.05) to 200 (±1) μl. Extraction of lead, cadmium and zinc from prepared solutions was carried out at potentials of: −0.999 V for lead, cadmium to −1.106 V and −1.035 V for zinc. Simultaneous determination of all three metals was carried out at a negative potential (−1.400 V) compared to the potential of mercury that is positive (Babincev, 2012). The simultaneous determination of metals was performed after adjusting the pH and potential of separation (reduction) because in the analysis of strongly acidic solutions, for the reduction potential that is more negative than −1 V, it comes to hydrogen evolution at the working electrode. For these reasons, the value for the hydrogen evolution potential is increased for the overvoltage of hydrogen on the metals tested. Simultaneous determination of metals was carried out with prior addition of Ga(III)-ions, in order to prevent the formation of intermetallic compounds of zinc and possibly the present copper. Intermetallic compound in the oxidation process leads to a decrease in signal for zinc, which depends on the ratio of copper and zinc. Studies were performed in model solutions with zinc concentrations of: 37.5, 187.5, and 375.0 μg dm^{-3}, and copper concentrations of 10.0, 20.0, 30.0 and 35.0 μg dm^{-3}. It was found that interference in the determination of zinc can come from the copper concentrations less than 10.0 μg dm^{-3} with an error of up to 30%. By adding gallium of 40.0 μg dm^{-3} in solutions containing copper from 35.0 μg dm^{-3}, for wider range of zinc concentration, the creation of their complex is prevented because more stable complex of gallium and copper is created.

In order to define the conditions of determination, the impact of the following was particularly examined: pH; stirring rate of solution, time of metals separation and time of working electrode formation.

After the conditions were established, the determination of lead, cadmium and zinc in real samples (river and groundwater) was performed.

RESULTS AND DISCUSSION

The influence of pH solution on the efficiency of determination was examined in the value range from 1.3−4.5 for metal concentrations of 224.30 μg dm^{-3} lead, 162.01 μg dm^{-3} cadmium and 375.00 μg dm^{-3} zinc. It was found that the results obtained deviate by ±2% when the determination were performed from solutions pH 1.3, 1.6 and 2.0. The ratio of oxidation time and content, represented as a constant of Potentiometric Stripping Analysis (K/s dm^3 mol^{-1}), has the highest value for lead when determination was performed from solution pH 1.6, for cadmium from solution pH 1.6 and 2.0, and for zinc from the solution pH 2.1−3.5. Simultaneous determination was performed at pH 2.1, because for a given value of pH constant of pH potentiometric stripping analyses for all three metals have the closest values (Fig. 1).

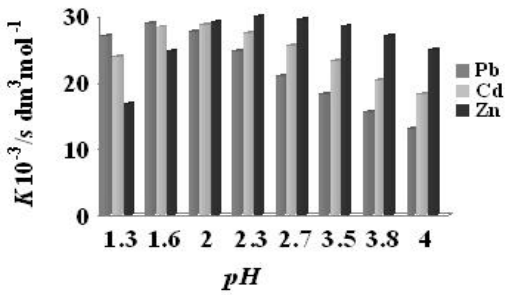

Figure 1. Dependence the constants Potentiometric Stripping Analysis for simultaneous determination of lead, cadmium and zinc by pH solutions

Effect of stirring rate on the determination of metals was investigated in the range of 1000□6000 min-1. The most efficient determinations have a stirring rate of 4000 min-1, which can be explained by the optimal thickness of diffusion layer of ions in solution. Metal extraction was tested during periods of: 180, 240, 300, 360 and 420 s. The results of the determination

showed that the most efficient metal extraction is achieved for the period of 300 s. Contents extracted for the time deviate from the actual by: 1.05% for lead, 1.90% for cadmium and 1.94% for zinc. The least time necessary for metal extraction is 240 s, metal contents extracted for that time deviate from real by: 3.34% for lead, 3.00% for cadmium and 3.76% for zinc.

Table 1. The results of the determination of lead concentration in model solutions

Concentration of lead µg dm^{-3}		S^c/µg	$K_v{}^d$/%	$E_r{}^e$/%
$X_s{}^a$	$\overline{X}{}^b$			
2.25	2.38	0.30	12.60	5.78
4.45	4.70	0.58	12.34	5.62
22.48	24.98	2.52	11.34	1.12
44.96	45.42	5.15	11.34	1.02
89.87	90.81	7.56	8.33	1.05
224.30	226.61	18.15	8.01	1.03
447.50	452.20	32.92	7.28	1.05
890.76	880.58	63.93	7.26	-1.14
1319.16	1298.56	98.04	7.55	-1.60
1763.84	1731.29	134.00	7.74	-1.84
2194.05	2150.56	169.24	7.87	-1.98
2700.00	2430.00	198.04	8.15	-10.00

$X_s{}^a$-concentration of elements in the standard solution, $\overline{X}{}^b$ -average measured concentration, number of measurements=5, S^c standard deviation, $K_v{}^d$ -coefficient of variation, $E_r{}^e$ -error determination

Table 2. The results of the determination of cadmium concentration in model solutions

Concentration of cadmium µg dm^{-3}		S^c/µg	$K_v{}^d$/%	$E_r{}^e$/%
$X_s{}^a$	$\overline{X}{}^b$			
1.62	1.73	0.03	13.96	6.79
3.25	3.45	0.47	13.74	6.15
16.23	16.54	1.56	9.45	1.91
32.47	33.09	2.49	7.54	1.90
64.90	66.13	4.98	7.53	1.89
162.01	165.09	12.20	7.39	1.90
323.22	329.31	24.45	7.43	1.88
643.25	634.15	45.59	7.19	-1.41
960.12	941.53	68.73	7.30	-1.93
1273.89	124323	105.79	8.51	-2.40
1584.59	1536.45	136.90	8.64	-3.04
1892.29	1789.80	156.07	8.72	-5.42

$X_s{}^a$-concentration of elements in the standard solution, $\overline{X}{}^b$-average measured concentration, number of measurements=5, S^c-standard deviation, $K_v{}^d$-coefficient of variation, $E_r{}^e$-error determination

The impact of the mercury layer thickness on metal determination was analyzed as the time required for the formation of the working electrode. The working electrode formation was done by separating the mercury on glassy carbon within: 120, 180, 240, 300 and 360 s. A good reproducibility was obtained for all three ions when the mercury layer was formed within 240 s. The mercury layer formed in 240 s, based on reproducibility, provides a good homogenization of extracted metal ions, easier and faster dissolution process and better separation. In order to determine detection limits of potentiometric analysis for lead, cadmium and zinc, solutions of 20.0 ml of deionized water and different working standard volumes from 0.5 to 600 µl were prepared. Metal extraction was performed within 300 s; solution stirring rate of 4000 min–1 and the pH values were 1.6 for lead and cadmium and 2.1 for zinc. The results for the determination are presented in Tables 1-3.

Table 3. The results of the determination of zinc concentration in model solutions

Concentration of zinc µg dm^{-3}		S^c/µg	$K_v{}^d$/%	$E_r{}^e$/%
$X_s{}^a$	$\overline{X}{}^b$			
1.88	2.02	0.23	11.39	7.45
3.75	3.97	0.46	11.59	5.86
18.75	19.09	1.99	10.42	1.81
37.50	38.21	3.96	10.36	1.89
187.50	191.15	15.96	8.35	1.95
375.00	379.77	28.22	7.43	1.27
750.00	737.74	57.47	7.79	-1.63
1125.00	1106.43	80.77	7.30	-1.65
1312.50	1286.83	111.70	8.68	-1.95
1500.00	1458.66	130.55	8.95	-2.76

$X_s{}^a$-concentration of elements in the standard solution, $\overline{X}{}^b$ -average measured concentration, number of measurements=5, S^c standard deviation, $K_v{}^d$ -coefficient of variation, $E_r{}^e$ -error determination

Based on results presented, the minimum contents of lead, cadmium and zinc that were determined with an error of ±2% are: 22.48 µg dm^{-3} of lead (determined with an error of 1.12%), 16.23 µg dm^{-3} cadmium (determined with an error of 1.91%) and 18.75 µg dm^{-3} zinc (determined with an error of 1.81%). In accordance with the standard deviations and the reproducibility, these contents can be considered the limits of determination. Standard deviations were 2.52 µg for lead, 1.56 µg of cadmium and 1.99 µg of zinc. The detection limit of Potentiometric Stripping Analysis for lead, cadmium and zinc is about 20 µg dm^{-3}. The highest concentrations that are determined by PSA with an error ±2% were: 2194.05 µg dm^{-3} for lead; 960.12 µg dm^{-3} for cadmium and 1312.50 µg dm^{-3} for zinc. These contents were determined with the error of: −1,98% for lead, −1.93% for cadmium, and −1.95% for zink and standard deviations of: 169.24 µg for lead, 68.73 µg for cadmium and 111.70 µg for zinc.

Simultaneous determinations

The determination of elements was studied simultaneously in 20.0 ml of deionized water and 10 µl working standard solutions of lead, cadmium and zinc, for metal concentrations of: 44.96 µg dm^{-3} lead, 32.47 µg dm^{-3} cadmium and 37.50 µg dm^{-3} zinc. Results of this study have shown that potential of the working electrode for the simultaneous determination of lead, cadmium and zinc is 490–510 mV more negative than the potential of zinc dissolution (an element with the lowest redox potential). It was determined that all three elements can be determined at a negative potential (–1.400 V) in relation to the

potential of mercury that is positive. For that reason, values for extraction potentials are increased by hydrogen overvoltage on mercury, lead, cadmium and zinc. The simultaneous determination of lead and cadmium has shown optimal values for pH 1.6. For pH 2.1, cadmium and zinc were simultaneously determined. Simultaneous determination of lead and zinc was examined for pH 1.3, 1.6, 2.0, the most effective determinations were for pH 2.0. Zinc is most accurately determined for pH value of 2.3–3.5, which may partly be explained by the qualitative properties of zinc. The simultaneous determination of all three elements was performed (with the mentioned separation potential) for pH 2.1, because the constants of Potentiometric Stripping Analysis for this value were the closest.

With prior pH adjustment, metal content was determined by standard addition method. During the determination, metals are firstly reduced (separated) on working electrode and then (after electrolysis) they are oxidized (returned) to the solution. After returning to the solution, oxidation potential is registered, which is changed until the entire separated contents of one metal is returned to the solution. After returning one element to the solution, working electrode potential increases to characteristic potential at which oxidation of the following takes place. Results of simultaneous determination of lead, cadmium and zinc are given in Table 4.

Table 4. The results of the simultaneously determination of lead, cadmium and zinc in model solution

Ion	Ion concentration, μg dm^{-3}			τ (s)	$K\cdot10^{-5}$ (s·dm^3/mol)	S (μg)	K_v (%)	E_r (%)
	X_s	X_i	$\overline{X}$					
Pb^{2+}	44.96	44.63	42.90	1.47	32.84	5.57	12.98	-4.58
		40.98		1.31	31.97			
		43.18		1.40	32.47			
		42.18		1.35	32.12			
		43.56		1.42	32.63			
Cd^{2+}	32.47	34.75	31.86	0.85	24.64	4.54	14.26	-1.91
		32.13		0.79	24.65			
		28.96		0.71	24.58			
		33.96		0.84	24.82			
		29.50		0.72	24.50			
Zn^{2+}	37.50	41.94	36.79	0.90	21.56	4.47	12.14	-1.89
		35.48		0.76	21.49			
		34.18		0.73	21.50			
		44.40		0.96	21.60			
		36.25		0.78	21.58			

[a]X_s-concentration of the elements in the model solution, [m]X_i-measured concentration, [b]$\overline{X}$-average measured concentration, number of measurements=5, [n]τ-time of oxidation, K_p-constant stripping analysis, [c]S-standard deviation, [d]K_v-coefficient of variation, [e]E_r-error determination

The obtained results suggest that there is a difference in the determinate contents when we take individual and simultaneous determinations into consideration. The results for the individual determinations deviated from the actual values by 1.02% for lead; 1.90% for cadmium and 1.89% for zinc. During the simultaneous determinations, the deviations were as follows: −4.58% for lead; −1.91% for cadmium and −1.89% for zinc. Results obtained for lead were less accurate. As it is about micro quantities, having in mind small standard deviations of simultaneous determination in relation to individual, simultaneous determination of these elements is considered possible. Potentiometric Stripping Analysis is applied in determination of heavy metals in samples of different nature (Kaličanin et al., 2001a; Kaličanin et al., 2001b; Kaličanin et al., 2001c; Suturović et al., 2001: Kaličanin et al., 2002). In this work, lead, cadmium and zinc in samples of waters are determined. The results for determination of the concentrations of lead, cadmium and zinc in river water (sampled successively every three months starting from april 2015 to february 2016) are shown respectively in Tables 5−8.

Table 5. The results of concentrations of lead, cadmium and zinc (μg dm^{-3}) in water of the river Ibar, april 2015

	Pb	Cd	Zn
1	4.28	0.51	29.23
2	1.98	1.12	78.12
3	9.24	5.25	258.43
4	10.93	4.91	180.04
5	8.82	4.96	288.02
6	12.11	3.85	249.11
MCL	10.00	3.00	3000.00

Sample 1. Ibar River, the entrance to KM (pontoon bridge), a few kilometers away from the river flows into minutiae, Trepčanska rivers and river peeler; Sample 2. The river Ibar, output from the KM, after casting sundries and peeler, below the city waste disposal Upper Field at Dudinog rubble; Sample 3. The river Ibar, rudarački bridge downstream from the waste disposal,, Trepča,, near the Trepča RMHK in Zvecan; Sample 4. River Ibar bridge Grabovac-Žitkovac, exit behind the city waste disposal Žitkovac; Sample 5. Ibar River, the village Kutnje, entrance to Leposavić, in addition to the city waste disposal Bostaniste in Leposavić; Sample 6. Ibar River, the village of Gornji Krnjin, exit from Leposavić, in addition tailing impoundments Gornji Krnjin in Leposavić; *MCL* maximum contaminant.

Results of testing in a small number of cases show exceeding the *MCL*. Lead concentrations above the allowed *MCL* in the spring season are registered only in the samples 4 and 6, which refer to water of Ibar. These samples are taken from the bridge Grabovac-Žitkovac behind the place of the waste disposal Žitkovac and in the village Upper Krnjin, the output from Leposavić, in addition to the landfill tailing upper Krnjin or Bostaniste in Leposavić

Table 6. The results of concentrations of lead, cadmium, zinc (μg dm^{-3}) in water of the Ibar, august 2015

	Pb	Cd	Zn
1	2.98	0.31	29.77
2	4.27	4.10	379.31
3	7.64	4.36	439.18
4	8.93	4.16	338.99
5	6.33	2.01	188.73
6	7.56	2.13	178.54
MCL	10.00	3.00	3000.00

Table 7. The results of concentrations of lead, cadmium, zinc (μg dm^{-3}) in water of the river Ibar, october 2015

	Pb	Cd	Zn
1	1.92	0.28	18.91
2	1.72	0.59	79.93
3	6.05	2.97	29.79
4	4.90	3.09	27.68
5	7.79	2.01	109.59
6	9.65	2.07	129.56
MCL	10.00	3.00	3000.00

Table 8. The results of concentrations of lead, cadmium, zinc (μg dm^{-3}) in water of the Ibar, february 2016

	Pb	Cd	Zn
1	2.53	0.21	37.96
2	3.98	0.49	456.01
3	5.99	2.38	337.89
4	5.43	2.97	579.77
5	4.12	1.97	455.99
6	4.43	1.78	337.97
MCL	10.00	3.00	3000.00

The increase in lead content in these samples there was probably washing and filtration with a delay of those cities, and cities delays that are located upstream or on the bank of the Ibar. Near the *MCL* and the concentration of lead in the samples 3 and 5, which were taken from the measuring points are also close to the waste disposal. Lead is present in the water at the measuring point 1, which was chosen as the site of male pollution. How is this place located a few kilometers from the flows of the river Sitnica Trepčanska river and river Lushta into the river Ibar, and of all places of disposal of industrial waste, it can be assumed that the lead content in the sample contribute to exhaust fumes of motor vehicles on the road that passes by the banks of the Ibar River, as well as washing with asphalt street.

The minimum content of lead in the Ibar river water was found in the sample 2, which can be explained by the fact that the sampling is done with the left bank of the Ibar river, opposite the city delay the Top Field. This measuring point is the furthest from the city traffic as a possible source of lead contamination. Increased concentrations of cadmium in the river water Ibar at the measuring points 3, 4, 5 and 6 above *MCL* is probably from the same causes as the increased concentration of lead. Sample 1 contains little cadmium. In sample 2 also has a low content of cadmium, but more than in a sample1.This measuring point is the first in a series in which the mixed water of the river Ibar, Sitnica, Trepčanska river and Lushta, which are before the casting of the Ibar already polluted. The content of zinc, compared with *MCL* is significantly lower compared to lead and cadmium. As his low concentrations it can be said that the existing pollutants in the area tested not significantly affect the water pollution zinc. The results of the content of heavy metals in water samples taken at the same measuring points and in different seasons of the year have shown that there are certain differences, but it is noted the same trend of the contamination, that is determined by the measuring points are more polluted than the other.

The highest concentrations of lead in the samples from the measuring points 3.4, 5, and 6 and the highest concentration of cadmium also at locations 3, 4 and 5. The results of determining the content of heavy metal in the spring and of Well water are shown in Tables 9–16.

Table 9. The results of concentrations of lead, cadmium and zinc (μg dm^{-3}) in natural spring water, april 2015

Samples	Pb	Cd	Zn
1	1.73	1.34	79.01
2	2.09	1.52	38.97
MCL	10.00	3.00	3000.00

Samples: 1. Village Grabovac, the source is above the alluvial plain. Water pumped from mountainous Lipe; 2. Devine water, 10 km from Zvecan

Table 10. The results of concentrations of lead, cadmium, zinc (μg dm^{-3}) in natural spring water

Samples	Pb	Cd	Zn
1	3.01	0.83	0.25
2	2.13	2.41	0.59
MCL	10.00	3.00	30000

Table 11. The results of concentrations of lead, cadmium, zinc (μg dm^{-3}) in natural spring water, octobert 2015

Samples	Pb	Cd	Zn
1	1.87	0.39	38.83
2	0.89	1.01	29.01
MCL	10.00	3.00	3000.00

Table 12. The results of concentrations of lead, cadmium, zinc (μgdm^{-3}) in natural spring water, february 2016

Samples	Pb	Cd	Zn
1	1.18	1.03	80.34
2	1.01	1.19	83.57
MCL	10.00	3.00	3000.00

Table 13. The results of concentrations of lead, cadmium and zinc (μg dm^{-3}) in groundwater, april 2015

Samples	1	2	3	4	5*	6*	7	8	9	10	*MCL*
Pb	3.17	2.02	6.43	1.97			1.13	3.24	1.07	6.81	10.00
Cd	0.69	0.84	1.89	2.27			1.47	1.48	1.38	2.66	3.00
Zn	28.03	39.12	149.21	59.33			178.56	177.92	98.16	247.77	3000.00

Samples groundwater-stone wells: 1. Žitkovac Village, 200 m of the Ibar, 2 m from the main road, the age of 5 years; 2. Village Grabovc, 100 m of the Ibar, the main road, 30 years old; 3. Village Žitkovac, 50 m from the landfill Žitkovac, 200 m of the Ibar; 4. The village Rudare, 50 m from Ibra, 30 years; 5. Village Srbovac, 20 m from Ibra, 40 years; 6. Village Srbovac, 20 m from Ibro, 40 years; 7. The upper Krnjin Village, 100 m of the Ibar, 10 y; Drilled wells: 8 village Rudare, 80 m from Ibra, 25 years; 9. Village Grabovac, 30 m from Ibra, 25 years; 10. Village Grabovac, 30 m from Ibra, 25 years; *The planned samples 5 and 6 were not taken due to heavy rainfall

Table 14. The results of concentrations of lead, cadmium and zinc (μg dm^{-3}) in groundwater, august 2015

Samples	1	2	3	4	5	6	7	8	9	10	*MCL*
Pb	3.42	0.81	9.84	5.99	4.13	3.25	1.38	5.72	3.17	14.99	10.00
Cd	0.21	0.15	0.91	0.07	0.13	0.36	0.57	0.02	0.47	0.41	3.00
Zn	49.01	198.91	49.02	38.97	29.03	48.91	79.05	598.13	129.44	189.21	3000.00

Table 15. The results of concentrations of lead, cadmium and zinc (μg dm^{-3}) in groundwater, october 2015

Samples	1	2	3	4	5	6	7	8	9	10	*MCL*
Pb	1.89	0.79	7.11	3.65	4.81	6.32	0.99	3.71	4.02	24.09	10.00
Cd	0.16	0.24	0.21	0.06	1.01	0.87	0.06	1.73	0.59	0.79	3.00
Zn	29.01	38.99	19.94	39.01	33.80	48.90	38.89	399.01	258.90	568.99	3000.00

Table 16. The results of concentrations of lead, cadmium and zinc (μg dm^{-3}) in groundwater, february 2016

Samples	1	2	3	4	5	6	7	8	9	10	*MCL*
Pb	2.58	2.61	6.13	4.23	3.81	3.74	1.02	4.13	4.43	4.21	10.00
Cd	0.18	0.51	0.11	0.69	1.84	1.49	0.09	1.21	0.75	1.68	3.00
Zn	249.3	138.1	149.2	189.9	60.2	97.8	43.9	279.9	462.5	431.3	3000.00

Significantly, based on the result of determining that the concentration of lead in all the samples wells and water sources is less than the *MCL* for drinking water. Variations may occur in the lead content at the measuring point 10 (in the drilled wells in the village Grabovac), wherein the concentration i Increased content of lead probably arose due to the reduced quantity of water (drought) and the pumping raises the sediment and stirred with water, which was noticeable by the color of the sample.n the summer and autumn rather above the *MCL* of the drinking water (Službeni glasnik Republike Srbije, 1994). In the colder period of the year (autumn and winter) lead content is generally lower. Concentrations of cadmium and zinc in well and spring waters are also less than the Maximum allowable concentrations at all measuring points and in different seasons.

CONCLUSION

The objective of this study is simultaneous determination of lead, cadmium and zinc by stripping analysis, as well as application of the same in water analysis, establishment of determination conditions, extraction potential, extraction time, optimal solution stirring rate, pH, time of working electrode formation, as well as manner of samples preparation, using the approach of comparing the results of simultaneous with the results of individual determination. It is obvious that there is a difference in results obtained. The efficiency of the individual determination was greater due to the better synchronization of the solution pH value and the extraction potential. Results accomplished in case of simultaneous determination have shown somewhat lower values which can be explained by the occurrence of hydrogen extraction in the analysis of acidic solutions, when extraction potential is more negative than −1 V. The maximum efficiency for all determinations was obtained at metal extraction time of 300 s, on electrode that is formed in 240 s and at solution stirring rate of 4000 min^{-1}. At higher stirring rates, the determination efficiency is reduced due to the decreased diffusion layer thickness. The lowest concentrations which can efficiently be determined by Potentiometric Stripping Analysis are: 22.48 μg dm^{-3} for lead, 16.23 μg dm^{-3} for cadmium and 18.75 μg dm^{-3} for zinc. Good efficiency is up to 2194.05 μg dm^{-3} for lead, 960.12 μg dm^{-3} for cadmium and 1312.50 μg dm^{-3} for zinc, which can be attributed to identical mechanism of mass transfer during extraction for the one during metal dissolution. For the simultaneous determination of all three metals, determination error was in range of 2–5%. The reproducibility of these measurements for lead, cadmium and zinc in the water samples ranged from: 10–13% for lead, 10–14% for cadmium and 8–9% for zinc. The obtained results indicate that Potentiometric Stripping Analysis is efficient in determination

of lead, cadmium and zinc, both individually and simultaneously, as well as in the analysis of water.

REFERENCES

Babincev, Lj. 2004. Analiza sadržaja teških metala u vodama oko jalovišta rudnika Suva ruda. Belgrade: Faculty of Technology and Metallurgy., p. 149. MSc thesis (in Serbian).

Babincev, Lj. 2012a. Heavy metals sorption woter from fiber natural. Voda i sanitarna tehnika, 41(2), pp. 59-64.

Babincev, Lj. M., Rajaković, Lj. V., Budimir, M. V., Perić−Grujić, A. A., & Sejmanović, D. M. 2011. Woody plant willow finction in river water protection. Hem. Ind., 65(4), pp. 397-401.

Babincev, Lj.M., 2012b. Zaštita vodenih resursa primenom prirodnih vunenih vlakana. Ecologica, 67(19), pp. 345-349.

Babincev, Lj. 2012c. Razvoj i primena potenciometrijske striping analize za određivanje teških metala u ekosistemu. Kosovska Mitrovica: Faculty of Technical Sciences., p. 170. PhD (in Serbian).

Jagner, D. 1979. Potentiometric stripping analysis in non-deaerated samples. Anal. Chem., 51, p. 324.

Jin, W. R., Nguyen, V. D., Valenta, P., & Nurnberg H. W., 1997. Simultaneous determination of 7 toxic trace and or ultratrace metals in environmental plants by differential-pulse voltammetry without change of solution and eledtrode. Anal. Lett., 30, p. 1235.

Kaličanin, B.M., Marjanović, N.J., & Suturović, Z. J. 2001a. Determination of the soluble lead in the glass ware by the potentiometric stripping analysis. APTEFF, 32, p. 61.

Kaličanin, B.M., Marjanović, N.J., & Suturović, Z.J. 2001b. The development of a gigh sensitivity method for the eleetrochemical determination of soluble lead in glassware. HMIDA, 8(55), p. 367.

Kaličanin, B.M., Todorović, Z.B., Marijanović, N.J., & Suturović, Z.J. 2001c. Potetntiometric stripping Anlysis of soluble lead in the glassware used for needs of food and pharmaceutical industry. J. Chem. Environ, 5, p. 7.

Kaličanin, B.M., Marjanović, N.J., & Suturović, Z.J. 2002. Application of Potentiometric stripping analysis with constant inverse current in the analytic step for determining lead in glassware. J. Serb. Chem. Soc., 67, p. 213.

Kastori, R. 1997. Heavy metals in the environment, Scientific Institute for Husbandry and Vegetable Crops. Novi Sad., p. 301.

Kastori, R., Bogdanović, D., Kádár, I., Milošević, N., Sekulić, P., & Pucarević, M. 2006. Soil and plant sampling in unpolluted and polluted habitats. Novi Sad: Scientific Institute for Husbandry and Vegetable Crops., p. 244.

Marjanović, N.J., Suturović, Z.J., Jankovitš, I.F., Ružić, N., & Branković, V. 1987. Compilation of works. Novi Sad, Serbia: Faculty of Technology., p. 53. 18.

Službeni glasnik Republike Srbije 1994. Pravilnik o dozvoljenim količinama opasnih i štetnih materija u zemljištu i vodi za navodnjavanje i metodama njihovog ispitivanja. Službeni glasnik Republike Srbije, 23, p. 553. (in Serbian).

Riso, R.D., Leccore, P., & Chaumery, C.J. 1999. Rapid and simultaneous analysis of trace metals (Cu, Pb and Cd) in seawater by potentiometric stripping analysis. Anal. Chim. Acta, 83, p. 351.

Sekulić, P., Kastori, R., & Hadžić, V. 2003. Degradation soil protection, Scientific Institute for Husbandry and Vegetable Crops. Novi Sad., p. 230.

Stanković, S., Čičkarić, D., & Marković, J. 2007. Determination of Pb and Cd in Water by potentiometric stripping analysis (PSA), Desalination 213, pp. 282−287.

Suturović, Z. 1985. Ispitivanje uslova predelektrolize kao prve faze elektrohemijske striping analize. Novi Sad, Serbia: Faculty of Technology., p. 115. MSc thesis (in Serbian).

Suturović, Z. 1992. Povećanje osetljivosti potenciometrijske striping analize. Novi Sad, Serbia: Faculty of Technology., p. 124. PhD thesis.

Suturović, Z.J. 2003. Elektrochem. Stripping Analysis. Novi Sad, Serbia: Faculty of Technology., p. 120.

Suturović, Z.J., Marjanović, N.J., Pekić, B., & Adamović, D. 2001. Potentiometric stripping analysis of selected heavy metals in roadside chamomile flower. APTEF, 32, p. 157.

Wang, J. 1985. Stripping Analysis.Derfield Beach, Florida: VCH Publishers., p. 119.

UNIVERSITY THOUGHT
Publication in Natural Sciences, Vol. 7, No. 1, 2017, pp. 24-31.
doi:10.5937/univtho7-14161
Original Scientific Paper

GAM MODEL AND TOURIST VALORIZATION OF GEOSITES PLOČNIK

MIROSLAV STANKOVIĆ[1], STEFAN MILOVANOVIĆ[1*]

[1]Faculty of Natural Sciences and Mathematics, University of Priština, Kosovska Mitrovica, Serbia

ABSTRACT

In Serbia, there are several sites from the Neolithic period, but there is only one site from the period of existence of the Vinča-Tordoš family (5500-4800 BC). In this paper, we will try to become familiar with the site named Pločnik by using two methods. This site is one of many archeological sites in Serbia, but it stands out uniquely because it is under state protection. The methods to be applied are GAM model and tourist valorization.

Keywords: Archaeological site, GAM model, tourist valorization, Neolithic, Pločnik, Vinča-Tordoš.

INTRODUCTION

Neolithic period was divided into early and late neoliths. The older neolith involves the material remains of old-age culture from the 7th to the mid 6th millennium BC. The beginning of early Neolithic brought many innovations. There was a settlement in one area, after which there was a transition from hunting and gatherings to agriculture and livestock breeding. New economic opportunities and sedentary lifestyles have spawned the emergence of new materials and new types of facilities. Clay, a new material suitable for its plasticity, has found wide application in the Neolithic period, but also in later periods. There are also tools of polished stones of different shapes, which are suitable for processing wood and leather and grinding grain. The late neolithic and eneolithic contents contain objects belonging to the period from the middle of the 6th to the middle of the 5th millennium BC. The Vinca culture flourished during the late Neolithic and Eneolithic. Livestock and agriculture represent the economic base of this culture, and its bearers have begun and gradually completely mastered the use of copper. Stone foods and tools for animal bones appear, as well as the first metal artefacts - copper chisels, axis hammers, needles, beads, pendants and moldings, which testify to the beginning of old metal and the innovative spirit of Vinca culture. Early Neolithic sites on the territory of Serbia are Starcevo Near Pančevo, Pavlovac (Čukar and Gumnište) near Vranje, Nosa-Pearl coast near Subotica, Tečić in Šumadija, Ajman, Mala Vrbica and Arija Babi in Đerdap, late neolithic sites Vinča-Belo Brdo in the Belgrade suburb, Pločnik near Prokuplje and Belovoda kod Petrovac na Mlavi.Na more important, the famous Neolithic site at the spa, causeway, was accidentally discovered in 1927, while he was digging for the route of the railway. Found objects, especially the storage of copper tools, which the Administration of the Ironworks gave to the Museum of Prince Pavle, were the reason why Dr. Miodrag Grbic made the first rescue excavation of this site the following year. On an area of about 500m2, they found baked dishes, figurines, stone tools and bones, and another copper tools storage. This material was the basis for a publication published by the Belgrade Museum in 1929 in German, which made Pločnik one of the main European locations from the Eneolithic period.

Research in Pločnik was restored in 1960, organized by the National Museum in Belgrade.

The work was led by Dr. Blaženka Stalio, and systematic drilling research, with interruptions, lasted until 1978. In nine campaigns, 765.5 m^2 were explored. The main purpose was to investigate and determine the boundaries of the village, whose stratigraphy is followed in the profile of the left coast of Toplica, where the 2-3.5 m thick cultural layer can be traced for almost kilometer in length, and where house foundations are clearly visible in the profile and pit profiles filled with a variety of amenities. The first probe was near the railway station and then probes followed the river profile, as this is the most vulnerable part of the village. Toplica in this part makes a meander, hits the high coast and undermines the gravel surface beneath the cultural layer. This way, only during the last 20 years, the river took almost 30 hectares of fertile land together with the site: http://muzejtoplice.org.rs/.

Research conducted in Pločnik gave plenty of material which characterized Pločnik as the Late Stone Age village, as well as the site from the period of Vinča culture, which in the region of the central Balkans lasted from 5500 to 4800 BC. In addition to the items which are usually found on the sites of this culture, foundations of houses, furnaces, fireplaces and pits, abundant ceramic material was discovered as well. A variety of vessels, from large and coarse to the polished ones, as well as various and extremely rich figural plastic with specific elements, have caused the late phase of the Vinča culture to be named after the site of Vinča-Pločnik.

Last survey campaign began in 1996 organized by the Belgrade National Museum and the Toplica National Museum from Prokuplje, under the leadership of MS. Dušan Šljivar from Prokuplje. Research gives excellent results and growing evidence of the beginning of copper metallurgy in this region: http://plocnik.org.rs/.

* Corresponding author: stefanmilovanovic2012@gmail.com

THEORETICAL PART

The Pločnik site stretches on 120 hectare. On the West, it is bordered by Paljevski creek. On the East, there is a river Bačka. On the South, there is Toplica River and on the North there are traces of settlement up to the foot of the hills that enclose the valley. Recent research has given an extraordinary material: copper artifacts that move the beginnings of metallurgy to 500 years earlier, exquisite works of art that the world admires which awakened the interest in the scientific world for this site. In the immediate vicinity of the site are: Roman baths, Church, Battle of Pločnik, spa Viča: http://www.prokuplje.org.rs/.

EXPERIMENTAL

Materials and methods

Methods for evaluating geosites that have been developed in previous years were mainly focused on geosites and their scientific value and later on, added value (Grandgirard, 1999; Bruschi & Cendrero, 2005; Coratza & Giusti, 2005; Reynard, 2005; Reynard & Panizza, 2005; Reynard et al., 2007; Pereira et al., 2007; Tomić, 2011; Vujičić et al., 2011; Boškov et al., 2015). Based on several of these methods, in 2005, Pralong (Pralong, 2005) has made a new model exclusively intended for the evaluation of geosite tourist value and the use of geosites in the tourism sector.

According to this method, the tourist value of the site is determined as the average value of aesthetic, scientific, cultural and economic values. In this model, as well as in many previous models, one of the main problems in the evaluation process is objectivity. None of these models include information on the needs, attitudes, interests and opinions of tourists visiting geosites which is of great importance especially in the evaluation of the tourist potential of the site. Including the visitors into the evaluation process is a good way to achieve greater objectivity.

Model for evaluation that was used in this study is based on the model for the evaluation of geosites (*Geosite Assessment Model* - hereinafter *GAM*), which was published in 2011 (Vujičić et al., 2011). During the creation of this model, extensive existing scientific literature in the field of the geosite evaluation was used (e.g. Hose, 1997; Hose et al., 2011; Bruschi & Cendrero, 2005; Coratza & Giusti, 2005; Pralong, 2005; Pereira et al., 2007; Serrano, González-Trueba, 2005; Zouros, 2007; Reynard et al., 2007; Reynard, 2008). GAM model is composed of two indicators: **the main value (*MV*)** and the **additional value (*AV*),** which are further divided into 12 or 15 sub-indicators (Table) which may have a value from 0.00 to 1.00. Table 1**.**

Table 1. Structure model for evaluating geosites (GAM)

Indicators/Subindicators	Description
Main values (*MV*)	
Scientific/Educational value (*VSE*)	
Rarity ($SIMV_1$)	Number of identical sites in the immediate environment.
Representativeness ($SIMV_2$)	Didactic and "school" characteristics of the site based on its own qualities and general configuration.
Site exploration ($SIMV_3$)	Number of publications in recognized journals, master and doctoral theses and other publications.
Interpretation level ($SIMV_4$)	Options for the interpretation of geological and geomorphological processes, forms and shapes.
Landscape / aesthetic value (*VSA*)	
Lookouts ($SIMV_5$)	Number of lookouts available to pedestrian walkways. Each must provide a view from a different angle and it must be located less than 1 km from the site.
Surface area ($SIMV_6$)	The total area of the site. Each locality is considered in the quantitative comparison with other localities.
Landscape and the nearby nature ($SIMV_7$)	The quality of the panoramic view, the presence of water and vegetation, the absence of damages caused by man, the vicinity of urban area, etc.
Incorporation of localities in the surroundings ($SIMV_8$)	The degree of contrast with nature, contrast, color, shape, etc.
Protection (*VPr*)	
Current situation ($SIMV_9$)	The current state of geosite.
Level of protection ($SIMV_{10}$)	Locality protected by local or regional associations, national or international institutions.
Sensitivity ($SIMV_{11}$)	Geosite Sensitivity Level / Vulnerability to natural or anthropogenic damage.
Bearing capacity ($SIMV_{12}$)	Adequate number of visitors to the site at the same time which will not jeopardize the current state of geosites.

Additional values (*AV*)	
functional values (*VFn*)	
Availability ($SIAV_1$)	Site access possibilities
Additional nature values ($SIAV_2$)	Number of additional natural values within 5 km (including other geosites)
Additional anthropogenic values ($SIAV_3$)	Number of additional natural values within 5 km
The proximity to the emitting centers ($SIAV_4$)	The proximity to the emitting centers
The proximity to important roads ($SIAV_5$)	The proximity to major roads within 20 km
Additional functional values ($SIAV_6$)	Parking, gas stations, car service, etc.
Tourist values (*VTr*)	
Promotion ($SIAV_7$)	The level of promotional activities.
organized visits ($SIAV_8$)	Annual number of organized visits to the geosite.
The proximity to vizitor centers ($SIAV_9$)	The proximity to vizitor centers to the geosite.
interpretative boards ($SIAV_{10}$)	Interpretive features of text and graphic material, quality, size and integration into the environment.
Number of visitors ($SIAV_{11}$)	Annual number of visitors.
Tourist infrastructure ($SIAV_{12}$)	The level of additional infrastructure for visitors (pedestrian paths, resting places, garbage cans, toilets, etc.)
Guide service ($SIAV_{13}$)	A level of expertise, knowledge of foreign languages, interpretive skills and so on, if there are those.
Accommodation ($SIAV_{14}$)	Accommodation services in the vicinity of the site.
Restaurant services ($SIAV_{15}$)	Reastaurant services in the vicinity of the site.
Mark (0.00-1.00)	

	0.00	0.25	0.50	0.75	1.00
$SIMV_1$	A common occurrence	Regional	National	International	Unique
$SIMV_2$	None	Low	Middle	High	The highest
$SIMV_3$	None	Local publications	Regional publications	National publications	International publications
$SIMV_4$	None	Middle level of process but difficult to explain to people outside of geology	Good example of process but difficult to explain to people outside of geology	Middle level of process but difficult to explain to an average visitor	Good example of process but difficult to explain to an average visitor
$SIMV_5$	None	1	2 to 3	4 to 6	More than 6
$SIMV_6$	Small	-	Middle	-	Big
$SIMV_7$	-	Low value	Middle	High	The highest
$SIMV_8$	Does not fit	-	Neutral	-	It fits
$SIMV_9$	Totally destroyed (as a result of human activity)	Very damaged (as a result of natural processes)	Moderately damaged (with preserved essential geomorphological features)	Lightly damaged	Undamaged
$SIMV_{10}$	Unprotected	Protected at the local level	Protected at the regional level	Protected at the national level	Protected at the international level
$SIMV_{11}$	Without the possibility of "recovery" (with the possibility of total loss)	High (can easily be damaged)	Middle (can be damaged by human or natural activities)	Low (can only be damaged by human activities)	It cannot easily be damaged
$SIMV_{12}$	0	0 to 10	10 to 20	20 to 50	More than 50
$SIAV_1$	Inaccessible	Low (only on foot with special equipment and professional guides)	Central (bicycle and other similar means of transport)	High (bus)	The highest (bus)

$SIAV_2$	None	1	2 to 3	4 to 6	More than 6
$SIAV_3$	None	1	2 to 3	4 to 6	More than 6
$SIAV_4$	More than 100 km	100 to 50 km	50 to 25 km	25 to 5 km	Less than 5 km
$SIAV_5$	There are not any in the vicinity	Local road	Regional road	National road	International road
$SIAV_6$	None	Low	Middle	High	The highest
$SIAV_7$	None	Local	Regional	National	International
$SIAV_8$	None	Less than 12 a year	From 12 to 24 a year	From 24 to 48 a year	More than 48 a year
$SIAV_9$	More than 50 km	From 50 to 20 km	From 20 to 5 km	from 5 to 1 km	Less than 1 km
$SIAV_{10}$	None	Low quality	Average quality	High quality	The highest quality
$SIAV_{11}$	None	Low (less than 5000)	Middle (from 5001 to 10 000)	High (from 10 001 to 100 000)	The highest (more than 100 000)
$SIAV_{12}$	None	Low level	Middle level	High level	The highest level
$SIAV_{13}$	None	Low quality	Average quality	High quality	The highest quality
$SIAV_{14}$	More than 50 km	25–50 km	10–25 km	5–10 km	Less than 5 km
$SIAV_{15}$	More than 25 km	10–25 km	10–5 km	1–5 km	Less than 1 km

This division has been created by the two most typical kinds of values: main values - mainly stemming from the natural geosite characteristics; and the additional values - which are mostly caused human influence and the adjustments made for the visitors' needs. **The main values (MV)** consist of three groups of indicators: scientific/educational value (*VSE*), landscape/ aesthetic value (*VSA*) and protection (*Vpr*). **Additional values** (*AV*) are divided into two groups of indicators, functional (*VFN*) and the tourist value (*VTR*) (Vujičić et al., 2011). So, we have a total of 12 sub-indicators of the main values and 15 sub-indicators of additional values which are assessed using values from 0.00 to 1.00, which defines GAM as the following equation:

$$GAM = MV + AV \quad (1)$$

where *MV* and *AV* represent the symbols for main value and added value. As the main and additional values consist of three or two groups of sub-indicators, we can derive the following two equations:

$$MV = VSE + VSA + VPr, \quad (2)$$

$$AV = VFn + VTr, \quad (3)$$

where, *VSE*, *VSA*, *VPr*, *VFn* and *VTr* represent scientific/educational value (*VSE*), landscape/aesthetic value (*VSA*), the protection (*VPr*), the functional value (*VFN*) and tourist value (*VTr*).

Now that we know that each group of indicators consists of sub-indicators, the equations (2) and (3) can be written as follows:

$$MV = VSE + VSA + VPr \equiv \sum_{i=1}^{12} SIMV_i \quad (4)$$

where is: $0 \leq SIMV_i \leq 1$.

$$AV = VFn + VTr \equiv \sum_{j=1}^{15} SIAV_i \quad (5)$$

where is: $0 \leq SIAV_j \leq 1$.

Here, $SIMV_i$ and $SIAV_j$ represent 12 sub-indicators of the main values (i = 1,...,12) and 15 sub-indicators (j = 1,...,15) of additional values. In accordance with the original definition of the *GAM* model (Vujičić et al., 2011), each of the sub-indicators can only be obtained from the following numerical values: 0.00, 0.25, 0.50, 0.75 and 1.00.

Based on the results of the evaluation, we created a matrix of basic and additional values, where the values are represented by *X* (main) and *Y* (added value) axes. The matrix is divided into nine fields (zones), which are divided by the main lines of the network represented by $Z(i,j)$, (i,j = 1, 2, 3). On the *X* axis, main line networks have a value of four, while on the *Y* axis they have five units. Compared to the hight of the mark, each estimated geosite belongs to a particular field.

The tourism potential of the given destination is determined by tourist valorization (evaluating the space and content), in terms of assessment of the possibilities for the tourism economy. It implies a qualitative and quantitative assessment of fair value of a tourist motive. The motives that get the highest value can expect the largest tourist demand so the priority is given to them. It represents the process of evaluating the space and objects and the phenomena in them as an opportunity for the activation of tourism and economy.

Necessary gradualism and systematization of the implementation of the tourist valorization process shall be based on research from the general to the particular, from literature to field observations from past to future.

According to the formula of the World Tourism Organization (WTO) we will provide an inventory and assessment of the tourism value of site Pločnik.

$$X=A+B+C+D \quad (6)$$

where in X is a summation of estimates of internal factors, A - assessment of urbanization, B - evaluation of infrastructure, C - evaluation of equipment and services, and D - the estimation of inherent characteristics.

$$Y=E+F+G+H \quad (7)$$

and Y is the sum of evaluation values of external factors of valorized values, E - accessibility assessment, F - assessment of the specificity of the resources, G- proximity to the emissive centers and H - value of resources assesment.

The research results are displayed numerically and they are ranked on a scale from 1 to 10 points.

NUMERICAL RESULTS

For this study, it is important to objectively assess the site and its 27 indicators, when using GAM model, so that the site can have its social benefits. In the group of scientific and educational value VSE, the subindicator rarity is 0.50, because in Serbia there are many sites from the Neolithic period, but this site is the only one from the Vinča-Tordoš period and in the vicinity there is only one in Macedonia.

Archaeological site Pločnik in our literature in the past is mentioned in the "color on the sidewalk" context, after 2009 the research began and it started getting the attention it deserves, that is why the representativeness is 0.25. Publications on the site for the first time appeared in 1927, they were published in German, also scientific-research works concerning the site are on international websites, and in Europe it is gaining in importance as one of the first centers of metallurgy - exploration of the site 1.00. Most of the phenomena, processes and forms can be interpreted to visitors, from the impression one gets – the level of interpretation 0.75.

All sub-indicators of landscape and aesthetic values VSA (lookouts, areas, landscapes and the surrounding nature, incorporation in the environment) are rated 0.50 on the ground that the site can clearly be seen from two angles, the area is 120 hectares, it is located in a relatively convenient location and surrounded by hospitable nature, and it partially merges with the environment. One of the important indicators of the site is the protection.

Subindicator *current state* receives a rating of 0.25 for the reason that a big problem is the ground on which the site is located because it is subject to erosion. The level of protection 0.75 at the state level and the site Pločnik is a monument of the neolithic culture (Gavrilović et al., 1998). The level of site sensitivity and erosion threatens the human factor and therefore the mark is 0.25. The number of visitors who remain in the vicinity of the site, meets a certain level of standard, the mark is 0.75.

From all the above mentioned information, we conclude that the main value of the site, in our opinion, after considering all the parameters, the site deserves 6.50 out of 12.

In the group of functional values VFn, subindicator *accessibility* deserves the highest mark of 1.00, the site can be reached by bus and train, the proximity to the highway and the railroad is 20m. Within 5km reach there are no other additional natural values of 0.00. In the vicinity of Pločnik there are sites of Roman thermal spa and the city of Milan Toplica (Vasić & Marinković, 1999) as additional anthropogenic value of 0.50. Important emissive centers nearby are Krušumlija, Prokuplje, Podujevo, Blace, therefore the subindicator deserves 0.75.

Table 2. Main and additional values of the geosite Pločnik MV

Indicators	Mark (0,00-1,00)
Scientific/educational value VSE	**2,50**
Rarity SIMV1	0,50
Representativity SIMV2	0,25
Exploration of the site SIMV3	1,00
The level of interpretation SIMV4	0,75
Landscape/aesthetic value VSA	**2,00**
Lookouts SIMV5	0,50
Surface area SIMV6	0,50
Landscape and nature around it SIMV7	0,50
Incorporation of the locality in the surroundings SIMV8	0,50
Protection VPr	**2,00**
Current state SIMV9	0,25
The level of protection SIMV10	0,75
Sensitivity SIMV11	0,25
Bearing capacity SIMV12	0,75
VSE+VSA+VPr	**6,50**
Additional values AV	
Functional values VFn	**3,00**
Accessibility SIAV1	1,00
Additional natural values SIAV2	0,00
Additional anthropogenic values SIAV3	0,50
The proximity to the emitting centers SIAV4	0,75
The proximity to the main roads SIAV5	0,75
Additional functional values SIAV6	0,00
Touristic values VTr	**2,50**
Promotion SIAV7	0,50
Organised visits SIAV8	0,25
The proximity to the visitor centres SIV9	0,25
Interpretation boards SIAV10	0,50
The number of visitors SIAV11	0,25
Tourist infrastructure SIAV12	0,00
Guide service SIAV13	0,50
The accommodation services SIAV14	0,50
Restaurant services SIAV15	0,25
VFn+VTr	**5,50**

Archaeological site Pločnik is located close to major roads, the highway E-80 Niš-Priština Fig. 2, roadway IIB No. 38 connects Blace-Beloljin as well as the roadway IIA number 213 which connects Kuršumlija-Blaževo, also in the immediate vicinity there is a railway line Niš-Kuršumlija, thus the

subindicator got 0.75. Additional functional values of 0.00 are in Kuršumlija Table 2.

Figure 1. Geographical location of Pločnik

Tourist values VTr, subindictor of site promotion 0.50, deserved its mark due to occasional conferences. Organized visits to the site appear in the form of school excursions and certain individuals, mark 0.25. In the vicinity of the site there is a visitor center Devil's Town at a distance of about 30 km and the mark is therefore 0.25. Interpretative tables deserve 0.50; there is a medium quality panel on the main road E-80, visible to visitors. Number of visitors deserves 0.25; it is not satisfactory because other than organized visits the individual visits are rare. Tourist infrastructure is 0.00, it is almost nonexistent. Travel Service, 0.50, the site meets the needs of visitors to a certain level. In the immediate vicinity of the site, there are only private accommodations and no other accommodation facilities, the closest are in Kursumlija, mark 0.50. Closest restaurant services, 0.25, can be obtained in nearby towns.

Table 3: Results of the GAM model

Results				
Main		Additional		
VSE+VSA+VPr 2,50+2,00+2,00	∑ 6,50	**VFn+VTr** 3,00+2,50	∑ 5,50	Field Z_{22}

The results of the archaeological site are shown in box Z_{22} in GAM chart. This means that the position from the obtained results represents an intermediate level Fig. 2. On the basis of mathematical and statistical analysis, the archaeological site Pločnik has a favorable "climate" for a tourist attraction .

From all of the above, we conclude that the added value of the site in our opinion, after considering all the parameters, of a possible 15 points, the site deserves 5.50 Table 3.

After a detailed analysis of the main and additional site values, following the pattern of M-GAM model, out of possible 27 points, the locality Pločnik achieved 12.00 points.

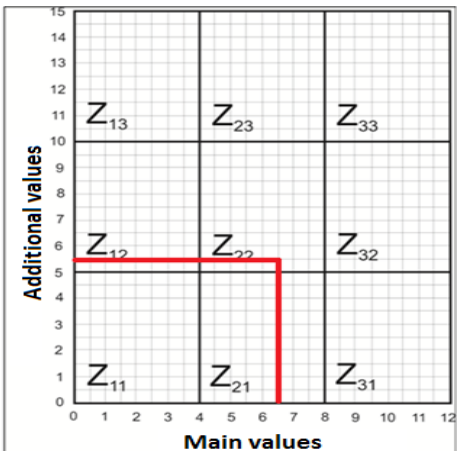

Figure 2. Graphic results of the site Pločnik GAM model

From all the above, we conclude that the site has the potential to become one of the visitor centers of the district where it is located, but in order to achieve this it must be valorized much better. That's why in the second part of our work we will try to make a sense of what should be done in order for the site to be recognized at national and even international level.

The universal formula for the calculation of tourist valorization (Stanković, 2008):

X = A + B + C + D (the sum of the assessment of internal factors)

Y = E + F + G + H (the sum of the assessment of external factors)

A – the assessment of the urbanization;

B – the assessment of infrastructure;

C – the assessment of equipment and services;

D - the assessment of inherent characteristics;

E– the assessment of accessibility;

F – the assessment of specificity of resources;

G – the assessment of the proximity to emissive centers;

H – the assessment of the importance of resources.

Site factors got relatively high marks because their condition is perfect but the problem is that they are not adequately valorized, we see in the Table 4.

Table 4. Internal and external factors of the site called Pločnik

	Factors	Mark										Total
X	Internal factors	1	2	3	4	5	6	7	8	9	10	
A	Urbanization assessment		*									
B	Infrastructure assessment								*			
C	Equipment and services assessment					*						
D	Inherent characteristics assessment								*			
	Total (X=A+B+C+D)											23
Y	External factors											
E	Accessability assessment									*		
F	The specificity of resources evaluation										*	
G	Assessment of proximity to the emitting centers					*						
H	Assessment of importance of resources										*	
	Total (Y=E+F+G+H)											34
	All together (X+Y)											57

CONCLUSION

By applying GAM model to the geosite called Pločnik and by its detailed elaboration, we recognize that the geosite is not on a satisfactory level taking into consideration the parameters set by the model. One of the key parameters that model prescribes is the appearance and rarity of the site, which by the model criterion got top marks, but the major drawback is that these two parameters are not sufficiently interpreted to the public. Another parameter which is not less important than the previous two, is the "consciousness", ie. disinterest of local population for the site, which is essential for its preservation.

On several occasions, it was attempted by means of tourist valorization to perceive all the shortcomings of the site, but each attempt was insufficiently developed. This locality, as an independent tourist value, could attract a number of tourists, but from certain groups because it represents a prehistoric way of being. Should there be unification of Toplica and Jablanica districts in terms of tourism potential, this site would be one of the major destinations on the tourist map of the district, and Serbia as well.

In an attempt to get to know the site called Pločnik, we applied two methods: GAM model and tourist valorization. We came to the conclusion that the site has resources, but it also has small shortcomings. In the vicinity of the site there is an important highway Niš-Priština, and there is also a plan for a highway leading to the Adriatic Sea to be built. Thus, with some effort, the site could become a waystation for all the users of this road.

Should there be a unification of the tourist offer of the district of Toplica, Jablanica, Ibar-Kopaonik as it did in Western Serbia, a tourist offer could be created and it would bring together all the potential of this part of Serbia including the site Pločnik.

In our opinion, for the tourists who travel from Bulgaria to Kopaonik, a tourism offer might look like this: Niš, Prokuplje, PLOČNIK, Prolom Spa, Devil's town, Prolom Spa, Kuršumlija's Spa, Kopaonik (the source of Toplice River) Jošanička banja, Župa's vineyards, Ćelije Lake and the church Lazarica in Kruševac. This way, we would get a round of complementary-complex tourist values.

REFERENCES

Bruschi, V.M., & Cendrero, A. 2005. Geosite evolution. Can we measure intantgible values?. II Quaternario, 18(1), pp. 293-316.

Coratza, P., & Giusti, C. 2005. Methodological proposal for the assessment of the scientific quality of geomorphosites. II Quaternario, 18(1), pp. 307-313.

Gavrilović, D., Menković, L.J., & Belij, S. 1998. Zaštita geomorfoloških objekata u geonasleđu Srbije.Beograd: Zavod za zaštitu prirode Srbije.

Hose, T.A. 1997. Geotourism-selling the earth to Europe. In P.D. Marinos, G.C. Koukis, G.C. Tsiambaos, & G.C. Stournaras Eds., Engineering geology and the environment. Rotterdam: A. A Balkema., pp. 2955-2960.

Hose, T.A., Marković, S.B., Komac, B., & Zorn, M. 2011. Geotourism: A short itroduction. Acta Geographica Slovenica, 51(3), pp. 339-342.

Pereira, P., Pereira, D., & Alves, C. 2007. Geomorphosite assessment in Montesinho Natural Park (Portugal). Geographica Helvetica, 62, pp. 150-168.

Pralong, J.P. 2005. A method for assessing the tourist potential and use of geomorphological sites. Géomorphologie. Relief, Processes, Environnement, 3, pp. 189-196.

Reynard, E. 2008. Scientific research and tourist promotion of geomorphological heritage. Geografia fisica e dinamica quaternaria, 31(2), pp. 225-230.

Reynard, E., Fontana, G., Kozlik, L., & Scapozza, C. 2007. A method for assessing "scientific" and "additional values" of geomorphosites. Geographica Helvetica, 62(3), pp. 148-158.

Serrano, E., & González-Trueba, J.J. 2005. Assessment of geomorphosites in natural protected areas: The Picos de Europa National Park (Spain). Géomorphologie, Formes, Processus, Environnement, 3, pp. 197-208.

Stanković, S. 2008. Turistička geografija. Beograd: Zavod za udžbenike.

Vasić, M., & Marinković, D. 1999. Prokuplje u Praistoriji, Antici i Srednjem veku. Beograd: Arheološki Institut.

Vujičić, M.D., Vasiljević, D.A., Marković, S.B., Hose, T.A., Lukić, T., Hadžić, O., & Janićević, S. 2011. Preliminary geosite assessment model (GAM) and its application on Fruška Gora Mountain, potential geotourism destination of Serbia. Acta Geographica Slovenica, 51(2), pp. 361-377.

Zouros, N.C. 2007. Geomorphosite assessment and management in protected areas of Greece. The case of the Lesvos island coastal geomorphosites. Geographica Helvetica, 62, pp. 169-180.

Retrieved from http://muzejtoplice.org.rs/

Retrieved from http://plocnik.org.rs/

Retrieved from http://www.prokuplje.org.rs/

UNIVERSITY THOUGHT
Publication in Natural Sciences, Vol. 7, No. 1, 2017, pp. 32-35.
doi:10.5937/univtho7-14156
Original Scientific Paper

ANALISYS OF THE INFLUENCE OF COMMUNICATION PARAMETERS OF FSO CHANNELS ON THE RECEPTION QUALITY

ALEKSANDAR MARKOVIĆ[1*], STEFAN PANIĆ[1], BRANIMIR JAKŠIĆ[2], PETAR SPALEVIĆ[2], MARKO SMILIĆ[1]

[1]Faculty of Natural Sciences and Mathematics, University of Priština, Kosovska Mitrovica, Serbia
[2]Faculty of Technical Sciences, University of Priština, Kosovska Mitrovica, Serbia

ABSTRACT

In this paper, the signal transmission in the Free-Space Optics (FSO) communication system using the software package OptiSystem 7.0 is analyzed. The influence of parameters FSO (Free-Space-Optics) channels (Range, Attenuation, Beam Divergence, Transmitter Loss, Receiver Loss, and Additional Losses) on the reception quality is considered. The reception quality is analyzed according to the values of BER (Bit Error Ratio) and Q factor. Graphics and tables of the changes of BER and Q factor depending on the parameters of FSO are given. Also, the eye diagrams for the characteristic parameter values are given.

Keywords: Free-Space Optics (FSO), BER (Bit Error Ratio), Additional Losses, Q factor.

INTRODUCTION

Some specific applications require relatively quick point-to-point high bandwidth and low cost connectivity. Typically, such applications aggregate multi-type traffic at an access enterprise point and transport it to another point located from hundreds of meters to few kilometers away. This technology does not use fiber on the link but a laser beam in free space and therefore it necessitates line of sight; typically from rooftop to rooftop. Because this technology does not need fiber installation and right-of-way licenses, it is deployed quickly and inexpensively (Kartalopoulos, 2008; Zyskind & Berry, 2002).

However, FSO (Free-Space-Optics) has a severe drawback. Laser light is severely absorbed by fog but not as much by rain. Interestingly, microwaves are affected by rain and not as much by fog. Thus, the two technologies are complementary and can work side by side. If fog is present, the microwave link switches in and if not the FSO does. FSO is preferred because it can transport much more bandwidth (more than 1 Gb/s) than the microwave link (few Mb/s) (Kartalopoulos, 2008).

FSO technology may also include multiple wavelengths thus utilizing WDM (Wavelength Division Multiplexing) technology, in which case the aggregate bandwidth is multiplied by the number of wavelengths in the beam (Agrawal, 2001; Agrawal, 2002).

FSO is already considered in satellite network applications to interconnect a cluster of satellites in a 3-D mesh topology (Kartalopoulos, 1997; Ramaswami & Sivarajan, 2002). Optical transmitters suited to this application use neodymium yttrium-aluminum-garnet (YAG) solid-state lasers. Although satellites are thousands of kilometers apart, space is free from atmospheric phenomena and exerts insignificant attenuation and thus a laser beam travels far. However, maintaining connectivity as satellites move requires good tracking. In addition, as the laser beam travels for many kilometers it diverges and thus the receiver must have a large aperture telescope, typically about 10 cm in diameter (Kartalopoulos, 2008).

Installation of FSO is relatively simpler and faster (about a day) than the typical fiber-optic network (weeks to months). FSO transceivers are installed on top of existing buildings (some deployments provide links from window to window). FSO needs no spectrum licensing since it does not use radio electromagnetic waves. It is immune to electromagnetic interference. It does not impose any hazard to life as the laser beam is few megawatts (it uses typical communication laser devices (800–1,550 nm).

FSO links are short (~ 2 km) as compared with fiber optic links (20–100 km). FSO links provide less bandwidth (~ 2.5 and perhaps 10 Gb/s) than fiber optic links, which can carry aggregate traffic exceeding Tb/s. FSO suffers from fog and heavy snow attenuation.

The attenuation and the wavelength over the FSO link is related to particle parameter $\sigma = 2\pi r/\lambda$, where it is assumed that particles are spherical with radius r. In general, the longer the wavelength, the lower the atmospheric attenuation and therefore most FSO systems prefer wavelengths at 1,550 nm over 800 nm, in addition (Kartalopoulos, 2008; Goralski, 2001).

FSO suffers from scattering caused by particles airborne in the atmosphere. Scattering is classified into three mechanisms: Rayleigh, Mie, and Geometric (Ramaswami & Sivarajan, 2002). FSO suffers from scintillation caused by air temperature fluctuations and atmospheric turbulence. However, attenuation due to scintillation is small (few dB/km) as compared with fog and snow (medium fog 30 dB/km attenuation and thick fog with >50 dB/km attenuation) (Kartalopoulos, 2008; Zyskind & Berry,

* Corresponding author: aleksandar.markovic@pr.ac.rs

2002). FSO requires accurate line of sight alignment. The transceiver aperture and tracking mechanisms must account for sway of tall buildings during strong winds to maintain alignment.

The output laser beams comply with the Gaussian beam distribution with beam divergences of 6 mrad for the 830 nm and 12 mrad at 1550 nm wavelengths (Pesek et al., 2010).

SYSTEM MODEL

The appearance of the network for analysis in OptiSystem (Spalevic et al., 2012) software is given in Fig. 1. It consists of an optical source, FSO channel, optical receiver, and BER analyzer. The intensity emitted by the source is 10 dBm. The system operates at a wavelength of 830 nm. FSO channel parameters are: Beam Divergence = 6 mrad, Transmitter Loss = 1 dB, Receiver Loss = 1 dB, Additional Losses = 1 dB. Range (R) is moving in the scale from 0.25 to 2 km, and Attenuation (A) has a value of 10 dB/km, 20 dB/km, 30 dB/km, 40 dB/km, 50 dB/km, 60 dB/km and 70 dB/km.

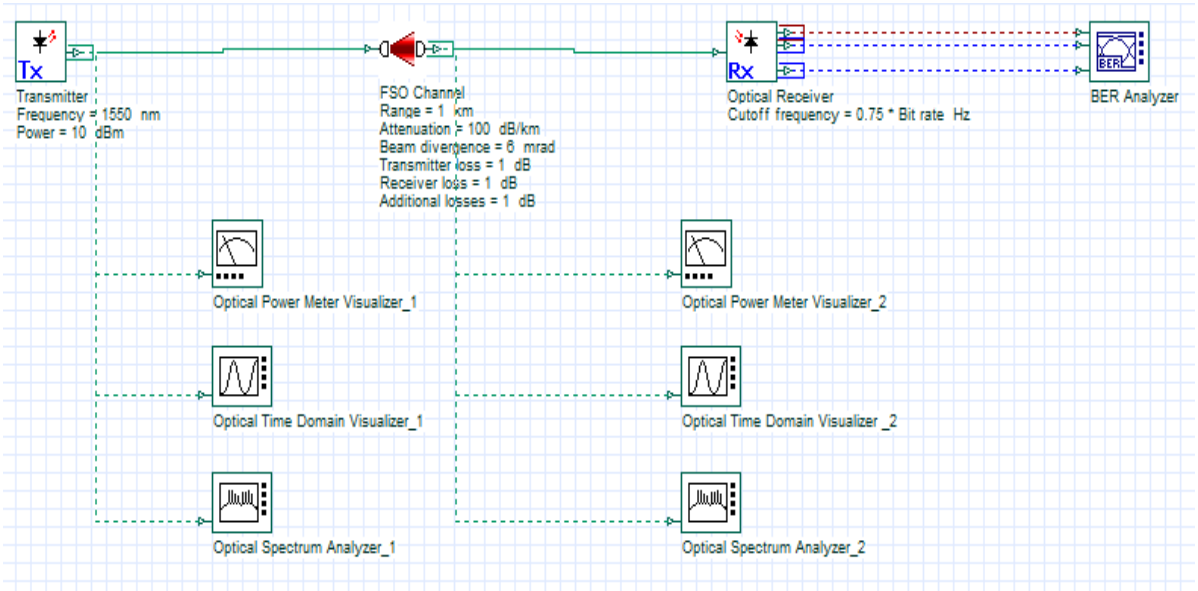

Figure 1. The change of the Q factor depending on the length of FSO channel

The criteria that is commonly applied to the optical receiver is that Bit Error Ratio (BER) is less than 10^{-9}. BER with optimal decision threshold adjustment depends only on Q parameter:

$$BER = \frac{1}{2} erfc\left(\frac{Q}{\sqrt{2}}\right) \approx \frac{\exp\left(-Q^2/2\right)}{Q\sqrt{\pi}}, \quad (1)$$

where *erfc* is complementary error function (Abramowitz & Stegun), defined as:

$$erfc(x) = \frac{2}{\sqrt{\pi}} \int_x^{+\infty} \exp\left(-y^2\right) dy. \quad (2)$$

Parameter Q can be written as (Agrawal, 2001; Agrawal, 2002):

$$Q = \frac{I_0 + I_1}{\sigma_0 + \sigma_1} \quad (3)$$

where σ_1^2 and σ_0^2 are respectively appropriate noise variance for the symbols 1 and 0. In WDM networks, the transmission quality is achieved for values of Q> 5.4.

SIMULATION RESULTS

Fig. 2 shows the change of Q factor depending on the length of the FSO channels, and for different values Attenuation (A) is shown.

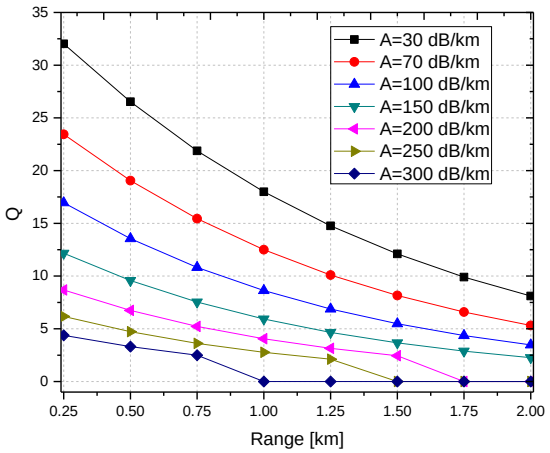

Figure 2. The change of the Q factor depending on the length of FSO channels.

This figure shows that Q factor decreases with the length of the FSO channel. If we take Q=5.4 as a border of transmission quality, we can see that only for A = 10 dB / km we have quality transmission over the entire section of 2 km. With the reduction of A = 60 dB / km and 70 dB / km, transmission quality cannot be achieved over 250 m.

Fig. 3 shows the curve of the Q factor for A=10 dB/km and for the Range 0.25 km and 1.5 km. The maximum value of the Q factor is lower for longer FSO channels.

In Table 1 are given the values of BER parameter, obtained in the simulation for the above mentioned parameters. The values of BER parameter increase with the increasing length of FSO channels and with increasing attenuation.

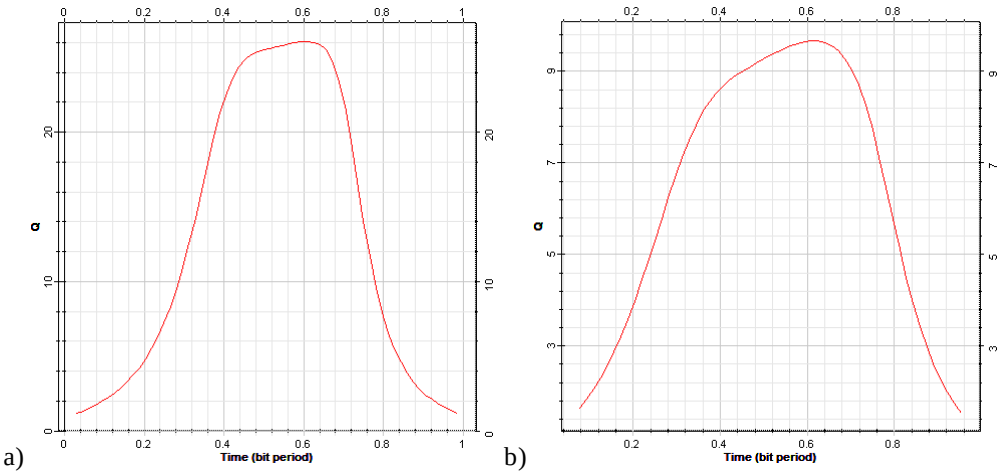

Figure 3. Diagram of Q factor for A=10 dB/km, and a) R=0.25 km, and b) R=1.5 km.

Table 1. BER values for different values of the length of FSO channels and attenuation

Attenuation	**0.25 km**	**0.5 km**	**0.75 km**	**1.0 km**
10 dB/km	2.3972E-255	2.2336E-155	1.9694E-106	1.1099E-072
20 dB/km	7.1062E-122	2.9390E-081	4.0252E-054	3.8309E-036
30 dB/km	8.9430E-065	3.8439E-042	1.4409E-027	3.2085E-018
40 dB/km	2.4592E-034	4.9831E-022	2.4326E-014	1.5470E-009
50 dB/km	1.9788E-018	7.9352E-012	8.4216E-008	2.4572E-005
60 dB/km	3.3589E-010	1.1310E-006	1.4633E-004	2.7726E-003
70 dB/km	5.9936E-006	4.6738E-004	6.1889E-003	1
Attenuation	**1.25 km**	**1.5 km**	**1.75 km**	**2.0 km**
10 dB/km	1.2298E-049	5.2744E-034	1.9268E-023	2.5616E-016
20 dB/km	2.7156E-024	1.6804E-016	2.2187E-011	5.2056E-008
30 dB/km	3.1220E-012	2.1608E-008	6.3911E-006	2.5368E-004
40 dB/km	1.5795E-006	1.2400E-004	1.9817E-003	1.1758E-002
50 dB/km	8.1565E-004	7.2588E-003	1	1
60 dB/km	1.6857E-002	1	1	1
70 dB/km	1	1	1	1

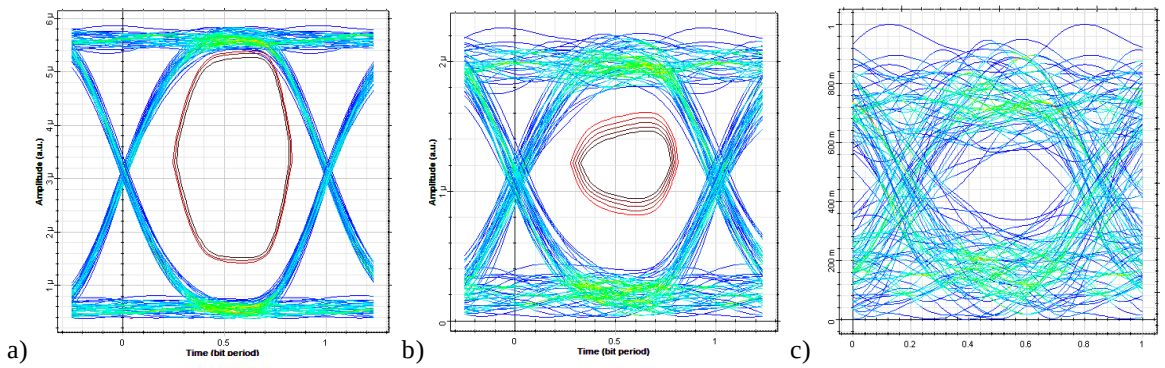

Figure 4. Eye diagram for the length of FSO channels of 0.25 km and a) A=10 dB/km, b) A=40 dB/km, and c) A=70 dB/km.

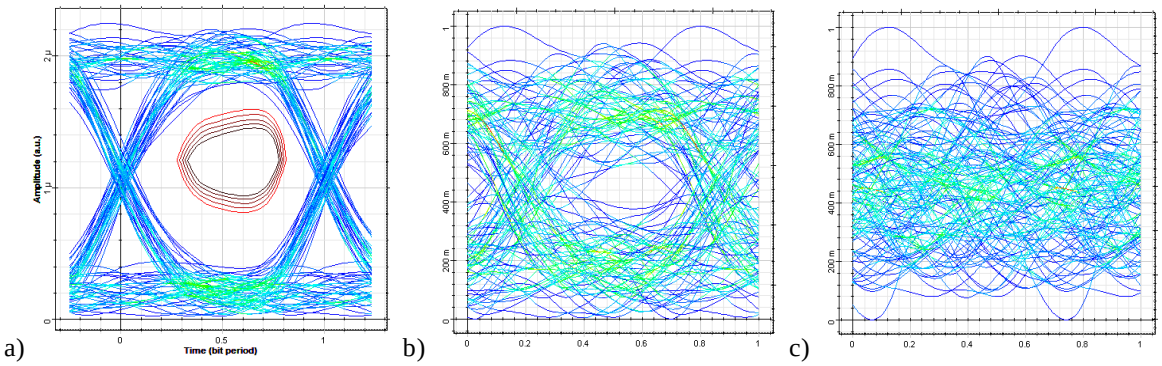

Figure 5. Eye diagram for the length of FSO channels of 1.5 km and a) A=10 dB/km, b) A=40 dB/km, and c) A=70 dB/km.

Fig. 4 gives the appearance of eye diagram for the case of the transmission of 0.25 km, and Fig. 5 gives eye diagram for the case of the transmission of 1.5 km of FSO channels. Closed curves represent sectors of BER values from 10^{-8} to 10^{-12}. The opening of the eye corresponds to a change of the Q-factor in Fig. 2, and to a change of BER parameter in Table 1.

CONCLUSION

The influence of communication parameters on quality transmission is shown by simulation of FSO channels in the software package OptiSystem. The quality of signal transmission is estimated based on the obtained value, the Q factor, and BER for different values of the length of FSO channels and Attenuation. Based on the obtained values, optimum FSO systems can be projected with high-quality signal transmission.

REFERENCES

Abramowitz, M., & Stegun, I.A. 1970. Handbook of Mathematical Functions.Dover.

Agrawal, G.P. 2001. Nonlinear Fiber Optics.Academic Press, Elsevier.

Agrawal, G.P. 2002. Fiber-Optic Comunication Systems.Wiley.

Goralski, W. 2001. Optical Networking & WDM.McGraw-Hill Companies.

Kartalopoulos, S.V. 1997. A global multi-satellite network for multi-media and PCS services with fault and disaster avoidance characteristics., pp. 694-698.

Kartalopoulos, S.V. 2008. Next Generation Intelligent OpticalNetworks: From Access to Backbone.Springer.

Pesek, J., Fiser, O., Svoboda, J., & Schejbal, V. 2010. Modeling of 830 nm FSO Link Attenuation in Fog or Wind Turbulence. Radioengeenering, 19(2), pp. 237-241.

Ramaswami, C.R., & Sivarajan, K. 2002. Optical Networks: A Practical Perspective.Elsevier.

Spalevic, P., Milic, D., Jaksic, B., Petrovic, M., & Temelkovski, I. 2012. Simulation influence of the thermal noise of PIN photodetector on performance DWDM optical network. ICEST, 2, pp. 315-318.

Zyskind, Z., & Berry, R. 2002. Optical Fiber Telecommunications IV-B.Academic Press, Elsevier.

UNIVERSITY THOUGHT
Publication in Natural Sciences, Vol. 7, No. 1, 2017, pp. 36-40.
doi:10.5937/univtho7-14347
Original Scientific Paper

CHARACTERISTICS OF HYBRID BROADCAST BROADBAND TELEVISION (HBBTV)

BRANIMIR JAKŠIĆ[1*], IVANA MILOŠEVIĆ[2], MILE PETROVIĆ[1], SINIŠA ILIĆ[1], SLOBODAN BOJANIĆ[3], SELENA VASIĆ[4]

[1]Faculty of Technical Sciences, University of Priština, Kosovska Mitrovica, Serbia
[2]High School of Electrical Engineering and Computers, Belgrade, Serbia
[3]ETSI Telecomunicacion, Universidad Politecnica de Madrid, Madrid, Spain
[4]Faculty of Information Technology, University of Metropolitan, Belgrade, Serbia

ABSTRACT

This paper describes the working principle of hybrid broadcast-broadband TV (Hybrid Broadcast Broadband TV - HbbTV). The architecture of HbbTV system is given, the principle of its operation, as well as an overview of HbbTV specification standards that are in use, with their basic characteristics. Here are described the services provided by Hybrid TV. It is also provided an overview of the distribution of HbbTV services in Europe in terms of the number of TV channels that HbbTV services offer, the number of active hybrid TV devices, HbbTV standards which are in use and models of broadcast networks used to distribute HbbTV service.

Keywords: Hybrid TV, HbbTV, broadcasting networks, broadband networks, digital terrestrial TV, cable, satellite, IPTV.

INTRODUCTION

The Internet has grown into a massive medium for delivering large amounts of data on various topics. Digitization of television, as second massive media, and the rapid development of the Internet lead to need to connect these two media. Hybrid broadcasting wideband television (Hybrid Broadcast Broadband TV - HbbTV) is a global initiative aimed at harmonizing standards for content delivery to the end user, while using, at the same time, the broadcasting (broadcast) and wideband (broadband) network via the linked TV devices (connected TV, Smart TV) and Set -Top-Boxes (HbbTV website, 2016), (Illinger, 2012). Actually, HbbTV is a technology that combines broadcasting services with services offered over the internet – all at one screen.

Unlike the traditional television, where the user is a passive observer, hybrid TV users can use interactive applications for entertainment or to obtain information.

A wide variety of additional services which Allows HbbTV can be divided into the following categories (Merkel, 2010):

- Voice subtitles, audio of other languages.
- E-Administration, "a digital counter" for the services of the national government or local authorities.
- "Super text" - an advanced teletext with a more attractive user interface with informations (news, weather, traffic, sports scores, stock market, etc.). Thanks to HTML (Hyper Text Markup Language) and connecting to the Internet, images, graphs, maps, and similarly can be displayed within the Super-text.
- Advanced Electronic Program Guide - EPG (Electronic Program Guides).
- Enhanced TV - Additional information on TV programs such as statistics in sports programs, adds with biographies, background events, etc.
- The vote, participation in TV shows, vote for candidates in shows and other.
- Additional services such as "catch up TV" - delayed viewing of the TV programs, restoration of the TV program, video on demand (VOD - Video on Demand), picture in picture and other.
- Direct access to additional TV channels which are not represented in cable systems, digital terrestrial or satellite television via live streaming (over 15,000 channels worldwide).
- Simple games on television.
- Home Shopping, courses, tele-education.

Fig. 1. HbbTV applications of RTL Germany.

* Corresponding author: branimir.jaksic@pr.ac.rs

Fig. 2. HbbTV applications of France 2 TV.

Fig. 3. Advanced EPG within the HbbTV applications of German ARD.

In Fig. 1 (Heise website, 2016), Fig. 2 (Forumdesforums website, 2016) and Fig. 3 (Parabola website, 2016), is given appereance of applications HbbTV RTL, France 2 and ARD TV.

ARCHITECTURE OF HBBTV SYSTEM

HbbTV uses two networks - broadcasting and broadband to deliver data and applications on hybrid devices (terminals). Typical hybrid devices are Internet-connected (Internet-connected) TV sets and Set-Top Boxes, computers with tuners and mobile phones with broadcast receivers. Today, many manufacturers of consumer electronics offer Internet-connected TVs and Set-Top-Boxes. There are different names for these solutions, such as Smart TV and NetTV (Clover, 2009).

Hybrid terminal has the ability to be connected to the two networks in parallel. On the one hand it can be one of broadcast DVB network (terrestrial DVB-T, DVB-S satellite or cable DVB-C). Through this broadcasting connection the hybrid terminal can receive the standard broadcasting A / V (ie. A linear A / V content), applications and signaling. Even if the terminal is not connected to a broadband network, its connection with the broadcasting network allows it to receive feasts applications. In addition, the signaling stream events in the application are possible via the broadcasting network.

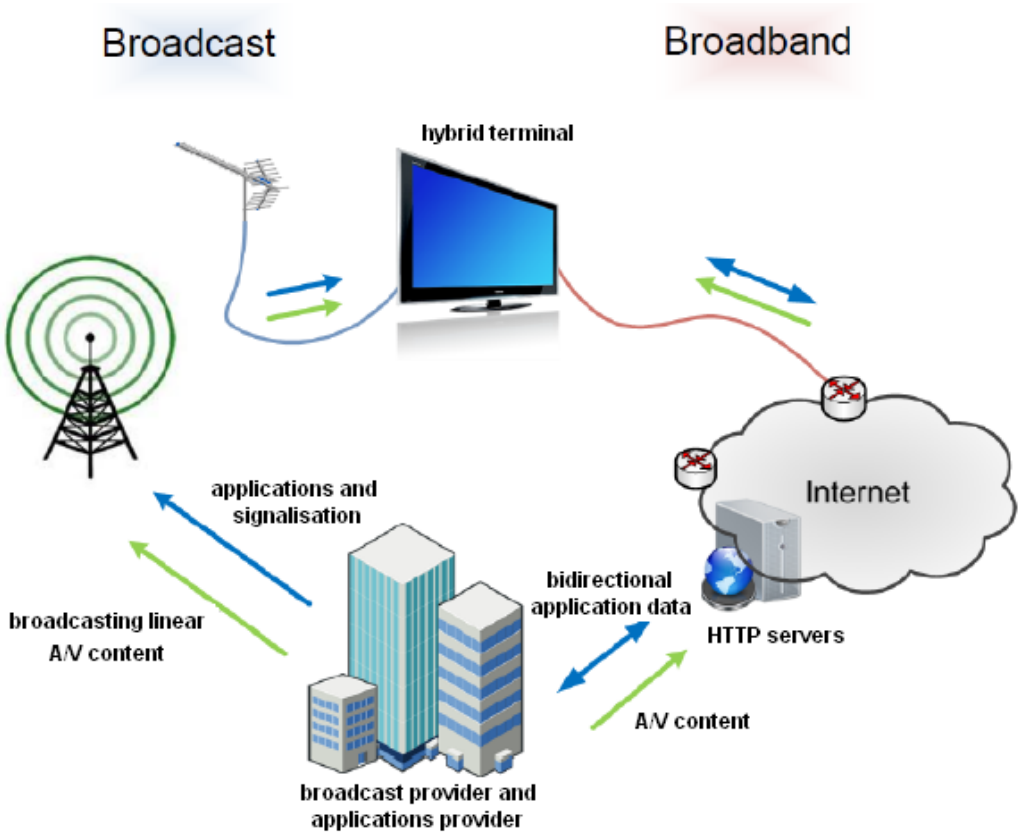

Fig. 4. Architecture of HbbTV system.

The hybrid terminal can be connected to the Internet via a broadband interface. This connection allows two-way communication with the provider applications. Through this interface terminal can receive the applications and the non-linear A / V content (e.g., streaming A / V content on the request). The hybrid terminal can support download A / V content is independent of the weather. Through broadband interface, the terminal can also be connected to other HbbTV terminals in the same local area network (HbbTV website, 2015).

Fig. 4 shows the architecture of a system with a hybrid terminal connected with the DVB-T network as an example of the broadcasting connection.

HBBTV SPECIFICATIONS

HbbTV standards are developed by the HbbTV Association, and published by the ETSI (European Telecommunications Standardization Institute). HbbTV Association was established in February 2009.

First demonstration of HbbTV was in 2009 in France by France Télévisions and two makers of Set-Top-Box technology, Inverto Digital Labs, Luxembourg, PLEYO from France, during Roland Garros using DTT transmission and IP connections and in Germany using satellite Astra 19.2° east, during IFA and the IBC exhibitions.

In June 2014, HbbTV Association is connected to the Open IPTV Forum (IPTV Forum website, 2016), a similar industrial organization for Internet Protocol television (IPTV) services established in 2007, which has worked closely with the HbbTV initiative on specification network connected TVs and Set-Top Boxes. Activities of Open IPTV Forum are transferred to the jurisdiction of the HbbTV Association. This extended the jurisdiction of HbbTV Association includes defining specifications for providers services which make it easier to accelerate the implementation of IPTV services

HbbTV Specification Version 1.0 (HbbTV specifications, 2010), was approved by ETSI as ETS TS 796, in June, 2010. In Table 1, are given the lables of HbbTV specification standards and appropriate ETSI approvals (HbbTV website, 2016).

Table 1. HbbTV Specifications.

HbbTV specifications	ETSI approval	Year
HbbTV 1.0	TS 102 796 v1.1.1	June, 2010.
HbbTV 1.5	TS 102 796 v1.2.1	November, 2012.
HbbTV 2.0	TS 102 796 v1.3.1	November, 2015.

HbbTV specification is built on existing standards and web technologies including OIPF (Open IPTV Forum), Consumer Technologies Association (CTA website, 2016), DVB-Digital Video Broadcasting) (DVB website, 2016) and the W3C (World Wide Web Consortium website, 2016). Standard provides the features and functionality which is required to meet the standards of good broadcasting and Internet services. By using the standards of Internet technologies, rapid development of applications is enabled.

HbbTV specification with label 1.5 provides the features and functionality needed to deliver a variety of services for broadcasting. HbbTV specification 1.5 introduces support for HTTP adaptive streaming based on MPEG-DASH specification, which improves video quality on too burdened or slow internet connections. Version 1.5 greatly improves access to informations which are related to the television program given by providers via EPG.

HbbTV Association has announced in 2015 a new HbbTV 2.0 specification. HbbTV Association expects that the manufacturers, broadcasters and operators will start to introduce a new generation of hybrid interactive TV service in 2016 (HbbTV website, 2016).

With HbbTV 2.0, consumers will be able to enjoy a wide range of new services, including (HbbTV website, 2016):

- Advanced user applications based on the HTML5.
- Watching video content via smartphone, PC and tablet devices.
- Advanced supporting applications about detailed review of the program, voting, games and more.
- Standardized delivery of Ultra HD content using HEVC compression standard.
- Improvement of services with better support for translation in multiple languages.
- Access to broadcasting content recorded on the hard disk of the receiver.
- Support for consumer privacy.

To achieve all these benefits, the new specification includes a series of new technologies, including support for HTML5, DVB CI Plus 1.4, HEVC video and TTML subtitles (Timed Text Markup Language). It also improves support for existing technologies, including MPEG DASH, DSM-CC (Digital Storage Media Command and Control) and synchronization applications on the TV. It is designed to ensure that HbbTV HbbTV 1.0 and 1.5 applications continue to work on the HbbTV 2.0 devices.

HBBTV IN EUROPE

At the moment HbbTV is the most developed in Germany, France and Spain. HbbTV is started in the German public service broadcasters - ARD and ZDF and France - France Télévision. Other countries where the HbbTV services are regularly provided are: United Kingdom, Belgium, Netherlands, Switzerland, Austria, Poland, Czech Republic, Denmark and Finland, and since 2016, and Norway and Sweden (Girons, 2015). Fig. 5 gives the situation in broadcasting HbbTV services in European countries on 1 January 2016.

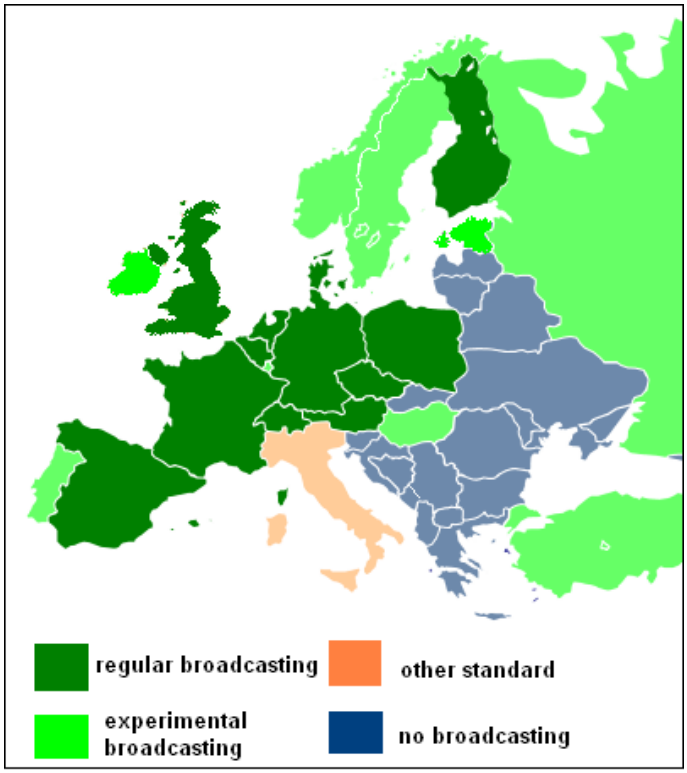

Fig. 5. Broadcast HbbTV services in Europe.

In European countries, forms of distribution of TV programs are variously represented. Table 2 contains the representation in% of digital terrestrial TV (DTT - Digital terrestrial television), satellite, cable, and IPTV in the distribution of TV channels to end-users in the second half of 2015 (Girons, 2015). The most common form of distribution in one country entails that the HbbTV services are most used in that system (broadcasting network).

Table 2. Representation of Terrestrial, Satellite, Cable and IPTV Systems in Europe

Country	Households [million]	DTT [%]	Satellite [%]	Cable [%]	IPTV [%]
Germany	38.5	9	43	43	4
France	27.0	42	18	6	34
Spain	19.0	81	4	15	
Austria	3.6	6	53	41	
Poland	13.5	28	54	16	2
Netherlands	17.0	6	6	62	26
Switzerland	3.3	3	10	56	31
Czech Rep.	4.5	44	38	13	5
Denmark	5.6	14	9	74	3
Finland	2.4	46	3	43	8
Sweden	4.5	25	15	50	10
Norway	2.2	10	31	59	
Hungary	4.2	18	23	55	4

The first HbbTV services in Germany started its work in 2010. Number of HbbTV devices in use in Germany in 2015 amounted to 12 million. HbbTV services are available in all broadcast networks (satellite, cable, terrestrial and IPTV) with 75 TV channels. Included standard is HbbTV 1.0 (Girons, 2015).

In France, the HbbTV services regularly begin to work in 2011. Number of active HbbTV devices in 2015 was about one million. HbbTV services are available in all broadcasting networks. In use are the standards HbbTV 1.0 and 1.5. Currently, the HbbTV service is available in about 15 TV channels. MyTF1 VOD is the first TNT2.0 service based on HbbTV 1.5 using MPEG-DASH adaptive streaming (Girons, 2015).

In Spain HbbTV services began to operate in 2013. Nearly 1.5 million HbbTV devices are in use in 2015. HbbTV services are the most represented in digital terrestrial TV and in 15 TV channels. In use is HbbTV standard 1.5. TDT Hibrida is the Spanish HbbTV DTT 1.5 specification.

The UK has a hybrid services that are broadcast through the MHEG-5.United Kingdom launched interactive television with the included MHEG-5 in its digital terrestrial TV since 2012. Since October 2015, launched the services Freeview Play platform by using standard HbbTV 2.0. Among the TV channels which provide these hybrid services are BBC, Channel 4, Channel 5, ITV and others. The service is available within the digital terrestrial and satellite TV.

In Poland HbbTV services are available in all broadcasting networks. In use is an upgraded version of the standard HbbTV 1.0 - 1.1 HbbTV. All public and a large number of TV channel offers HbbTV services (Dziadul, 2015).

In Austria, all HbbTV services are available for all types of broadcast networks. HbbTV services are available in 6 TV channels, as well as in the German TV channels available via satellite. They use about one million HbbTV devices. Used HbbTV 1.0 standard (ORF website, 2015).

In Belgium, the HbbTV services are available through the Walloon RTBF in the digital terrestrial network (DTT).

Dutch broadcasters for distributing HbbTV services are using standard HbbTV 1.5. The most significant emitters are NSO and SPS.

In Switzerland in 2015. were already 2 million HbbTV devices. In use is the HbbTV standard 1.0, and 1.5 and 2.0 are tested. HbbTV services provide all public broadcasters (6 TV channels in French, Italian and German), as well as other German and French broadcasters. HbbTV services are distributed through satellite and cable systems (Girons, 2015).

Broadcasters in the Czech Republic for distribution HbbTV services using standard HbbTV 1.0 (RTS website, 2014). During 2015, there were 740,000 hybrid connected TV devices.

In Denmark, the distribution of HbbTV services uses standard HbbTV 1.1 and services are available in cable, terrestrial and IPTV systems. During 2015, there were 240,000 active hybrid TV devices.

In Finland, the distribution of HbbTV services uses standard HbbTV 1.1 and HbbTV 1.5. HbbTV services are mostly represented in the digital terrestrial TV (DTT) (Sofiadigital website, 2015).

In Norway and Sweden HbbTV services will regularly begin with operations during 2016. Since 2014. They are in the test phase, and for distribution HbbTV services uses the standard HbbTV 1.5.

In Hungary HbbTV services are provided by Antenna Hungaria (Antenna Hungária website, 2016) in the digital terrestrial network, using standard HbbTV 1.0. In 2015, there were 200,000 active HbbTV devices.

Russia has been got in 2013., within the DVB-T2 network, the first HbbTV services. HbbTV services are available in some pay TV operators (RTS website, 2013).

In Estonia, the HbbTV services were launched in the beginning of 2015. in the context of digital terrestrial TV (RTS website, 2015).

In Italy is not in use HbbTV standard, for Interactive TV is used MHP (Multimedia Home Platform) Hybrid TV. It was developed by the DVB Project in 2000. MHP is a Java-based middleware system originally designed for telephone line with interactive channels. Fast internet now allows that potential of MHP can be fully realized. Interactive TV has been a fundamental element for the launch of digital terrestrial television in Italy and MHP was at the center of this offer.

CONCLUSION

The introduction of the Hybrid Broadcast Broadband TV (HbbTV) enabled offering a wide range of interactive services to the end users. HbbTV provides a direct connection between the linear programs and online content. HbbTV is directly implemented at the so-called. "Connected TV" or appropriate Set-Top-Boxes, without purchasing additional equipment. Providers only need to develop applications in accordance with one of the HbbTV standard, instead of creating different versions of applications for each model of TV or for each model of Set-Top-Box. A large number of European countries included HbbTV services and the most common are in Germany, France, Spain, Austria and Poland. During 2015, more than 90% of all manufacturers of TV equipment have adopted the HbbTV standard (Gesellschaft für Konsumforschung website, 2016). It is estimated that in 2016 more than 50% of all TVs available in homes in Europe will be compatible for HbbTV.

ACKNOWLEGMENTS

This work was done within the Erasmus Plus Capacity-Building projects in the field of Higher Education: “Implementation of the Study Program - Digital Broadcasting and Broadband Technologies (Master Studies)”, Project No. 561688-EPP-1-2015-1-XK-EPPKA2-CBHE-JP.

REFERENCES

-Antenna Hungária. (2016). . website. Retrieved from www.ahrt.hu

Clover, J. 2009. EBU General Assembly backs HBB.Broadband TV News.

-Consumer Technology Association (CTA). (2016). . website. Retrieved from https://www.cta.tech/

-Digital Video Broadcasting (DVB). (2016). . website. Retrieved from https://www.dvb.org/

Dziadul, C. 2012. HbbTV starts in Poland.Broadband TV News.

-Forumdesforums. 2016. Forumdesforums website. Retrieved from http://www.forumdesforums.com/modules/news/article.php?storyid=62067

-Gesellschaft für Konsumforschung (Gfk SE). (2016). . website. Retrieved from www.gfk.com

Girons, R.S. 2015. Country Review Europe. . In: HbbTV Symposium, 2015-12-08, London.

-European Telecommunications Standards Institute (ETSI). 2010. HbbTV specifications. TS 102 796 V1.1.1..

-HbbTV Association. 2015. HbbTV 2.0 Specification. Retrieved from https://www.hbbtv.org/wp-content/uploads/2015/07/HbbTV_specification_2_0.pdf

-HbbTV. (2016). . website. Retrieved from http://www.hbbtv.org/

-Heise. 2016. RTL startet HbbTV Regelbetrieb mit HD. website. Retrieved from http://www.heise.de/newsticker/meldung/RTL-startet HbbTV-Regelbetrieb-mit-HD-Videotext 1070641.html?view=zoom;zoom=1

Illgner, K. 2012. HbbTV Roadmap.HbbTV Consortium.

Merkel, K. 2010. HbbTV: A hybrid broadcast-broadband system for the living room.Munich: IRT.

-Open IPTV Forum. (2015). . website. Retrieved from www.oipf.tv

-Österreichischer Rundfunk (ORF). (2015). . website. Retrieved from www.orf.at

-Parabola. (2016). . website. Retrieved from http://www.parabola.cz/clanky/4738/hbbtv-jiz-take-na-pristrojich-vu-plus/

-RTS. 2013. HbbTV platforma u Rusiji. website. Retrieved from www.rts.rs/page/rts/sr/Digitalizacija/story/1578/Svet/1453053/HbbTV+platforma+u+Rusiji.html

-RTS. 2014. HbbTV napreduje u Češkoj. website. Retrieved from http://www.rts.rs/page/rts/sr/Digitalizacija/story/1578/Svet/1770379/HbbTV+napreduje+u+%C4%8Ce%C5%A1koj.html

-RTS. 2015. HbbTV stiže u Estoniju. website. Retrieved from http://www.rts.rs/page/rts/sr/Digitalizacija/story/1578/Svet/1857203/HbbTV+sti%C5%BEe+u+Estoniju.html

-Sofiadigital. 2015. Finland is setting the standard for connected TV services. website. Retrieved from http://sofiadigital.com/finland-is-setting-the-standard-for-connected-tv-services/

-World Wide Web Consortium. (2016). . website. Retrieved from https://www.w3.org/

UNIVERSITY THOUGHT
Publication in Natural Sciences, Vol. 7, No. 1, 2017, pp. 41-45.
doi:10.5937/univtho7-14337
Original Scientific Paper

DETERMINATION OF ACCELERATED FACTORS IN GRADIENT DESCENT ITERATIONS BASED ON TAYLOR'S SERIES

MILENA PETROVIĆ[1*], NATAŠA KONTREC[1], STEFAN PANIĆ[1]

[1]Faculty of Natural Science and Mathematics, University of Priština, Kosovska Mitrovica, Serbia

ABSTRACT

In this paper the efficiency of accelerated gradient descent methods regarding the way of determination of accelerated factor is considered. Due to the previous researches we assert that the use of Taylor's series of posed gradient descent iteration in calculation of accelerated parameter gives better final results than some other choices. We give a comparative analysis of efficiency of several methods with different approaches in obtaining accelerated parameter. According to the achieved results of numerical experiments we make a conclusion about the one of the most optimal way in defining accelerated parameter in accelerated gradient descent schemes.

Keywords: Line search, gradient descent methods, quasi-Newton method, convergence rate.

INTRODUCTION

We analyze nonlinear optimization methods for the minimization of an objective function f: $\Re^n \to \Re$:

$$\min f(x), \quad x \in \Re^n \tag{1}$$

In this paper we suppose that f is uniformly convex and twice continuously differentiable function. For these classes of functions, furthermore we adopt the next often used representation of optimization models:

$$x_{k+1} = x_k + t_k d_k \tag{2}$$

where x_{k+1} denotes the function value in the next iterative point, x_k presents the function value in the current iteration, t_k is the iterative step size value and d_k is the search direction vector.

Since the first methods for solving non-linear minimization problems have been developed it was clear that the two main characteristics of these iterations: the step length and the search direction (parameters t_k and d_k in (2)) crucially determine accelerated features of the optimization method. Therewith, we expect the value of an iterative step size to be optimal at the sense that it is not too high to misses out the minima and at the same time not too small to provide unnecessary high number of iterations. In order to obtain the minimal value of the objective function we assume that the search direction vector fulfills the descent condition: this paper we suppose that f is uniformly convexand:

$$g_k^T d_k < 0,$$

where with g_k we denote a gradient of the objective function in the $k-$th iteration.

THEORETICAL PART

One of the first choices for descending search direction vector, which satisfies the previous condition, is proposed in classical gradient descent method (GD method). In this iteration $d_k = -g_k$. This is the one of the oldest iterations for solving nonlinear optimization problems. Theoretically, GD method has good convergence properties. In practical sense GD iteration is very slow and not really useful for the problems with large number of variables. In order to prevent these disadvantages but at the same time conserving the descending property of the negative gradient, some authors developed iterative gradient descent schemes more efficient in practical usage than GD method (Fletcher & Reeves, 1964; Polak & Ribiére, 1969; Polyak, 1969).

$$x_{k+1} = x_k - \theta_k t_k d_k \tag{3}$$

where the acceleration parameter θ_k is calculated as $\theta_k = a_k/b_k$. Here $a_k = t_k g_k^T g_k$, $b_k = -t_k y_k^T g_k$ and $y_k = g_{k+1} - g_k$. The value of iterative step-length t_k is derived using backtracking line search procedure. This iteration is noted as AGD-method. The AGD method is compared with gradient descent GD-method. In numerical experiments, obtained for 340 test problems, notably better results in favor to the AGD scheme are registered. The analyzed characteristics are the number of iterations, the CPU time and the number of function evaluations. Regarding all three tested properties, the AGD iteration has provided considerably reduction of measured values comparing to the GD scheme.

Considering the obtained results from Andrei (2006) in Stanimirovic & Miladinovic (2010) the authors identify a class of accelerated gradient descent methods. On their opinion all gradient descent schemes with somehow defined accelerated factor belong to this class of methods. They have offered their way of deriving accelerated factor and described it in (Stanimirovic & Miladinovic, 2010). For that purpose they have constructed accelerated gradient descent SM-method as next:

* Corresponding author: milena.petrovic@pr.ac.rs

$$x_{k+1} = x_k - t_k \gamma_k^{-1} d_k \quad (4)$$

To define an accelerated factor, noted in (4) as γ_k, the authors used a Taylor's expansion of the objective function f_{k+1}:

$$f(x_{k+1}) = f(x_k) - t_k g_k^T \gamma_k^{-1} g_k + \frac{1}{2} t_k^2 \left(\gamma_k^{-1} g_k\right)^T \nabla^2 f(\xi) \gamma_k^{-1} g_k \quad (5)$$

where $\xi \in [x_k, x_{k+1}]$ is a point:

$$\xi = x_k + \alpha\left(x_{k+1} - x_k\right) = x_k - \alpha t_k \gamma_k^{-1} d_k, \quad 0 \le \alpha \le 1 \quad (6)$$

Hessian $\nabla^2 f(\xi)$ in (5) is replaced by $\nabla^2 f(\xi) = \gamma_{k+1} I$, which transforms expression (5) into:

$$f(x_{k+1}) = f(x_k) - t_k \gamma_k^{-1} \|g_k\|^2 + \frac{1}{2} t_k^2 \gamma_{k+1} \gamma_k^{-2} \|g_k\|^2 \quad (7)$$

From the previous relation arises the value of the accelerated parameter γ_{k+1} of the *SM*-method:

$$\gamma_{k+1} = \frac{\gamma_k \left| f(x_{k+1}) - f(x_k) \right| + t_k \|g_k\|^2}{t_k^2 \|g_k\|^2} \quad (8)$$

Linear convergence for so defined SM iteration is proven as well as improvements in performances comparing to the GD and AGD- methods. Achieving a reduction in number of iterations, CPU time and in number of function evaluations in comparison with GD scheme was expected. But prominently reduction of resulted values achieved by the SM-method in all three tested characteristics compered to the accelerated AGD iteration leads us to conclusion that defining an accelerated parameter using the Taylor's expansion gives better practical results.

Later on in (Petrovic & Stanimirovic 2014; Petrovic 2015; Stanimirovic et al., 2015) authors use a favorable results from Stanimirovic & Miladinovic (2010) and continue to explore the way of defining an accelerated parameter using the Taylor's expansion and different forms of iterations for solving nonlinear unconstrained optimization problems. For this investigation we consider results from (Petrovic, 2015). In Petrovic (2015), an iteration with two step lengths, α_k and β_k is presented as:

$$x_{k+1} = x_k - \left(\alpha_k \gamma_k^{-1} + \beta_k\right) d_k \quad (9)$$

Using the Taylor's expansion applied on a scheme (9) and an approximation of Hessian in a current iterative point by the product $\gamma_{k+1} I$ where an accelerated parameter γ_{k+1} is included, the value of accelerated factor of the ADSS-method in $(k + 1)$-iterative point is:

$$\gamma_{k+1} = 2 \frac{f(x_{k+1}) - f(x_k) + \left(\alpha_k \gamma_k^{-1} + \beta_k\right) \|g_k\|^2}{\left(\alpha_k \gamma_k^{-1} + \beta_k\right)^2 \|g_k\|^2} \quad (10)$$

Like in Stanimirovic & Miladinovi (2010) we assume that $\gamma_{k+1} > 0$ otherwise the Second-Order Necessary Condition and Second-Order Sufficient Condition will not be fulfilled. However, in the case when $\gamma_{k+1} < 0$ we take $\gamma_{k+1} = 1$. This way we ensure that when Gk is not positive definite matrix than taking $\gamma_{k+1} = 1$ produces that the search direction is $-g_k$ and that is a descent direction indeed. The next iterative point x_{k+2} is then calculated as:

$$x_{k+2} = x_{k+1} - \left(\alpha_{k+1} \gamma_{k+1}^{-1} + \beta_{k+1}\right) d_{k+1}$$

which presents an accelerated gradient descent iteration. In all three mentioned accelerated gradient descent models (AGD, SM, ADSS) the values of iterative step sizes are computed by the Armio's backtracking line search procedures which is generally described through the next three steps. Applying the SM and the ADSS methods linear convergence is proven on the set of uniform convex functions and under additional assumptions for the strictly convex quadratics as well. Algorithms (0.2) and (0.3) display the SM and the ADSS accelerated models respectively.

Algorithm0.1 The backtracking line search starting from $t = 1$.

Require: Objective function $f(x)$, the direction of the search (d_k) at the point x_k and numbers $0 < \sigma < 0.5$ and $\beta \in (0, 1)$.
1: $t = 1$.
2: While $f(x_k + td_k) > f(x_k) + \sigma t g_k^T d_k$, take $t := t\beta$.
3: Return $t_k = t$.

Algorithm0.2 SM-method.

Require: Objective function $f(x)$ and chosen initial point $x_0 \in dom(f)$.
1: Set $k = 0$ and compute $f(x_0)$, $g_0 = \nabla f(x_0)$ and take $\gamma_0 = 1$.
2: If test criteria are fulfilled then stop the iteration; otherwise, go to the next step.
3: (Backtracking) Find the step size $t_k \in (0, 1]$ using Backtracking procedure with $d_k = -\gamma_k^{-1} g_k$.
4: Compute $x_{k+1} = x_k - t_k \gamma_k^{-1} g_k$, $f(x_{k+1})$ and $g_{k+1} = \nabla f(x_{k+1})$.
5: Determine the scalar approximation γ_{k+1} of the Hessian of f at the point x_{k+1} using (8).
6: If $\gamma_{k+1} < 0$, then take $\gamma_{k+1} = 1$.
7: Set $k := k + 1$, go to the step 2.
8: Return x_{k+1} and $f(x_{k+1})$.

Algorithm0.3 Accelerated Double Step Size method (*ADSS* method).

Require: $0 < \rho < 1$, $0 < \tau < 1$, x_0, $\gamma_0 = 1$.
1: Set $k = 0$, compute $f(x_0)$, g_0 and take $\gamma_0 = 1$.
2: If $\|g_k\| < \xi$, then go to Step 9, else continue by the next step.
3: Find the step size α_k applying Backtracking1 procedure.
4: Find the step size β_k applying Backtracking2 procedure.
5: Compute x_{k+1} using (9).
6: Determine the scalar γ_{k+1} using (10).
7: If $\gamma_{k+1} < 0$, then take $\gamma_{k+1} = 1$.
8: Set $k := k + 1$, go to Step 2.
9: Return x_{k+1} and $f(x_{k+1})$.

NUMERICAL COMPARATIONS

In Stanimirovic & Miladinovic (2010) authors have tested 30 test functions from Andrei (2008) given in generalized or extended form as a large scale unconstrained test problems. They considered for each test function 10 different numerical experiments with the number of variables: 100, 500, 1000, 2000, 3000, 5000, 7000, 8000, 10000 and 15000. A substantial outcome of these numerical experiments is that the SM method shows the best results for 20 test functions in the sense of number of iterations needed to achieve requested accuracy, while AGD is the best in the remaining 10 test problems. Considering the CPU time and the number of function evaluations, the SM method shows better performance for 23 test functions.

Since the both of the methods, the SM and the AGD, belong to the class of accelerated gradient descent methods we can conclude that computing an accelerated variable using the Taylor's expansion provides a far better practical results in reducing the number of iterations, the number of function evaluations and needed CPU time. That was the reason to continue with this way of computing the parameter of acceleration. The similar approaches are applied in (Petrovic & Stanimirovic, 2014; Petrovic, 2015; Stanimirovic et al., 2015). In this work we consider results published in Petrovic (2015).

Table 1. Summary of numerical results for SM and ADSS tested on 25 large scale test functions regarding number of iteration.

Test function	Nomber of iterations	
	ADSS	SM
Extended Penalty	589	50
Perturbed quadratic	111972	397
Raydan-1	21125	34
Diagonal 1	10417	37
Diagonal 3	10574	49
Generalized Tridiagonal -1	278	77
Extended Tridiagonal -1	3560	70
Extended Three Expon	164	40
Diagonal 4	80	780
Extended Himmelblau	168	70
Quadr. Diag. Perturbed	53133	393
Quadratic QF1	114510	425
Extended Quad. Penalty QP1	224	60
Extended Quad. Penalty QP2	162	60
Quadratic QF2	118801	60
Extended EP1	68	40
Extended Tridiagonal - 2	584	80
Arwhead	10	64
Almost Perturbed Quadratic	110121	397
Engval1	185	70
Quartc	190	70
Generalized quartic	156	70
Diagonal 7	90	2201
Diagonal 8	96	2213
Diagonal 9	11235	43

Numerical tests presented in Petrovic (2015) confirm noticeably better performance of accelerated double step size ADSS method comparing to the accelerated gradient descent SM scheme with one step length parameter. This also lead us to conclusion that properly defined values of iterative step lengths (as well as the number of step sizes involved in method) substantially causes the level of efficiency of analyzed method.

Table 2. Summary of numerical results for SM and ADSS tested on 25 large scale test functions regarding CPU time.

Test function	CPU time	
	ADSS	SM
Extended Penalty	5	4
Perturbed quadratic	1868	0
Raydan-1	178	4
Diagonal 1	116	0
Diagonal 3	209	1
Generalized Tridiagonal -1	2	0
Extended Tridiagonal -1	35	0
Extended Three Expon	1	0
Diagonal 4	0	0
Extended Himmelblau	0	0
Quadr. Diag. Perturbed	1193	1
Quadratic QF1	2127	0
Extended Quad. Penalty QP1	12	2
Extended Quad. Penalty QP2	7	4
Quadratic QF2	2544	1
Extended EP1	1	0
Extended Tridiagonal - 2	0	0
Arwhead	0	3
Almost Perturbed Quadratic	2148	0
Engval1	7	0
Quartc	0	0
Generalized quartic	0	0
Diagonal 7	0	33
Diagonal 8	0	40
Diagonal 9	118	0

To confirm this ascertainment in this work the SM and the ADSS schemes are numerically compared and the numerical outcomes from Petrovic (2015) are used. First, let us point it out on the common features of these two iterations:

- Computation of accelerated factor for each of these models is achieved in a similar way, using the Taylor's expansion and in accordance with the posed formulation of the iteration;
- The value of the single step size in the *SM* is obtained by the Backtracking line search technique as well as each of the value of two needed step length parameters in the *ADSS* scheme;
- Both methods have a negative gradient for the search direction, i.e. both methods are gradient descent.

For each of the 25 test functions ten experiments are taken for the larger number of variables:1000, 2000, 3000, 5000, 7000, 8000, 10000, 15000, 20000 and 30000. Analyzed characteristics

are number of iterations, needed CPU time of execution and the number of function evaluations. Taking the next exit criteria:

$$\|g_k\| \le 10^{-6} \text{ and } \frac{|f(x_{k+1}) - f(x_k)|}{1+|f(x_k)|} \le 10^{-6}$$

results are displayed in the following Tables 1, 2, 3.

From the given Tables the next conclusions follows:

- By using the ADSS scheme in 21 out of 25 test functions considerably lower number of iterations is realized then by using the SM scheme;
- The ADSS iteration is faster than the SM for 17 functions and for 5 test functions both methods need the same CPU time; which presents an accelerated.
- By using the *ADSS* scheme in 20 out of 25 test functions much lower number of function evaluations is achieved then using the *SM* scheme.

Expand view of the previous statements is given trough the average values, arranged in Table 4.

Table 3. Summary of numerical results for SM and ADSS tested on 25 large scale test functions regarding number of evaluation..

Test function	No. of funct. evaluation	
	ADSS	SM
Extended Penalty	2987	1780
Perturbed quadratic	632724	1714
Raydan-1	116757	4844
Diagonal 1	56135	1448
Diagonal 3	59425	1048
Generalized Tridiagonal -1	989	719
Extended Tridiagonal -1	30686	420
Extended Three Expon	1224	350
Diagonal 4	530	2590
Extended Himmelblau	566	480
Quadr. Diag. Perturbed	547850	1719
Quadratic QF1	649643	1755
Extended Quad. Penalty QP1	2566	841
Extended Quad. Penalty QP2	2057	843
Quadratic QF2	662486	836
Extended EP1	764	487
Extended Tridiagonal - 2	2144	420
Arwhead	30	1082
Almost Perturbed Quadratic	1712	1712
Engval1	2177	460
Quartc	430	390
Generalized quartic	423	614
Diagonal 7	220	6633
Diagonal 8	594	6709
Diagonal 9	60566	3646

Generally, from 250 testings we can conclude that the *ADSS* outperforms the *SM* respect to all tested characteristics: number of iterations, CPU time and number of function evaluations. Considering the number of iterations, the *ADSS* exceeds *SM* about 70 times. Needed CPU time is averagely 113 times less in favor to *ADSS* comparing to *SM* and regarding function evaluations about 80 times lower number is needed with regard to the *SM*.

Remark 0.1. *In Stanimirovic et al. (2015); Petrovic et al. (2016) two more accelerated gradient descent schemes with accelerated parameters derived from the features of the Taylor's series are presented. Linear convergence of these methods and their numerical efficiency is proved and tested. All of these improved results that are mentioned or analyzed confirm that it is reasonable to detected a class of accelerated gradient descent methods with accelerated parameter obtained by the Taylor's expansion of posed iteration.*

Table 4. Average numerical outcomes for 25 test functions tried out on 10 numerical experiments in each iteration..

Average performances	ADSS	SM
Number of iterations	314	22739.68
CPU time (sec)	3.72	422.84
Number of function evaluations	1741.6	138450.4

CONCLUSION

In this paper the efficiency of an accelerated gradient descent method with accelerated parameter achieved using the properties of the Taylor's expansion is described and numerically proved. For that purpose we have pointed out on a different ways of defining a factor of acceleration. The results of the numerical tests in Stanimirovic & Miladinovic (2010) which show the benefits of calculating the acceleration parameter trough the Taylor's expansion instead of means stated in Andrei (2006), were the reason to continue investigation of developing an accelerated parameter this way applied on a different form of a gradient descent iteration.

Double step size gradient descent ADSS model proposed in Petrovic (2015), with all three crucial elements of iteration (an accelerated parameter, step sizes and search direction) similarly defined, is compared with the SM method. The efficiency of the ADSS model regarding all analyzed characteristics (number of iterations, CPU time and number of function evaluations) in comparison to the accelerated gradient descent single step size SM method has been numerically confirmed.

At the end we can indicate that the problem stated in this paper can be exploited in some new ways. More precisely, the problem of finding an acceleration parameter with some different forms of gradient descent iterations is still actual.

REFERENCES

Andrei, N. 2006. An acceleration of gradient descent algoritham with backtracing for unconstrained optimization. Numer. Algor, 42.

Andrei, N. 2008. An unconstrained optimization test functions collection. Advanced Modeling and Optimization, 10(1).

Fletcher, R., & Reeves, C. 1964. Function minimization by conjugate gradients. Comput. J., 7, pp. 149-154.

Petrović, M. 2015. An Accelerated Double Step Size Method In Unconstrained Optimization. Applied Mathematics and Computation, .

Petrović, M., Rakočević, V., Kontrec, N., Panić, S., & Ilić, D. 2016. Hibridization of accelearted gradient descent method. Numer. Algor., . under review.

Petrović, M., & Stanimirović, P. 2014. Accelerated Double Direction Method For Solving Unconstrained Optimization Problems. Mathematical Problems in Engineering, 2014, pp. 309-319.

Polak, E., & Ribiére, G. 1969. Note sur la convergence de méthodes de directions conjuguées. Revue Francaise Informat. Reserche Opérationnelle, 16, pp. 35-43.

Polyak, B.T. 1969. The conjugate gradient method in extreme problems. USSR Comp. Math. Math. Phys., 9, pp. 94-112.

Stanimirović, P.S., & Miladinović, M.B. 2010. Accelerated gradient descent methods with line search. Numer. Algor, 54, pp. 503-520.

Stanimirović, P.S., Milovanović, G.V., Petrović, M., & Kontrec, N.Z. 2015. Transformation of Accelerated Double Step Size Method for Unconstrained Optimization. Mathematical Problems in Engineering, .

UNIVERSITY THOUGHT
Publication in Natural Sciences, Vol. 7, No. 1, 2017, pp. 46-50.
doi:10.5937/univtho7-13884
Original Scientific Paper

ON THE STARK BROADENING OF Ar VII SPECTRAL LINES

MILAN S. DIMITRIJEVIĆ[1*], SYLVIE SAHAL-BRÉCHOT[2]

[1]Astronomical Observatory, Volgina 7, Belgrade, Serbia
[2]LERMA, Observatoire de Paris, PSL Research University, CNRS, Sorbonne Universities, UPMC Univ. Paris 06, 5 Place Jules Janssen, Meudon Cedex, France

ABSTRACT

Stark broadening parameters, full width at half maximum of spectral line and shift, have been calculated for 3 spectral lines of Ar VII, for broadening by electron, proton, and He III impacts. For calculations, the semiclassical perturbation approach in the impact approximation has been used. The results are provided for temperatures from 20 000 K to 500 000 K and for an electron density of 10^{17} cm^{-3}. Obtained results will be included in the STARK-B database which is also included in Virtual atomic and molecular data center (VAMDC).

Keywords: Stark broadening, atomic data, atomic processes, line profiles.

INTRODUCTION

Data on the Stark broadening of spectral lines are important for diagnostics, modeling and investigation of laboratory plasmas (Konjević, 1999; Torres et al., 2006), inertial fusion plasma research (Griem, 1992), laser produced plasma analysis and diagnostics (Gornushkin et al., 1999; Sorge et al., 2000), as well as for different plasmas in technology, like for example for welding and piercing with laser produced plasma (Hoffman et al., 2006), or for design and development of light sources based on plasmas (Dimitrijević & Sahal-Bréchot, 2014a), and lasers (Csillag & Dimitrijević, 2004). An important topic where Stark broadening data are needed are astrophysical plasmas (Beauchamp et al., 1997; Dimitrijević & Sahal-Bréchot, 2014b), in particular atmospheres of white dwarfs, pre white dwarf stars, and post AGB (Asymptotic Giant Branch) stars (Tankosić et al., 2003; Milovanović et al., 2004; Simić et al., 2006; Dufour et al., 2011).

Additionally, since for temperatures higher than around 10 000 K hydrogen is mainly ionized, Stark broadening is, in such a case, the principal pressure broadening mechanism (Griem, 1974). Consequently, in some atmospheric layers of A and late B stars, where such plasma conditions are typical, it should be taken into account. Such cases have been analysed for example in Simić et al. (2005b,a) and Simić et al. (2009).

Due to development of satellite-born spectroscopy, data on trace elements, which have been without significance for astrophysics, become more and more important for analysis of stellar spectra. It is also worth to notice that Rauch et al. (2007) accentuated that accurate Stark broadening data for as much as possible large number of atoms and ions and the corresponding spectral lines "are of crucial importance for sophisticated analysis of stellar spectra by means of NLTE model atmospheres".

Spectral lines of Ar VII have been found by Taresch et al. (1997) in the spectrum of extremely hot and massive galactic O3 If supergiant HD 93129A. Also Werner et al. (2007), by analyzing high-resolution spectra taken with the Far Ultraviolet Spectroscopic Explorer (FUSE), have identified Ar VII lines in some of the hotest known central stars of planetary nebulae, with the effective temperatures of 95000 - 110000 K, and in (pre-) white dwarfs, where Stark broadening is very important and the corresponding Stark brooadening data are needed for a reliable analysis and modelling.

In order to provide the needed Stark broadening parameters for Ar VII spectral lines, completely missing in the existing literature, Stark Full Widths at Half intensity Maximum (FWHM) W and shifts d for three transitions have been calculated by using semiclassical perturbation method (SCP, Sahal-Bréchot (1969a,b)) for colissions of Ar VII ions with electrons, protons and He III ions, which are the main constituents of stellar atmospheres.

THE IMPACT SEMICLASSICAL PERTURBATION METHOD

For the calculations of Stark broadening parameters, full width at half intensity maximum (FWHM - W) and shift of spectral line (d) here is usede the semiclassical perturbation formalism (SCP), developed in Sahal-Bréchot (1969a,b). Further innovations and modernisations are presented in Sahal-Bréchot (1974, 1991); Dimitrijević et al. (1991); Dimitrijević & Sahal-Bréchot (1996); Sahal-Bréchot et al. (2014).

The Stark broadened profile $F(\omega)$ of an isolated spectral line has Lorentzian form and can be represented as:

$$F(\omega) = \frac{W/2\pi}{\left(\omega - \omega_{if} - d\right)^2 + \left(W/2\right)^2}. \qquad (1)$$

Here,

* Corresponding author: mdimitrijevic@aob.rs

$$\omega_{if} = \frac{E_i - E_f}{\hbar}.$$

In the upper equation E_i and E_f are energies of the initial and final states, while (W) and (d), in angular frequency units, are given by equation:

$$W = N\int vf(v)dv\left(\sum_{i'\neq i}\sigma_{ii'}(v) + \sum_{f'\neq f}\sigma_{ff'}(v) + \sigma_{el}\right),$$

$$d = N\int vf(v)dv\int_{R_3}^{R_D} 2\pi\rho d\rho\sin(2\varphi_p). \quad (2)$$

with N is here denoted the electron density and with f(v) the Maxwellian velocity distribution function for electrons, ρ is the impact parameter of the incoming electron, and with i', f' are denoted the perturbing levels of the initial and final state. The inelastic cross section $\sigma_{jj'}(v)$, $j = i, f$ is given with the formula:

$$\sum_{i'=i}\sigma_{ii'}(v) = \frac{1}{2}\pi R_1^2 + \int_{R_1}^{R_D} 2\pi\rho d\rho\sum_{i'=i}P_{ii'}(\rho,v). \quad (3)$$

where $P_{Jj'}(\rho,v)$, $j=i, f$; $j'=i', f'$ is transition probability. The elastic cross section is

$$\sigma_{el} = 2\pi R_2^2 + \int_{R_1}^{R_D} 2\pi\rho d\rho\sin^2\delta + \sigma_r,$$

$$\delta = \left(\varphi_p^2 + \varphi_q^2\right)^{\frac{1}{2}}. \quad (4)$$

The phase shifts due to the polarization potential is $\varphi_p(r^{-4})$ and due to the quadrupolar potential $\varphi_q(r^{-3})$. They are defined in Section 3 of Chapter 2 in Sahal-Bréchot (1969a). The cut-offs R_1, R_2, R_3, and the Debye radius R_D are described in Section 1 of Chapter 3 in Sahal-Bréchot (1969b). The contribution of Feshbach resonances, σ_r is explained in details in (Fleurier et al.,1977).

All approximations and the details of the theory are discussed in detail in Sahal-Bréchot et al. (2014). The electrons are moving along hyperbolic paths while for ionic perturbers the paths are different because for them the Coulomb force is repulsive and for them, in Eqs. (2-4), there is no the contribution of Feshbach resonances.

STARK BROADENING PARAMETER CALCULATIONS

Within the frame of semiclassical perturbation theory (Sahal-Bréchot, 1969a,b; Sahal-Bréchot et al., 2014) we have calculated using Eqs. (2-4) widths (FWHM) and shifts for three multiplets of six time charged argon ion Ar VII. Energy levels necessary for present calculations have been taken from Saloman (2010). The needed oscillator strengths have been calculated within the Coulomb approximation by using the method of Bates & Damgaard (1949) and the tables of Oertel & Shomo (1968). For higher levels, when there is no the corresponding data in Oertel & Shomo (1968), the required oscillator strengths have been calculated according to the article of Van Regemorter et al. (1979).

In Table 1, the obtained results of our calculations of Stark widths (FWHM) and shifts for electron- proton- and doubly charged helium ion-impact broadening, for a perturber density of 10^{17} cm^{-3} and for a set of temperatures from 20 000 K to 500 000 K, are shown. The temperature range covers needs in astrophysics, laboratory plasma, fusion research, technology and the topic of lasers and laser produced plasma. Extrapolation to perturber densities lower than 10^{17} cm^{-3} is linear. For higher perturber densities the influence of Debye screening should be checked and eventualy taken into account (see e.g. (Griem, 1974)). With known Stark broadening parameters, W and d it is easy to obtain the line profile using Eq. (1).

One can see from Table 1, that spectral line width due to collisions with electrons is always dominant in comparison with line widths produced by ionic collisions, since ions are much heavier than electrons and their velocities are much smaller. At low temperatures ion width is completely neglibigle but its influence increases with temperature and it should not be neglected at high temperatures. One can see as well that widths due to collisions with doubly charged helium ions are larger than widths produced by collisions with protons. Shifts are much smaller and they are of the same order of magnitude for collisions with electrons as well as with both species of ions. At higher temperatures ion shifts are larger than electron ones and proton shifts are smaller than He^{++} ones.

It should be noticed that wavelengths given in Table 1 are calculated ones, so that they are different from experimental ones. However, they are correct in angular frequency units since then, for the calculation of Stark broadening parameters, relative and not absolute positions of energy levels are significant. In order to transform the Stark widths in Å-units to the width in angular frequency units the following formula can be used:

$$W(\text{Å}) = \frac{\lambda^2}{2\pi c}w(s^{-1}). \quad (5)$$

where c is the speed of light. If the correction of widths and/or shifts for the difference between calculated and experimental wavelength is needed, this can be performed for the width as:

$$W_{cor} = \left(\frac{\lambda_{\exp}}{\lambda}\right)^2 W. \quad (6)$$

Here, with W_{cor} is denoted the corrected width, λ_{exp} is the experimental, λ the calculated wavelength and W the width from Table 1. Formulas for the shifts are analogous to Eqs. (5) and (6).

Parameter C (Dimitrijević & Sahal-Bréchot, 1984) in Table 1, enables to estimate the maximal perturber density for which the line may be treated as isolated, when it is divided by the corresponding full width at half maximum.

ON THE IMPLEMENTATION OF RESULTS IN THE STARK-B DATABASE

The presented in Table 1 Stark broadening parameters for Ar VII spectral lines, will be also implemented in the STARK-B

database (Sahal-Bréchot et al., 2015, 2017), intended for the investigations, modelling and diagnostics of the plasma of stellar atmospheres, diagnostics of laboratory plasmas, and investigation of laser produced, inertial fusion plasma and for plasma technologies.

The STARK-B database contains Stark widths and shifts calculated by authors of this article and their coauthors, by using the SCP computer code for spectral lines, and published in more than 150 publications. Actually, in this database are SCP data for the following elements and ionization degrees: Ag I, Al I, Al III, Al XI, Ar I, Ar II, Ar III, Ar VIII, Au I, B II, B III, Ba I, Ba II, Be I, Be II, Be III, Br I, C II, C III, C IV, C V, Ca I, Ca II, Ca V, Ca IX, Ca X, Cd I, Cd II, Cl I, Cl VII, Cr I, Cr II, Cu I, F I, F II, F III, F IV, F V, F VI, F VII, Fe II, Ga I, Ge I, Ge IV, He I, Hg II, I I, In II, In III, K I, K VIII, K IX, Kr I, Kr II, Kr VIII, Li I, Li II, Mg I, Mg II, Mg XI, Mn II, N I, N II, N III, N IV, N V, Na I, Na X, Ne I, Ne II, Ne III, Ne IV, Ne V, Ne VIII, Ni II, O I, O III, O IV, O V, O VI, O VII, P IV, P V, Pb IV, Pd I, Rb I, S III, S IV, S V, S VI, Sc III, Sc X, Sc XI, Se I, Si I, Si II, Si IV, Si V, Si VI, Si XI, Si XII, Si XIII, Sr I, Te I, Ti IV, Ti XII, Ti XIII, Tl III, V V, V XIII, Y III, Xe VI, Xe VIII and Zn I.

Table 1. This table gives electron-, proton-, and doubly charged helium-impact broadening parameters for Ar VII spectral lines, for a perturber density of 10^{17} cm^{-3} and temperatures from 20 000 to 500 000 K. Calculated wavelength of the transitions (in Å) and parameter *C* are also given. This parameter, when divided with the corresponding Stark width, gives an estimate for the maximal pertuber density for which the line may be treated as isolated. W_e: electron-impact full width at half maximum of intensity, d_e: electron-impact shift, W_p: proton-impact full width at half maximum of intensity, d_p: proton-impact shift, $W_{He^{++}}$: doubly charged helium ion-impact full width at half maximum of intensity, $d_{He^{++}}$: doubly charged helium ion-impact shift.

Transition	T(K)	W_e (Å)	d_e (Å)	W_{H^+} (Å)	d_{H^+} (Å)	$W_{He^{++}}$ (Å)	$d_{He^{++}}$ (Å)
Ar VII $3s^2\ ^1S$ - $3p\ ^{1Po}$	20000.	0.144E-02	0.504E-04	0.414E-06	-0.397E-06	0.789E-06	-0.716E-06
585.7 Å	50000.	0.919E-03	-0.130E-05	0.164E-05	-0.109E-05	0.316E-05	-0.210E-05
C = 0.59E+20	100000.	0.653E-03	-0.449E-05	0.447E-05	-0.221E-05	0.865E-05	-0.438E-05
	200000.	0.465E-03	-0.587E-05	0.106E-04	-0.434E-05	0.206E-04	-0.869E-05
	300000.	0.386E-03	-0.496E-05	0.155E-04	-0.621E-05	0.304E-04	-0.124E-04
	500000.	0.309E-03	-0.637E-05	0.222E-04	-0.902E-05	0.438E-04	-0.181E-04
Ar VII $4s\ ^1S$ - $4p\ ^{1Po}$	20000.	0.860E-01	0.166E-03	0.126E-03	-0.194E-03	0.241E-03	-0.349E-03
2445.8 Å	50000.	0.546E-01	-0.106E-02	0.488E-03	-0.524E-03	0.948E-03	-0.101E-02
C = 0.24E+21	100000.	0.396E-01	-0.903E-02	0.109E-02	-0.952E-03	0.215E-02	-0.189E-02
	200000.	0.297E-01	-0.126E-02	0.186E-02	-0.145E-02	0.369E-02	-0.292E-02
	300000.	0.255E-01	-0.121E-02	0.239E-02	-0.176E-02	0.474E-02	-0.355E-02
	500000.	0.213E-01	-0.113E-02	0.289E-02	-0.210E-02	0.578E-02	-0.425E-02
Ar VII $3s\ ^3S$ - $4p\ ^{3Po}$	20000.	0.534E-01	0.172E-02	0.781E-04	-0.877E-04	0.149E-03	-0.158E-03
1982.0 Å	50000.	0.333E-01	-0.387E-03	0.295E-03	-0.239E-03	0.571E-03	-0.460E-03
C = 0.20E+21	100000.	0.240E-01	-0.512E-03	0.653E-03	-0.449E-03	0.128E-02	-0.892E-03
	200000.	0.179E-01	-0.607E-03	0.110E-02	-0.714E-03	0.219E-02	-0.144E-02
	300000.	0.153E-01	-0.649E-03	0.139E-02	-0.865E-03	0.277E-02	-0.174E-02
	500000.	0.128E-01	-0.572E-03	0.169E-02	-0.107E-02	0.338E-02	-0.216E-02

STARK-B contains also our Stark broadening data obtained by using the Modified SemiEmpirical method (MSE) (Dimitrijević & Konjević, 1980; Dimitrijević & Kršljanin, 1986; Dimitrijević & Popović, 2001).These data are of lower accuracy than SCP data but this approach is convenient for the cases where atomic data are not sufficiently complete for an adequate SCP calculation. MSE Stark line widths, in some cases together with line shifts, of the following emitters are in STARK-B

database: Ag II, Al III, Al V, Ar II, Ar III, Ar IV, As II, Au II, B III, B IV, Be III, Bi II, Bi III, Br II, C III, C IV, C V, Cd II, Cd III, Cl III, Cl IV, Cl VI, Co II, Co III, Cu III, Cu IV, Eu II, Eu III, F III, F V, F VI, Fe II, Ga III, Ge III, Ge IV, I II, Kr II, Kr III, La II, La III, Lu III, Mg III, Mg IV, Mn II, Mn III, N II, N III, Na III, Na VI, Nb III, Ne III, Ne IV, Ne V, Ne VI, Ne VII, Ne VIII, O III, O IV, P III, P IV, P VI, Pt II, Ra II, S IV, Sb II, Sc II, Se II, Se III, Si IV, Si V, Si VI, Si XI, Sn III, Sr III, Ti II, Ti III, V II, V III, V IV, Xe II, Y II, Zn II, Zn III, Zr II and Zr III.

We note as well that STARK-B database is one of the databases which are in the Virtual Atomic and Molecular Data Center - VAMDC (Dubernet et al., 2010; Rixon et al., 2011; Dubernet et al., 2016). VAMDC is created in order to enable an efficacious search and mining of atomic and molecular data scattered in different databases and to make more convenient their adequate use. It has been the principal aim of a FP7 founded project of the same name (Dubernet et al., 2010), which started on July 1 2009 and lasted 42 months. During this project an interoperable e-infrastructure for atomic and molecular data upgrading and integrating European (and wider) A&M database services has been build, and a forum of data producers, data users and databases developers has been created. Currently in VAMDC are 30 databases with atomic and molecular data, including STARK-B, and can be accessed and searched through VAMDC portal: http://portal.vamdc.org/. The web site of VAMDC Consortium is: http://www.vamdc.org/.

CONCLUSION

We have performed a SCP calculation of Stark broadening parameters for three multiplets of Ar VII. Stark broadening parameters - widths and shifts, have been calculated for collisions of Ar VII ions with electrons, protons and doubly charged helium ions. The obtained data will be implemented in STARK-B database. There is no neither theoretical, nor experimental data for Stark broadening of Ar VII spectral lines and we hope that the obtained results will be of interest. for a number of problems in astrophysical, laboratory, laser produced, inertial fusion and technological plasmas.

ACKNOWLEGMENTS

This work is a part of the project 176002 "Influence of collisional processes on astrophysical plasma line shapes" supported by the Ministry of Education, Science and Technological Development of Serbia.

REFERENCES

Bates, D.R., & Damgaard, A. 1949. The Calculation of the Absolute Strengths of Spectral Lines. Philosophical Transactions of the Royal Society of London. Series A. Mathematical and Physical Sciences, 242(842), pp. 101-122.

Beauchamp, A., Wesemael, F., & Bergeron, P. 1997. Spectroscopic Studies of DB White Dwarfs: Improved Stark Profiles for Optical Transitions of Neutral Helium. Astrophysical Journal Supplement, 108, pp. 559-573.

Dimitrijevic, M.S., & Csillag, L. 2004. On the Stark broadening of the 537.8 nm and 441.6 nm Cd+ lines excited in a hollow cathode laser discharge. Applied Physics B: Lasers and Optics, 78(2), pp. 221-223. doi:10.1007/s00340-003-1368-3

Dimitrijević, M.S., & Konjević, N. 1980. Stark widths of doubly- and triply-ionized atom lines. Journal of Quantitative Spectroscopy & Radiative Transfer, 24, pp. 451-459.

Dimitrijević, M.S., & Kršljanin, V. 1986. Electron-impact shifts of ion lines: Modified semiempirical approach. Astronomy and Astrophysics, 165, pp. 269-274.

Dimitrijević, M.S., & Popović, L.Č. 2001. Modified Semiempirical Method,. Journal of Applied Spectroscopy, 68(6), pp. 893-901. doi:10.1023/A:1014396826047

Dimitrijević, M.S., & Sahal-Bréchot, S. 1984. Stark broadening of neutral helium lines. Journal of Quantitative Spectroscopy & Radiative Transfer, 31, pp. 301-313.

Dimitrijević, M.S., & Sahal-Bréchot, S. 1996. Stark broadening of Li II spectral lines. Physica Scripta, 54, pp. 50-55.

Dimitrijević, M.S., & Sahal-Bréchot, S. 2014. On the Application of Stark Broadening Data Determined with a Semiclassical Perturbation Approach. Atoms, 2, pp. 357-377.

Dimitrijević, M.S., Sahal-Bréchot, S., & Bommier, V. 1991. Stark broadening of spectral lines of multicharged ions of astrophysical interest. I - C IV lines. Astronomy and Astrophysics Supplement Series, 89, pp. 581-590.

Dubernet, M.L., Antony, B.K., Ba, Y.A., & et al., 2016. The virtual atomic and molecular data centre (VAMDC) consortium. Journal of Physics B: Atomic, Molecular and Optical Physics, 49(7). 074003.

Dubernet, M.L., Boudon, V., Culhane, J.L., & et al., 2010. Virtual atomic and molecular data centre. Journal of Quantitative Spectroscopy & Radiative Transfer, 111(15), pp. 2151-2159.

Dufour, P., Nessib, B.N., Sahal-Bréchot, S., & Dimitrijević, M.S. 2011. Stark Broadening of Carbon and Oxygen Lines in Hot DQ White Dwarf Stars: Recent Results and Applications. Baltic Astronomy, 20, pp. 511-515.

Fleurier, C., Sahal-Bréchot, S., & Chapelle, J. 1977. Stark profiles of some ion lines of alkaline earth elements. Journal of Quantitative Spectroscopy and Radiative Transfer, 17, pp. 595-603.

Gornushkin, I.B., King, L.A., Smith, B.W., Omenetto, N., & Winefordner, J.D. 1999. Line broadening mechanisms in the low pressure laser-induced plasma. Spectrochimica Acta, Part B: Atomic Spectroscopy, 54(8), pp. 1207-1217.

Griem, H.R. 1974. Spectral line broadening by plasmas.New York: Academic Press, Inc.

Hoffman, J., Szymanski, Z., & Azharonok, V. 2006. Plasma Plume Induced During Laser Welding of Magnesium Alloys. . In: AIP Conference Proceedings. , pp. 469-472 812,

Konjević, N. 1999, Plasma broadening and shifting of nonhydrogenic spectral lines: present status and applications, Physics Reports, 316 (6), 339–401.

Milovanović, N., Dimitrijević, M.S., Popović, L.Č., & Simić, Z. 2004. Importance of collisions with charged particles for stellar UV line shapes: Cd III. Astronomy and Astrophysics, 417, pp. 375-380.

Oertel, G.K., & Shomo, L.P. 1968. Tables for the Calculation of Radial Multipole Matrix Elements by the Coulomb Approximation. Astrophysical Journal Supplement, 16, pp. 175-218.

Rauch, T., Ziegler, M., Werner, K., & et al., 2007. High-resolution FUSE and HST ultraviolet spectroscopy of the white dwarf central star of Sh 2-216. Astronomy and Astrophysics, 1, pp. 317-329.

Rixon, G., Dubernet, M.L., Piskunov, N., & et al., 2011. VAMDC: The Virtual Atomic and Molecular Data Centre: A New Way to Disseminate Atomic and Molecular Data-VAMDC Level 1 Release. . In: AIP Conference Proceedings. , pp. 107-115 1344.

Sahal-Bréchot, S. 1969. Impact theory of the broadening and shift of spectral lines due to electrons and ions in a plasma. Astronomy and Astrophysics, 1, pp. 91-123.

Sahal-Bréchot, S. 1969. Impact theory of the broadening and shift of spectral lines due to electrons and ions in a plasma. Astronomy and Astrophysics, 2, pp. 322-354. (continued).

Sahal-Bréchot, S. 1974. Stark broadening of isolated lines in the impact approximation. Astronomy and Astrophysics, 35, pp. 319-321.

Sahal-Bréchot, S. 1991. Broadening of ionic isolated lines by interactions with positively charged perturbers in the quasistatic limit. Astronomy and Astrophysics, 245, pp. 322-330.

Sahal-Bréchot, S., Dimitrijević, M.S., & Nessib, B.N. 2014. Widths and Shifts of Isolated Lines of Neutral and Ionized Atoms Perturbed by Collisions With Electrons and Ions: An Outline of the Semiclassical Perturbation (SCP) Method and of the Approximations Used for the Calculations. Atoms, 2, pp. 225-252.

Sahal-Bréchot, S., Dimitrijević, M.S., & Moreau, N. 2017. STARK-B database.Observatory of Paris, LERMA / Astronomical Observatory of Belgrade. Retrieved from http://starkb.obspm.fr.

Sahal-Bréchot, S., Dimitrijević, M.S., Moreau, N., & Nessib, B.N. 2015. The STARK-B database VAMDC node: A repository for spectral line broadening and shifts due to collisions with charged particles. Physica Scripta, 50, p. 8. 054008.

Saloman, E.B. 2010. Energy Levels and Observed Spectral Lines of Ionized Argon, Ar II through Ar XVIII. Journal of Physical and Chemical Reference Data, 39(0331), p. 1.

Simić, Z., Dimitrijević, M.S., & Kovačević, A. 2009. Stark broadening of spectral lines in chemically peculiar stars: Te I lines and recent calculations for trace elements. New Astronomy Review, 53(7-10), pp. 246-251.

Simić, Z., Dimitrijević, M.S., Milovanović, N., & Sahal-Bréchot, S. 2005. a, Stark broadening of Cd I spectral lines. Astronomy and Astrophysics, 441(1), pp. 391-393.

Simic, Z., Dimitrijevic, M.S., Popovic, L.C., & Dacic, M.D. 2005. Stark Broadening of F III Lines in Laboratory and Stellar Plasma. Journal of Applied Spectroscopy, 72(3), pp. 443-446. doi:10.1007/s10812-005-0095-4

Simić, Z., Dimitrijević, M.S., Popović, L.Č., & Dačić, M. 2006. Stark broadening parameters for Cu III, Zn III and Se III lines in laboratory and stellar plasma. New Astronomy, 12(3), pp. 187-191.

Sorge, S., Wierling, A., Röpke, G., Theobald, W., Sauerbrey, R., & Wilhein, T. 2000. Diagnostics of a laser-induced dense plasma by hydrogen like carbon spectra. Journal of Physics B: Atomic, Molecular and Optical Physics, 33(16), pp. 2983-3000. doi:10.1088/0953-4075/33/16/304

Tankosić, D., Popović, L.Č., & Dimitrijević, M.S. 2003. The electron-impact broadening parameters for Co III spectral lines. Astronomy and Astrophysics, 399, pp. 795-797.

Taresch, G., Kudritzki, R.P., Hurwitz, M., & et al., 1997. Quantitative analysis of the FUV, UV and optical spectrum of the O3 star HD 93129A. Astronomy and Astrophysics, 321, pp. 531-548.

Torres, J., van de Sande, M.J., van der Mullen, J.J.A.M., Gamero, A., & Sola, A. 2006. Stark broadening for simultaneous diagnostics of the electron density and temperature in atmospheric microwave discharges. Spectrochimica Acta, Part B: Atomic Spectroscopy, 61(1), pp. 58-68.

van Regemorter, H., Binh, H.D., & Prud'homme, M. 1979. Radial transition integrals involving low or high effective quantum numbers in the Coulomb approximation. Journal of Physics B: Atomic, Molecular and Optical Physics, 12, pp. 1053-1061.

Werner, K., Rauch, T., & Kruk, J.W. 2007. Discovery of photospheric argon in very hot central stars of planetary nebulae and white dwarfs. Astronomy and Astrophysics, 466, pp. 317-322.

Griem, H.R. 1992. Plasma spectroscopy in inertial confinement fusion and soft x-ray laser research. Physics of Fluids, 4(7), str. 2346-2361.

UNIVERSITY THOUGHT
Publication in Natural Sciences, Vol. 7, No. 1, 2017, pp. 51-54.
doi:10.5937/univtho7-13753
Original Scientific Paper

AN ANALYSIS OF FACTORS AFFECTING THE HIGH RADON CONCENTRATION IN DIFFERENT TYPES OF HOUSES

LJILJANA GULAN[1*]

[1]Faculty of Natural Sciences and Mathematics, University of Priština, Kosovska Mitrovica, Serbia

ABSTRACT

This paper presents an analysis of indoor radon measurements carried out in municipality of Zubin Potok, northwestern part of Kosovo and Metohija. Annual measurements in two rooms of each house were performed by solid state nuclear track detectors commercially known as Gammadata. Average indoor radon concentration in different type of houses varied from 29-326 Bq/m^3. A different year of house's construction including various types of building materials were selected for survey. A detail analysis showed that the differences in radon concentration occur between various building materials used for construction, flooring level, type of room and behavior of inhabitants. It was found that building materials in some houses contribute additionally to indoor radon.

Keywords: Indoor radon concentration, house, building materials.

INTRODUCTION

Radon is unique gaseous product in uranium and thorium decay series. Two, the most prominent isotopes are radon (Rn-222) and thoron (Rn-220) which occurs in disintegration of series U-238 and Th-232, respectively. Their importance increases with their half-lives; 3.825 days for radon, and 55.6 seconds for thoron (UNSCEAR, 2006). The occurrence of Rn-222 in mineral grains is the result of direct emanations of radium Ra-226. The most significant sources of radon are granite, uranium ores, volcanic and phosphate rocks, gneisses, *etc*. Since soil originates by the decomposition of rocks, it could be a major source of radon in indoor air. Soil gas radon can enter buildings through cracks by pressure-driven mechanism. The relatively long half-life allows it enough time to transport and homogenous mixing in a room (UNSCEAR, 2006; Gulan, 2015; Vuckovic et al., 2016). Radon exhalation from the soil depends on several factors: concentrations of radium in soil, permeability and moisture of soil, state of vegetation cover, weather conditions. Meteorological conditions, lifestyle and occupant's habits could contribute more-less to the radon variations in indoor environments.

Average annual effective dose from different sources of radiation is presented in Fig. 1. Major contribution to public exposure relate to inhalation of radon and thoron (UNSCEAR, 2008). This is because people spend more time indoors in homes or workplaces (about 80%); that's the way to radon inhalation, and hence increasing the potential risk to lung cancer (UNSCEAR, 1993; ICRP, 1993; Darby et al., 2005; WHO, 2009). No level of radon is considered to be safe.

A number of European countries (United Kingdom, Sweden, Norway, Spain) established national guidelines for radon of 200 Bq/m^3 for both existing houses and new construction; other countries (Finland, Germany, Greece, Italy) determined 400 Bq/m^3 as upper limit for existing houses and 200 Bq/m^3 for new construction (CEC, 1990; Alghamdi & Aleissa, 2014).

Worldwide indoor radon concentrations vary widely from a few Bq/m^3 to more than $7 \cdot 10^4$ Bq/m^3 in high-background area (UNSCEAR, 2006). The higher indoor radon concentrations occur in the autumn or early winter and lower in the summer (Kurnaz et al., 2011; Alghamdi & Aleissa, 2014). Seasonal variation of radon indoors affects several parameters: the object, the source of radon, household habits, air ventilation and heating.

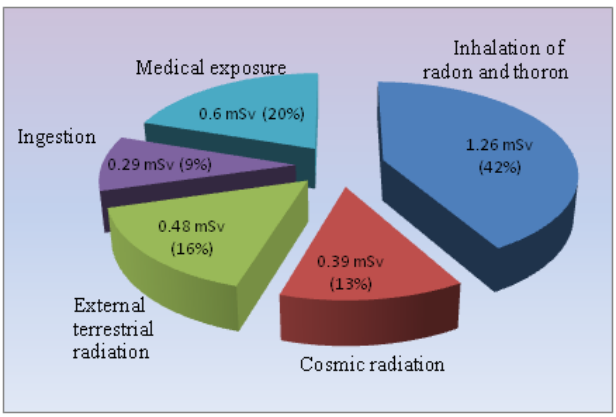

Figure 1. Average annual effective dose from different sources of radiation (UNSCEAR, 2008)

Active and passive methods (techniques) for radon monitoring have been developed. First method is used for short-term radon measurements and for preliminary inspection of sites. Second method which allows long time measurements (from 1 month to 1 year) is more suitable. Some recent large-scale surveys in Balkan region were performed with passive monitoring devices (Kavasi et al., 2007; Forkapic et al., 2007; Žunić et al., 2010; Milić et al., 2011; Stojanovska et al., 2012; Gulan et al., 2012; Gulan et al., 2013; Gulan, 2015; Vuckovic et al., 2016).

* Corresponding author: ljiljana.gulan@pr.ac.rs

The aim of this paper was to investigate possible differences and influence of building characteristics on indoor radon concentration based on specific analysis, as well to estimate impact of geology on high indoor radon.

EXPERIMENTAL

Materials and methods

Annual indoor radon measurements were conducted from April 2011-2012 in Zubin Potok municipality, northwest part of Kosovo and Metohija. In order to investigate the factors affecting the indoor radon, the preliminary survey was carried out in two rooms of five specific houses selected according to few criterion. This included the following items:

a) different types of house;

b) different year of house's construction;

c) different types of building materials used for house's construction;

d) different room's type;

e) measurement points at different floor of house.

Passive method of radon measurements with solid state nuclear track detectors (SSNTD) was applied. The CR-39 detectors, known as Gammadata were deployed on shelves of furniture at height of 1.5 m above floor and at the distance of 20 cm from the walls of living rooms/kitchens and bedrooms.

After exposure, the detectors were collected, packed and transported for the shortest possible time to laboratory. They were subjected to standard protocols of etching and readout of alpha tracks in well-controlled calibration chambers for radon. Uncertainty of radon measurements was less than 16% (Gulan, 2015).

In the term of geomorphology, Ibar valley is dominated on the relief of investigated area; this was a result of exogenous influences: glacial erosion, fluvial erosion and denudation; orogenesis was created on the basis of the huge mass of limestone rocks. The alluvial surface around River Ibar was created due to the erosive expansion of soft phyllites. Extensions consist of Quaternary sediments with alluvial (river terraces) and dilluvial horizons in the sludge layer, the sand and gravel. Terraces consist of gravel, marl and limestone, and rather than serpentinite and crystalline schists, which also depends on the geological composition of the terrain (Strategija razvoja opštine Zubin Potok, 2013).

RESULTS AND DISCUSSION

A range of indoor radon concentration in different houses varied from 29-421 Bq/m^3. Some important notes were observed. An analysis for each investigated house follows.

The lowest, but the same value of radon concentration in both rooms was measured in a floor house built from bricks 30 years ago. The approximate uniformity in radon distribution exists in the different rooms on the same floor. If the walls, ceilings and floors are made of the same building materials on the same floor, possible differences in the concentration of radon between the two rooms on the same floor can appear due to habits of the household, heating and ventilation (Denman, 2007).

Two floor houses of different age were subjected to investigation; one built 3 years (new house) and other 30 years (old house) before measurements. Radon concentrations were higher at ground level of both, new and old houses (246 Bq/m^3 and 156 Bq/m^3), respectively. It was expected, since earlier studies about impact of floor level on radon concentration confirmed that radon concentrations in multi-story building were higher in basement, *i.e*. ground level (Chao et al., 1997; Kurnaz et al, 2011; Popovic & Todorovic, 2006). Surprisingly, relatively high radon concentrations of 192 Bq/m^3 and 86 Bq/m^3 were noted at floor rooms of new and old houses, respectively. On the one hand unexpected, the average radon concentration was higher in new house. A type of this house is large ground-living room with open stairways to first floor. One reason for difference in radon concentration is tightly closed PVC doors and windows in new house in comparison to wooden joinery in old house. Also, high radon concentration in these cases could be probably induced by exhalation from walls of mortar and lime. The old house had wallpapers. Some building materials have been recognized as possible sources of high radon concentration, like materials containing by-product gypsum. Nonetheless, high content of radionuclides in nearby soil could affect radon accumulation.

Radon concentrations were 73 Bq/m^3 in living room and 65 Bq/m^3 in bedroom of prefabricated ground-floor house built 10 years ago. This is very rarely type of house in Kosovo and Metohija, and because of that it was very interesting for survey. Construction is quite different from commonly built houses in this area, since it only has strong concrete slab, wooden floor and plasterboard walls filled with Styrofoam (polystyrene foam). It is notable that radon is almost equal in both rooms, although their purpose and distance from front door are different.

The highest radon was measured in ground-floor house built from local stone and mud approximately 70 years ago. This house is without slab and floor is decking. The relevant differences in radon occurred between rooms of the house; concentration was 231 Bq/m^3 in the kitchen and 421 Bq/m^3 in the bedroom. The first reason of such a large difference could be existence of radon source in certain parts of the house. Secondly, purpose of room (*i.e.* bedroom), as well as its higher distance from the front door could affect the difference in concentration of 190 Bq/m^3. Bedrooms are usually smaller than living rooms or kitchen, and more often closed, and consequently less ventilated (Alghamdi & Aleissa, 2014). Some studies found that building materials used for construction of houses represent a significant source of indoor radon (Righi & Bruzzi, 2006). Useful information about geological features near building was obtained

from occupants; since Ibar River flows through Zubin Potok, there are mostly sandy soils. Some authors reported that a significant correlation has been found between indoor radon and geological characteristics of nearby soil (Sundal et al., 2004).

Seasonal variation in indoor radon concentration (such are various meteorological conditions, usage of ventilation systems, *etc*.) was avoided by annual measurements. Using the active method for radon measurements in certain sites can show accurate reason for obtained results. Further investigation will include more houses; a survey will be focused to determination of soil radioactivity near houses, with aim to get any correlation between indoor radon and radium in soil.

CONCLUSION

Indoor radon concentration in bedroom of old house exceeds level of 400 Bq/m^3, and also, 200 Bq/m^3 in other room. The main reasons of higher indoor radon accumulation in ground houses could be radionuclides in the nearby soil, building materials, poor ventilation and behavior of inhabitants.

Remark: One can conclude that the factors responsible for the degree of radon hazard in investigated houses could be assigned to one of groups:

- characteristics of underlying geology,
- type of building materials used for construction.

But, some abovementioned parameters by clubbing together could more-less contribute to higher radon levels, too.

ACKNOWLEGMENTS

The present work was supported by the Serbian Ministry of Education, Science and Technological Development, Project No. 41028.

REFERENCES

Alghamdi, A.S., & Aleissa, K.A. 2014. Influences on indoor radon concentrations in Riyadh, Saudi Arabia. Radiation Measurements, 62, pp. 35-40.

-CEC. Commission of the European Communities. 1990. Commission recommendation of 1990 on the protection of the public against indoor exposure to radon. European Journal of Communication, 80, pp. 26-28.

Chao, C.Y.H., Tung, T.C.W., & Burnett, J. 1997. Influence of Ventilation on Indoor Radon Level. Building and Environment, 32(6), pp. 527-534.

Denman, A.R., Groves-Kirkby, N.P., Groves-Kirkby, C.J., Crockett, R.G.M., Phillips, P.S., & Woolridge, A.C. 2007. Health implications of radon distribution in living rooms and bedrooms in U.K. dwellings: A case study in Northamptonshire. Environ Int, 33(8), pp. 999-1011. pmid:17399788

Forkapić, S., Bikit, I., Slivka, J., Conkić, L.J., Vesković, M., Todorović, N., . . . Hulber, E. 2007. Indoor radon in rural dwellings of the South-Pannonian region. Radiat Prot Dosimetry, 123(3), pp. 378-83. pmid:17077094

Gulan, L., Milic, G., Bossew, P., Omori, Y., Ishikawa, T., Mishra, R., . . . Zunic, Z.S. 2012. Field experience on indoor radon, thoron and their progenies with solid-state detectors in a survey of Kosovo and Metohija (Balkan region). Radiation Protection Dosimetry, 152(1-3), pp. 89-197.

Gulan, L., Bochicchio, F., Carpentieri, C., Milic, G., Stajic, J., Krstic, D., . . . Zunic, Z.S. 2013. High annual radon concentration in dwellings and natural radioactivity content in nearby soil in some rural areas of Kosovo and Metohija (Balkan region). Nuclear Technology and Radiation Protection, 28(1), pp. 60-67.

Gulan, L. 2015. Radon i toron u vazduhu zatvorenih prostorija na Kosovu i Metohiji - korelacija i mape rizika, Monografija. Beograd: Akademska misao.

-ICRP, International Commission on Radiological Protection. 1993. Protection against Radon-222 at Home and at Work. Annals of the ICRP, . Pergamon, Oxford, ICRP 65 Publication.

Kávási, N., Németh, C., Kovács, T., Tokonami, S., Jobbágy, V., Várhegyi, A., . . . Somlai, J. 2007. Radon and thoron parallel measurements in Hungary. Radiat Prot Dosimetry, 123(2), pp. 250-3. pmid:16891349

Kurnaz, A., Küçükömeroğlu, B., Cevik, U., & Celebi, N. 2011. Radon level and indoor gamma doses in dwellings of Trabzon, Turkey. Applied radiation and isotopes, 69(10), pp. 1554-9. pmid:21783373

Milić, G., Yarmoshenko, I., Jakupi, B., Kovačević, M., & Žunić, Z.S. 2011. Indoor radon measurements in Kosovo and Metohija over the period 1995-2007. Radiation Measurements, 46, pp. 141-144.

Popović, D., & Todorović, D. 2006. Radon indoor concentrations and activity of radionuclides in building materials in Serbia. Facta Universitatis: Physics, Chemistry and Technology, 4, pp. 11-20.

Righi, S., & Bruzzi, L. 2006. . Natural radioactivity and radon exhalation in building materials used in Italian dwellings. Jornal of Environmental Radioactivity, 88, pp. 158-170.

Stojanovska, Z., Januseski, J., Boev, B., & Ristova, M. 2012. Indoor exposure of population to radon in the FYR of Macedonia. Radiation Protection Dosimetry, 148(2), pp. 162-7. pmid:21406429

-Opština Zubin Potok. 2013. Strategija razvoja opštine Zubin Potok 2013-2017.

Sundal, A.V., Henriksen, H., Soldal, O., & Strand, T. 2004. The influence of geological factors on indoor radon concentrations in Norway. Sci. Total Environ., 328(1-3), pp. 41-53. pmid:15207572. doi:10.1016/j.scitotenv.2004.02.011

-UNSCEAR. United Nations Scientific Committee on the Effects of Atomic Radiation. 1993. Sources and effects of ionizing radiation. Report to General Assembly with Scientific Annexes.New York: United Nations.

-UNSCEAR. United Nations Scientific Committee on the Effects of Atomic Radiation. 2006. Report: Effects of ionizing radiation ANNEX E. Sources-to-effects assessment for radon in homes and workplaces.New York: United Nations.

-UNSCEAR. United Nations Scientific Committee on the Effects of Atomic Radiation. 2008. Sources and effects of ionizing radiation. Annex B: Exposure of the public and workers from various sources of radiation.New York: United Nations.

Vuckovic, B., Gulan, L., Milenkovic, B., Stajic, J.M., & Milic, G. 2016. Indoor radon and thoron concentrations in some towns of central and South Serbia. J. Environ. Manage., 183(Pt 3), pp. 938-944. pmid:27681871

-WHO. World Health Organization. 2009. WHO Handbook on Indoor Radon. A Public Health Perspective. WHO Press Geneva.

Žunić, Z.S., Bossew, P., Ristic, N.C., Bochicchio, F., Carelli, V., Vaupotic, J., . . . Tollefsen, T. 2010. The indoor radon survey in Serbian schools: Can it reflect also the general population exposure? Nukleonika, 55(4), pp. 419-427.

CIP - Каталогизација у публикацији
Народна библиотека Србије, Београд

5

The UNIVERSITY thought. Publication in natural sciences / editor in chief Nebojša Živić. - Vol. 3, no. 1 (1996)- . - Kosovska Mitrovica : University of Priština, 1996- (Kosovska Mitrovica : Art studio KM). - 29 cm

Polugodišnje. - Prekid u izlaženju od 1999-2015. god. - Je наставак: Универзитетска мисао. Природне науке =
ISSN 0354-3951
ISSN 1450-7226 = The University thought. Publication in natural sciences
COBISS.SR-ID 138095623

Available Online

This journal is available online. Please visit http://www.utnsjournal.pr.ac.rs to search and download published articles.